DISSERTATION

OVERACTIVE NF-KB SIGNALING AS A DRUGGABLE TARGET AND EVALUATION OF PARTHENOLIDE AN NF-KB INHIBITOR IN CANINE CANCER

Submitted by

Lisa Janelle Schlein

Graduate Degree Program in Cell and Molecular Biology

In partial fulfillment of the requirements

For the Degree of Doctor of Philosophy

Colorado State University

Fort Collins, Colorado

Fall 2022

Doctoral Committee:

Advisor: Douglas H. Thamm

Paul Avery
Dawn Duval
Amy MacNeill

ABSTRACT

OVERACTIVE NF-KB SIGNALING AS A DRUGGABLE TARGET AND EVALUATION OF PARTHENOLIDE AN NF-KB INHIBITOR IN CANINE CANCER

This study provides a unique translational research opportunity to help both humans and dogs diagnosed with diseases that carry dismal prognoses in both species: histiocytic sarcoma (HS), hemangiosarcoma (HSA), and disseminated mastocytosis (MCT). Lymphoma is one of the most common cancer types affecting dogs and humans, and therefore, novel therapeutic approaches are always needed. For all of these cancer types, dogs and human cancers share common molecular abnormalities, consistent with a conserved pathogenesis between species. Relative to traditional murine models for human cancers, dogs are genetically diverse, large mammals with heterogeneous, spontaneous tumors. Dogs generally receive good medical care and share the environmental factors with humans, and accordingly, dogs with spontaneous tumors are an excellent model for human oncology generally. Additionally, although disseminated HS, MCT and visceral HSA are exceedingly rare diseases in humans, they are more common in some dog breeds, giving us the opportunity to study this disease in a larger population than would otherwise be available. Therapeutics evaluated in dogs with these diseases stand to benefit both canine and human patients.

NF-kB proteins are a family of structurally related, eukaryotic transcription factors that have 400+ genetic targets, and are involved in many vital cellular processes, including innate immunity, inflammatory responses, development, cellular growth, and survival. Not surprisingly, overactivation of NF-kB is a feature of many chronic disease processes, including cardiac disease, neurodegenerative disease, immune-mediated disease, and cancer. While NF-kB overactivation has been documented extensively in human oncology, there is a relative paucity of data documenting the same phenomenon in veterinary medicine. As part of this study, large scale validation of NF-kB overactivation was performed in canine cancer via immunohistochemistry of 215 tumor samples (lymphoma, HS, HSA, and MCT). Antibodies were validated for use via western blot, immortalized cell pellets, and evaluation of normal canine tissues.

In addition to validation of NF-kB overactivation, assays were performed to assess the therapeutic potential of parthenolide (PTL), a known, canonical NF-kB signaling inhibitor with additional mechanisms of antineoplastic activity, including alteration of cellular redox balance. Growth inhibition assays were performed with canine cell lines and primary lymphoma cells isolated from canine patients, using PTL alone or in combination with redox-perturbing standard-of-care therapeutics. Cell death was assessed using flow cytometry. Immunofluorescence was used to assess NF-kB localization, western blot was used to assess NF-kB activity with and without PTL, and canine cells were transfected with a reporter gene cassette containing the NFkB consensus sequence followed by firefly luciferase gene to study the effect of PTL on NF-kB-related luminescence. PTL's effects on glutathione and reactive oxygen species

generation were assessed with a colorimetric assay and a fluorescent H2DCFDA assay, respectively. Genetic expression changes were assessed with RNA sequencing of HS cells, with and without PTL treatment. A mouse model of disseminated HS was created with NF-kB luminescent cells to study the effect of PTL on this disease *in vivo*.

Many spontaneous canine tumor samples have nuclear p65 and p100/p52 IHC staining that is of greater magnitude than observed in comparable, normal cell populations, indicating the promise of PTL and other therapeutics that target aberrant NF-kB signaling. Canine cell lines and primary cells are sensitive to PTL and undergo dose-dependent apoptosis following exposure to drug. PTL exposure also leads to glutathione depletion, reactive oxygen species generation, and NF-kB inhibition in canine cells. Standard-of-care therapeutics broadly synergize with PTL. In two canine HS cell lines, genetic expression of NF-kB pathway signaling partners is downregulated with PTL therapy. Preliminary data suggest that PTL inhibits NF-kB activity of cells in a mouse model of disseminated HS.

Overall, these data support further investigation of compounds that can antagonize canonical and alternative NF-kB pathway signaling, which are overactivated in canine lymphoma, HS, HSA, and MCT disease. PTL is one promising therapeutic that acts, in part, via canonical NF-kB antagonism in canine neoplasms. Further investigation of this compound *in vivo* is underway in a mouse model of disseminated HS, and if this study is successful, it will provide strong justification for clinical trials with this compound in dogs.

ACKNOWLEDGEMENTS

It is common knowledge that no one is an island, and that projects on this scale take significant investment not only from the individual doing most of the science, but from an entire village of supporters. In writing these acknowledgements, I am humbled by the size of the village that supported this particular project.

In my junior year of vet school, I heard Dr. Doug Thamm talk about the Cancer Biology PhD program and, as a student with literally no research experience, I sought his advice about finding research project in a field that I knew little about but found fascinating. Now, a decade later, I can say that the path that meeting set me on has been filled with adventure, intellectual challenge, and fulfillment in a rewarding discipline. I am deeply grateful to Doug for his guidance, both during veterinary school (at a meeting that I am confident he does not remember) and as my academic advisor in the PhD program. His truly tireless enthusiasm and support for students are an inspiration to everyone around him.

While I was not able to get official approval to add Dr. Craig Jordan to my PhD committee in time for the thesis defense, he has served as a key advisor for this project. His immense experience in hematopathology and the use of parthenolide have been vital in shaping this project, and his very generous donation of a water-soluble formulation of drug was critical to mouse experiments that are presented in this research and are ongoing.

Dr. Dawn Duval and Dr. Amy MacNeill are members of my committee who have been present every step of the way in the PhD program, from the very beginning of my

research time at CSU. Their perspectives and experience have been invaluable in shaping my understanding of cancer biology. In supporting my desire to work on my teaching skillset, Dawn was kind enough to allow me to lecture in the Cancer Biology course. Although I am still learning to set a reasonable speaking pace, this was a wonderful experience. In addition to acting as a research mentor, Amy's dedication and excellence as a pathologist and teacher have decidedly helped me to develop my clinical skillset, and I am incredibly grateful for the time I have been able to spend with Amy at CSU.

Dr. Paul Avery and Dr. Mark Ewalt are amazing pathologists who have been inspiring as committee members and mentors in my field. I admire their quick wit and candor on the clinic floor, as well as their tremendous work ethic, which is evident in every report and conversation they have with mentees, students, and colleagues.

In my time in the Thamm laboratory, I have worked with five incredible laboratory managers: Barb Rose, Dr. Kristen Farrell, Rupa Idate (Dawn's lab manager), Jade Kurihara (Steve Dow's lab manager), and Laura Chubb (Nicole Ehrhart's lab manager). These women are all wonderful scientists, as well as friends, confidants, and coworkers. Their work makes everything in the lab seamless, and they have always been available to troubleshoot assay issues or listen to ideas about other approaches. I am also very grateful to all of my coworkers in the lab. Dr. Travis Meuten has helped with my research since I started my project, and always has some unique method or MacGyver-style device that makes everything easier. Dr. Samantha Schlemmer ("Schlem") is someone I could always brainstorm with, candidly, at any level, without feeling small. I am in constant awe of Travis and Schlem's incredible attention to detail, willingness to

help others, brilliance, and humility. Sam Brill and Dr. Rachel Brady have always been available and kind, as I've needed help, support, and camaraderie throughout this journey.

Dr. Sunetra Das and Dr. Kathryn Cronise were instrumental in assisting with coding and interpretation of genetic expression data. Allister Aradi and other members of the Clinical Trials team retrieved more clinical samples for this project than I can recall. Any work remotely involving histopathology would not have been possible without the tireless efforts of Todd Bass and his team, and especially Laura Ashton. Dr. Mohammad Minhajuddin performed the EMSA assay that is presented in this work. SK Richman has been very helpful in adjusting graphics to make them visually appealing and publication ready.

Throughout my PhD experience, I have also received support and consultation regarding research methods and ideas from many other individuals at CSU, including Drs. Daniel Regan, Amanda Guth, William Wheat, Anne Avery, Daniel Gustafson, Lyndah Chow, Steve Dow, EJ Ehrhart, A Russell Moore, Adam Harris, Kelly Santangelo, Samantha Evans, Marika Klosowski, Christine Olver, and Linda Vap. I am confident that I am leaving people out of this list who have helped along the way. Thank you to Dr. Rodney Page and the entire Flint Animal Cancer Center for creating a wonderful environment for learning and scientific exploration.

In my time in the program, faculty in the Cell and Molecular Biology Program have been instrumental in my success. I would like to thank the past and current directors of the program, Dr. Howard Liber and Dr. Carol Wilusz, for their leadership and support. Charlene Spencer has ensured that I always submit the correct paperwork to

succeed in the program, even when my status as a post-doctoral student has complicated her work. Drs. Michael Weil, Lucas Argueso, Susan Bailey, Claudia Wiese, and Jac Nickoloff delivered lectures that sparked interest in new areas of cancer biology and were always very supportive when I sought guidance during my program. Thank you to Drs. Paige Ostwald, Kathryn Cronise, Platon Selemenakis, Jared Luxton, Elena Pires, Taghreed Alturki, Nouf Alyami, and Heather Deel for your camaraderie in the program.

I am very grateful for all of the funding I received for this program, which came from the Morris Animal Foundation Cancer Biology program (administered by Dr. Rodney Page), the TOTTS TL1 program (administered by Dr. Lisa Cicutto), and a Morris Animal Foundation Fellowship Grant.

Drs. Peter Moore and Bill Vernau were very helpful in characterizing circulating neoplastic histiocytic cells in two dogs, which will be presented in this study. Dr. Laura E. Brandt, clinical pathologist and my incredibly supportive, current supervisor, was very kind in providing funding for immunocytochemical staining for these cells, and for supporting construction of an ASVCP abstract and manuscript by an intern who worked on this project. I would also like to thank the former Wheat Ridge Animal Hospital intern, Dr. Jillian Hickey, who performed heroics to collect diagnostic samples from one of these patients for publication. I am very thankful that the owners of these dogs and supervising clinicians at WRAH (Dr. Stacy Meola and Dr. Kayla Harding) saw value in allowing additional characterization and culture of cells from these patients.

On a more personal note, I am grateful to my husband, Neal, and daughter, Rachel, for their unwavering support throughout the program. I would also like to thank

my parents, Terry and Paul, and Neal’s mom and her cousin, Catherine and Melanie, for their support and for taking such wonderful care of Rachel. Dr. Alycen Lundberg and Dr. Kimberly Pattullo have been with me every step of the way in research and has always spared an ear to listen to new ideas. Last but certainly not least, I am thankful for my Zoetis and Wheat Ridge Animal Hospital work families for support and understanding at the end of my program, particularly Drs. Laura Brandt, Noa Safra, and Jennifer Owen.

DEDICATION

This dissertation is dedicated to canine oncology patients and their owners. Without their participation in research studies and steadfast desire to conquer cancer, work like this would be impossible.

TABLE OF CONTENTS

ABSTRACT ii
ACKNOWLEDGEMENTS iii
DEDICATION iv

Chapter 1: Literature Review 1
Overview 1
Introduction 1
Types of neoplasia explored in this research 2
Leukemias and lymphomas 2
Histiocytic Sarcoma 3
Hemangiosarcoma 4
Mast cell neoplasia 5
PTL as an antineoplastic compound 6
Redox balance in cancer cells 8
Examples of redox chemotherapeutics 11
Mechanisms of resistance to antioxidants and redox chemotherapeutics 12
NF-kB Activation in Canine Cancer 13
NF-kB signaling in health 14
NF-kB dysregulation and cancer development 16
NF-kB signaling in cancer 19
Evasion of apoptosis 19
Acquisition of limitless replicative potential 22
Induction of angiogenesis 22
Induction of invasion and metastasis 23
NF-kB inhibition in cancer therapy 24
NF-kB overactivation in canine cancer 24
Leukemias and lymphomas 24
Hemangiosarcoma 27
Mammary cancer 27
Malignant Melanoma 29
Glioma 29
Osteosarcoma 29
Prostate Cancer 30
Studies including multiple cancer types 31
Specific Aims and Project Rationale 31
References 33

Chapter 2: Parthenolide as a Therapeutic in Canine Neoplasia 46
Overview 46
Introduction 47
Materials and Methods 49
Results 64

1. Sensitivity of canine tumor cell lines to parthenolide 64
1a: Broad characterization of PTL's effects across all cell lines in the FACC collection 64
1b: Further characterization of canine cell line responses to PTL 67
1c: NF-kB signaling in selected cell lines treated with parthenolide ... 69
2. Redox balance in canine cell lines treated with parthenolide 88
3. PTL in combination with other therapeutic agents in canine cell lines 92
4. Effects of PTL in patient-derived tumor samples 93
5. PTL in a mouse model of disseminated canine HS 98
Discussion and Conclusions 111
References 115

Chapter 3: Immunohistochemical Characterization of NF-kB Activation in Canine Neoplasms 118
Overview 118
Introduction 118
Materials and Methods 120
Results 128
Discussion and Conclusions 142
References 145

Chapter 4: Conclusions and Future Directions 149

CHAPTER 1: LITERATURE REVIEW

Overview

This review begins with a brief discussion of the similarities that canine cancers share with their human counterparts, features of a drug called parthenolide (PTL) and its promise as a therapeutic, and discussion of two primary mechanisms of action by which PTL may act in canine neoplasms: NF-kB inhibition and perturbation of redox balance in the cell.

Introduction

Cancer is the most common cause of death in dogs and affects approximately 4 million dogs per year.[41] Dogs have recently gained attention as a viable large animal model of human cancer for several reasons. Relative to rodent models, dogs are genetically diverse and share many environmental exposures with humans; unlike laboratory-induced cancer in rodents, dogs develop spontaneous neoplasms over a long period of time, which more closely mirrors cancer development in humans; and for many tumor types, canine cancers are remarkably similar to their human counterparts in microscopic appearance and biologic behavior.[40,118,41]

The purpose of this work is to explore the therapeutic potential of parthenolide (PTL), a naturally derived compound, in the treatment of canine cancer, and by extension, human cancers that receive little research attention due to their relatively low incidence. Although our data will show that PTL is a promising therapeutic for diverse

cancer types in dogs, this body of work focuses on hematopoietic cancers, which are malignancies derived from immune system cells.[1] Leukemias, or so-called “liquid tumors” circulate in blood and are derived from hematopoietic precursor cells in the bone marrow or mature hematopoietic cells in the blood.[1] The leukemic cell lines studied in this work are of lymphoid origin. Solid lymphoid malignancies, or lymphomas, are one major focus of this work, as are histiocytic sarcomas (HS, tumors of dendritic cells/macrophages), mast cell tumors (MCT), and hemangiosarcomas (HSA). Disseminated forms of HS, HSA, and MCT, both in humans and in dogs, are uniformly fatal, and novel therapeutic strategies are needed to improve therapeutic outcomes in both species.

Types of neoplasia explored in this research

Leukemias and lymphomas

There are clinical entities, both in humans and in animals, which are ultimately classified as leukemias or lymphomas, and are derived from a broad range of both lymphoid and myeloid cells at various stages of development, and with myriad normal functions in the body. Lymphomas are among the most frequently diagnosed cancers in dogs, with chemotherapy (commonly “CHOP” or cyclophosphamide, doxorubicin, vincristine, prednisone) being the gold standard of care in dogs.[21] Clinically and molecularly, canine disease often mirrors human disease. For example, many features of canine diffuse large B-cell lymphoma (DLBCL) resemble the ABC form of this human disease and peripheral T cell lymphoma in both humans and dogs is an aggressive

disease.[7] In this work, the canine cell lines used are lymphoid in origin, and primary cells were derived from patients with both T cell and diffuse large B cell lymphoma.

Histiocytic sarcoma

Histiocytic cells differentiate from CD34+ stem cell precursors into splenic red pulp +/- bone marrow macrophages and dendritic cells.[96] Canine HS has an aggressive clinical course, with most dogs having evidence of metastasis or locally disseminated disease at the time of diagnosis, and a median survival time of 3-6 months with chemotherapy; most commonly, therapy with lomustine/CCNU (1-(2-Chloroethyl)-3-cyclohexyl-1-nitrosourea), a long-acting nitrosourea alkylating agent, is used, although some reports have evaluated CCNU with doxorubicin and/or cyclophosphamide as well.[32,126,18,134] This disease is exceptionally rare (<1% of hematopoietic neoplasms) and is similarly fatal in humans receiving chemotherapy, with a median survival time of <6 months.[75] Because HS is relatively overrepresented in some dog breeds, such as Bernese mountain dogs, golden retrievers, and flat-coated retrievers,[96] dogs provide a natural study population for this rare and deadly human disease.

In most cases, HS cells are derived from interstitial dendritic cells, which are ubiquitous in the body, and can therefore arise in almost any tissue; these cells express CD1a, CD11c, and MHC class II. A variant of HS, called hemophagocytic HS (HHS), arises from splenic red pulp +/- bone marrow macrophages, and expresses CD11d/CD18 rather than CD1a and CD11c/CD18.

Some recent research has identified genetic alterations in HS of Bernese mountain dogs and flat-coated retrievers that are similar to those described in human

HS, implying a conserved pathogenesis for both species. These include CDKN2A/B, RB1, PTEN, PTPN11, and KRAS.[55,96,122,134] Loss of CDKN2A/B via mutation, deletion, or silencing is frequently observed in human cancers, including HS.[122,77] Mutations result in loss of tumor suppression by $p16^{INK4A}$, which inhibits DNA damage-related apoptosis.[122] RB1 (retinoblastoma 1) is a tumor suppressor gene with altered expression in many human solid tumors, as well as in acute myeloid leukemia and dendritic sarcomas.[55,48,62,73] PTEN plays a role in inducing cell cycle arrest and in induction of apoptosis, and has been deleted in a large number of human and canine tumors, including HS in both species.[55,19,88] PTPN11 and KRAS are gain-of-function mutations that are associated with upregulation of the mitogen-activated protein kinase (MAPK) pathway.

Hemangiosarcoma

Angiosarcomas (AS) are rare vascular tumors of endothelial origin, comprising approximately 1-2% of sarcomas in humans. The exact etiology of this neoplasm in humans, dogs, and rodents is unknown; it may arise from the transformation of endothelial cells that are resident within tissues, or alternatively, from circulating stem cells that are recruited from bone marrow or sites of extramedullary hematopoiesis.[161,78,25 15]

In humans, there are three different clinical presentations, including post-radiation therapy, cutaneous AS secondary to solar radiation, and infrequently, spontaneous disease that develops in visceral organs.[152] Because these tumors are exceptionally rare in humans, research efforts to identify driver mutations, identify

actionable drug targets, and conduct human clinical trials have stopped short of the need to address this deadly disease. By contrast, visceral canine hemangiosarcoma (HSA) is also deadly and forms vascular structures that are histologically similar to human AS, but is much more common in dogs, affecting up to 50,000 dogs per year in the United States alone.[144,152] Studies have found mutations in P53 and PTEN in both human AS and canine HSA, implying shared pathogenesis for these cancer types.[33,137,100,151]

While cutaneous HSA is generally treated via surgical excision in dogs, visceral HSA is uniformly fatal, with a MST of 140-202 days with various doxorubicin-based chemotherapeutic protocols.[69,24] Outcomes are similar in human patients with visceral angiosarcoma.[128]

Mast cell neoplasia

Normal mast cells are critical in both innate and adaptive immunity, and in addition, these cells are chronic offenders in allergic/inflammatory disease, progression of other cancer types, and autoimmune disease.[28] Clonal expansions of mast cells resulting in tumor formation can occur in the skin, or can be of a disseminated or systemic form in both dogs and humans, and are commonly caused in both dogs and humans by activating mutations of the KIT receptor tyrosine kinase.[28,106,138,154] This research is focused on evaluation of disease that affects both species systemically (the disseminated form). In humans, systemic mastocytosis can be a single disease process (median survival time of 41 months) or associated with development of another, non-mast cell hematopoietic neoplasm (median survival time 24 months).[106] Dogs with

systemic disease may be treated with lomustine/CCNU, vinblastine, and/or toceranib/Palladia™ (a KIT receptor tyrosine kinase inhibitor), with median reported survival times of 227 days for CCNU/vinblastine and 118 days for toceranib.[95]

PTL as an antineoplastic compound

Sesqueterpine lactones (SLs) are the active components of many medicinal plants from the Asteraceae (daisy plant) family, and several of these compounds inhibit the action of NF-kB, a transcription factor that is critical for normal innate immune and inflammatory responses.[39] PTL is a SL that was first isolated from the flowers and leaves of the feverfew plant (*Tanacetum parthenium)* and has been used for centuries to treat fever, migraine headaches, rheumatoid arthritis, and as a general anti-inflammatory agent. It was first recognized as having antineoplastic properties in 1973, and has been found to be effective, both *in vitro* and in mouse models, for numerous types of human cancers, including leukemias and lymphomas. Importantly, apoptosis in cancer cell populations is observed at PTL concentrations that are not cytotoxic (~1-10 μM).

PTL induces apoptosis in neoplastic cell populations via multiple mechanisms, which include NF-kB, AP-1, MAP kinase, and JAK-STAT inhibition, as well as disruption of the mitotic spindle, activation of p53, perturbation of redox balance within the cell, and epigenetic mechanisms (global DNA hypomethylation and proteasomal-mediated degradation of histone deacetylase 1 activity). On one hand, a drug with pleiotropic effects like PTL holds promise for anticancer therapy, as various sub-clones within a tumor may have different vulnerabilities that can all potentially be targeted by one drug,

and may therefore be uniquely situated to overcome cancer cell drug resistance. On the other hand, in the age of molecularly targeted, “personalized” anticancer strategies, such compounds can be viewed with less enthusiasm as “dirty drugs,” due to the tendency of such compounds to induce toxic or off-target effects.[157]

Two major mechanisms of PTL’s action that are explored in this research include NF-kB inhibition and perturbation of redox balance in the cell. In NF-kB/p65, Cys 38 participates in DNA binding by forming a hydrogen bond with the sugar-phosphate backbone. Parthenolide targets the DNA binding domain of RelA/p65 via covalent cysteine adduction at Cys 38.[39] Additionally, PTL demonstrates inhibition of IkB degradation via inhibition of IKKB, which is mediated via Michael addition between PTL and Cysteine 179 of IKKB.[157]

Despite PTL’s promise as an antineoplastic agent, a major previous limitation was its lipophilicity/poor water solubility, a characteristic shared by other natural lactones.[70] To address this limitation, a number of water-soluble, aminoparthenolide analogs were synthesized, including the fumarate salt of dimetylaminoparthenolide (DMAPT), which has 1000-fold increased water solubility, and has demonstrated apoptosis in cultured human AML, CLL (chronic lymphocytic leukemia) and CML (chronic myeloid leukemia), as well as dogs with acute leukemia.[102]

Intriguingly, in addition to causing death in bulk leukemic cell populations, PTL appears to prevent engraftment and metastasis of human acute myeloid leukemia (AML) cells, which indicates that it inhibits the action of leukemia stem cells, or LSCs.[51] These are a small subpopulation of primary cancer cells expressing stem-cell markers that are difficult to treat, as they are capable of initiating and re-establishing disease and

tend to divide slowly, and are therefore resistant to therapeutics that target rapidly dividing cells (chemotherapeutics and radiation). Although exploration of stem cell-like sub-populations is not an aim of this research, the possibility that PTL may target highly resistant clones of cells makes it a promising therapeutic for many cancer types.

Parthenolide effectively inhibits growth in canine cancer cell lines of different types, often at achievable, single-agent doses (data to be presented in Chapter 2). However, since tumor subclones develop therapeutic resistance over time, and for any given cancer type or patient, multiple agents may be desirable or even necessary, it is important to note that for human cancers, PTL appears to be broadly synergistic with a range of other therapeutics.[43]

Although PTL's use has been explored in a variety of leukemias and solid cancer types in mouse models and in humans, to our knowledge, this is the first research that explores PTL as a candidate therapeutic for human mast cell neoplasia, HS, or HSA/angiosarcoma.

Redox balance in cancer cells

Reactive oxygen species, or ROS, exist in a delicate balance with cellular antioxidants. While moderate increases in ROS can, in fact, be beneficial to the cell and promote proliferation and differentiation, excessive amounts can cause oxidative damage to lipids, proteins, and DNA.[141] Disruptions of redox homeostasis, or "oxidative stress" in cells may be due to increased ROS production or a relative decrease in the ability of the cell to counter that production (via scavenging systems such as superoxide dismutases, glutathione peroxidase, and thioredoxin).[141] Relatively increased oxidative

stress has been documented in cancer cell lines, as well as primary cells and tissues that have been directly isolated from patients. Leukemia cells freshly isolated from patients have increased ROS production compared with normal lymphocytes, studies of solid tumors have shown increased levels of oxidative damage products, and the levels of ROS-scavenging enzymes, such as glutathione peroxidase, have been shown to be significantly altered in malignant cells and in primary cancer tissues.[133,23,65,108,76] Importantly, oxidative stress in cancer cells has been observed in very aggressive tumors with poor prognoses, such as glioblastoma multiforme.[127] Greater understanding of oxidative stress, as well as investigation of therapeutics that can target aberrant redox status of tumor cells, is needed to improve therapeutic outcomes for these cancers.

While an increase in oxidative stress may play an important role in cancer initiation and progression, it has the potential to simultaneously increase cellular vulnerability to additional ROS insults that are introduced by exogenous agents, such as chemotherapeutics that may alter redox balance. Potential mechanisms of increased oxidative stress in cancer cells include alterations in the tumor microenvironment (hypoxia, inflammation), activation of oncogenes, aberrant metabolism, mitochondrial dysfunction, and loss of functional p53.[141,109,105] For example, constitutive activation of RAS protein signaling via overexpression or mutational activation is one of the most common genetic events in carcinogenesis, and is associated with increased ROS production and increased cellular oxidative stress.[140] However, RAS-transformed cells are more susceptible to glutathione depletion than non-transformed cells.[142,13]

There are many mechanisms by which cancer cells may achieve adaptation to oxidative stress over time. There is some evidence that exposure of normal epithelial cells to constant, low-level oxidants confers resistance to additional oxidative stress at a higher level.[22,141] As various subclones of a tumor cell population are exposed to oxidative stressors, it is likely that those that are most resistant survive to continue proliferation. These more resistant cells are likely to have adaptive mechanisms, such as increased ability to scavenge ROS and the ability to promote cell survival pathways.[141] For example, p53, the so-called "guardian of the genome," has a critical role in preventing oxidative genetic mutation and instability, and acts as a transcription factor to regulate both pro-oxidant and antioxidant genes. Many tumors (both human and canine) exhibit loss of functional p53, which is associated with high oxidative stress and aggressive tumor growth.[56,71,141,50] Redox adaptation via activation of ROS-scavenging enzymes seems to be a major means by which cancer cells additionally adapt to maintain redox homeostasis. For example, multiple pathways may activate one or more redox-sensitive transcription factors, including NF-kB, Nrf2, and HIF-1, which lead to increased expression of antioxidant molecules. Some of these transcription factors can also promote expression of cell-survival molecules, such as BCL2.[141] Furthermore, these same transcription factors offer additional survival advantages, leading to cell signaling that favors proliferation, angiogenesis, and metastasis. At an advanced stage of disease, cancer cells may enter a vicious cycle, whereby ROS induce genetic mutations that lead to further metabolic aberrations and ROS production.

Therapeutics that modulate oxidative stress and preferentially target neoplastic cell populations have been referred to as "redox chemotherapeutics."[157] Some cancer

drugs that are well-established have also been shown to generate ROS, which in turn, contributes to apoptosis of cancer cells; these agents include paclitaxel, cisplatin, bortezomib, and etoposide.[114,72,84,124] Actions of redox chemotherapeutics can occur via a structure-based mechanism (in which the activity of a molecular target is altered via binding of a ligand), or more commonly, a reactivity-based mechanism (in which the activity of the molecular target is altered through a chemical reaction).[157] Some of these compounds have promising single-agent activity, while others may best be used as combinatorial drugs to achieve synergistic cytotoxicity.

Examples of redox chemotherapeutics

"Redox cyclers" react with flavoprotein reductases such as cytochrome P450 reductase and NADPH:quinine oxidoreductase (NQO1) in the presence of reduced NADPH and generate superoxide in the presence of molecular oxygen.[157] Examples of redox cyclers include anthracyclines, such as daunorubicin and doxorubicin. Doxorubicin can also chelate iron, which may trigger a Fenton-type reaction leading to the generation of a highly reactive hydroxyl radical.[157,159,93]

Most redox-modulating enzymes relying on the pool of reduced glutathione (GSH) in the cell, so one therapeutic strategy is to decrease the reduced GSH pool within cancer cells.[157,103] In theory, this would have a profound effect on cellular survival and drug sensitivity. Numerous compounds are electrophilic Michael acceptors, including curcumin, PTL, and cinnamic aldehyde. Typically, these Michael acceptors target thiol-group containing reaction partners via covalent adduction (thioalkylation).[17,157,39,125] Therefore, redox alterations in target cells originate from

glutathione adduction and ROS formation downstream of glutathione depletion.[157] Covalent adduction of critical thiol residues also occurs in redox-sensitive target proteins that regulate cellular redox status, including components of NF-kB signaling or thioredoxin redox systems.[157] Glutathione depletion can also be achieved by targeting its synthesis. Buthionine sulphoximine (BSO) is an inhibitor of gamma-glutamylcysteine synthetase (gamma-GCS), a rate-limiting enzyme for GSH synthesis.[157,57] Inhibitors of the xc-cystine/glutamate antiporter, such as sulfasalazine, inhibit uptake of cystine, which is a rate-limiting substrate for GSH synthesis as well.[49]

The thioredoxin system is also upregulated in cancer cells, and its upregulation has been specifically noted in aggressive and drug-resistant cancers. Some thioredoxin inhibitors include PX-12, which is a Trx-1 inhibitor with potent *in vivo* activity.[157]

Mechanisms of resistance to antioxidants and redox chemotherapeutics

Treatment with antioxidants is a double-edged sword; although increased oxidative stress is associated with the potential for tumor development, some antioxidants in clinical trials were surprisingly associated with increased cancer incidence, which may be related to inhibition of ROS-mediated apoptosis and promotion of tumor survival.[11,141] Antioxidant treatment also has the potential to decrease the antitumor effects of some agents that depend on ROS-mediated actions for cytotoxicity.

Since cancer cells have adapted to increased oxidative stress, some cells not only increase their ability to scavenge ROS, but also inhibit cellular apoptosis despite ROS-mediated damage, which can potentially necessitate treatment with agents that target multiple vulnerabilities in cancer cells. For example, multidrug resistant HL-60

leukemia cells are resistant to the cytotoxic effect of H_2O_2, which is apparently due to increased catalase activity.[81,141] Several studies have shown that resistance to agents that induce intracellular ROS are correlated with increased antioxidant capacity.[53,111,108] One strategy to overcome redox adaptation in cancer cells is to target both the level of ROS and the function of survival proteins. PTL is such an agent which, depending on the cell type, exerts its antineoplastic activities via glutathione inhibition, redox perturbation, and inhibition of survival signaling via NF-kB. A concern with this multifaceted approach is a theoretically increased risk of promoting mutations in normal cells as well.

NF-kB Activation in Canine Cancer

Nuclear factor kappa-light-chain-enhancer of B cells (NF-kB) is a transcription factor that is constitutively active in most human hematopoietic and solid tumor cell lines, and has also been demonstrated in tumor tissues from human patients with diverse cancer types, including multiple myeloma, acute myeloid leukemia (AML), acute lymphoblastic leukemia (ALL), chronic myelogenous leukemia (CML), prostate, and breast cancer.[3,34]

The aim of this section is to provide an overview of what is currently known about NF-kB signaling in human health and cancer, and to collate available evidence documenting NF-kB overactivation in canine cancer. In addition to highlighting a pathway that is commonly dysregulated in both human and canine cancers, the literature suggests that NF-kB inhibition may be a viable treatment strategy for several canine cancer types.

NF-kB signaling in health

NF-kB is a family of structurally related transcription factors that were first described in 1986 and are highly conserved in animals.[80,120,131] Inactive NF-kB is sequestered in the cell cytoplasm until it is activated, when it translocates to the nucleus to bind DNA and initiate transcription of over 400 target genes that are important in normal immunity, growth, apoptosis, and inflammation.[120,66,34] Target genes include inflammatory cytokines, adhesion molecules, inflammatory enzymes (such as cyclooxygenase-2), telomerase, anti-apoptotic proteins, and cell cycle-regulatory genes.[120]

NF-kB may become activated via a canonical or an alternative signaling pathway (see **Fig. 1.1**). The canonical pathway is activated by diverse factors, including tumor necrosis factor alpha (TNF-a), interleukin-1 (IL-1), and lipopolysaccharide (LPS), and this pathway is critical for innate immunity, inflammation, and inhibition of apoptosis.[131] In the canonical pathway, NF-kB is a heterodimer made up of p50 and RelA subunits. NF-kB is sequestered in an inactive form in the cell cytoplasm with one of many inhibitory molecules containing ankyrin repeats that function as protein-protein interaction domains that interact with the Rel homology domains (RHDs) of NF-kB members; the most common inhibitory molecule is IkBa.[120,131,66,34] Upon activation of a specific IkB kinase (IKK), phosphorylation of two conserved serine residues on the N-terminal domains of IkB proteins leads to polyubiquitination and proteasomal degradation of the inhibitory molecule, which unmasks a nuclear localization signal,

allowing the NF-kB heterodimer to enter the cell nucleus and initiate transcription of downstream target genes.[120,66,34]

The alternative pathway, by contrast, is important for B cell maturation, formation of secondary lymphoid organs, and production of high-affinity antibodies, and is activated by NF-kB inducing kinase (NIK).[131,120] NIK phosphorylates IKKa, which then phosphorylates pre-existing p100/NF-kB2:RelB heterodimers, triggering the processing of inhibitory p100/NF-KB2 to p52. Active p52:RelB complexes can then translocate and activate downstream target genes.[120,132,66,34]

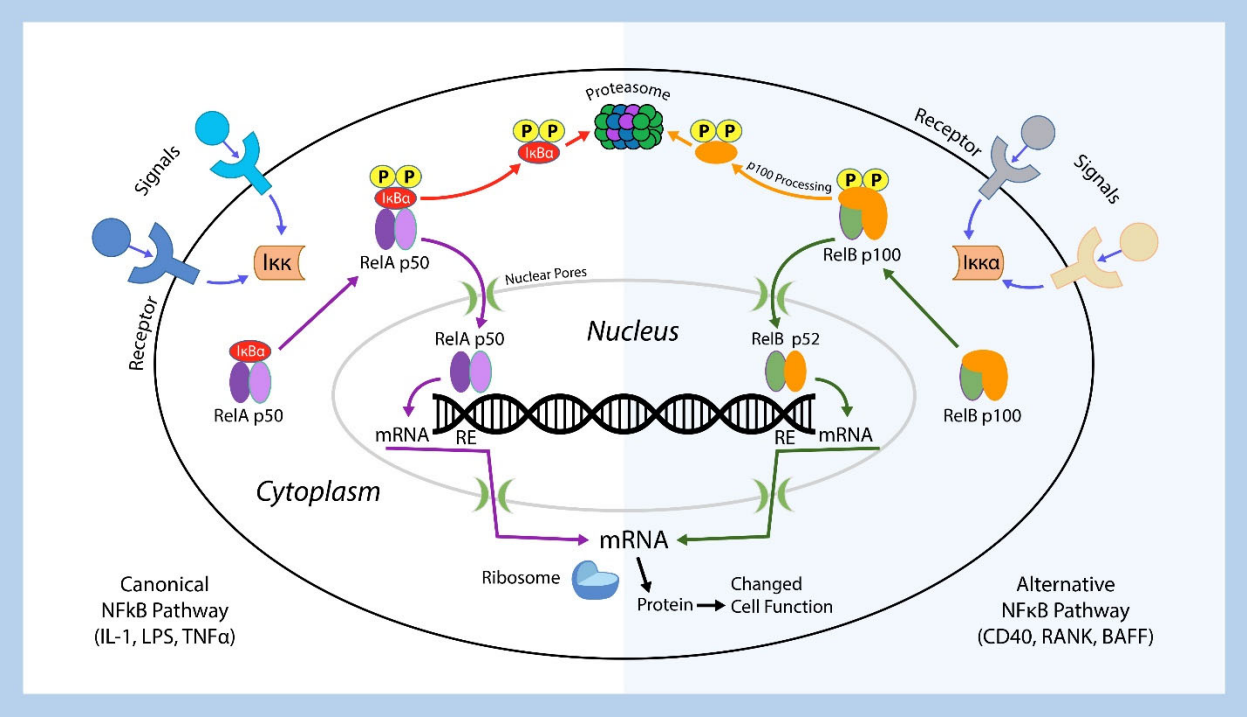

Figure 1.1: *NF-kB signaling cascade.* The left side of the diagram (white background) shows the canonical signaling pathway, while the alternative pathway is on the right side of the diagram (blue background). The canonical pathway is critical for innate immunity, inflammation, and inhibition of apoptosis, and in this pathway, NF-kB is a heterodimer made up of p50 and RelA subunits (shown above in purple). This heterodimer is sequestered in an inactive form in the cell cytoplasm by an inhibitory molecule; IkBa is most common and is shown above in red. Upon activation of a specific IkB kinase (IKK), phosphorylation of two conserved serine residues on the N-terminal domains of inhibitory IkB proteins leads to polyubiquitination and proteasomal degradation of the inhibitory molecule, which unmasks a nuclear localization signal, allowing the

NF-kB heterodimer to enter the cell nucleus and initiate transcription of downstream target genes. In the alternative pathway, which is important for appropriate B cell maturation, formation of lymphoid organs, and production of high-affinity antibodies, NF-kB inducing kinase (NIK) phosphorylates inhibitory IKKa, which then phosphorylates pre-existing p100/NF-kB2:RelB heterodimers (shown in green and orange above). This triggers the processing of inhibitory p100/NF-KB2 to p52. Active p52:RelB complexes can then translocate and activate downstream target genes. RE = response element, a binding site for active NF-kB.

In health, NF-kB overactivation is prevented via tightly regulated negative feedback loops that limit the duration of NF-kB nuclear localization. IKBa has a nuclear export sequence that can bind to NF-kB and remove it from the nucleus. In addition, there are several deubiquitinating enzymes (CYLD, A20, and Cezanne) that are induced by pro-inflammatory signaling and block IKK activation by removing polyubiquitin chains from IKBa. This results in stabilization of newly synthesized IKBa and prevents additional NF-kB activation.[120]

NF-kB has many important roles, but most of the inducible activity of NF-kB appears to be important in mounting effective immune responses and functioning as an anti-apoptotic, pro-survival factor, which may help the body's immune cells avoid death during infection.[131]

NF-kB dysregulation and cancer development

While acute inflammation is self-limiting and readily resolved, overexuberant or chronic inflammation can lead to a permissive state in which pre-cancerous cells evade normal immunosurveillance and are more vulnerable to DNA damage and epigenetic change.[36,148,110,38] The link between inflammation and cancer was suspected by Rudolph Virchow over 150 years ago, when he documented tumor-infiltrating

inflammatory cells in human breast carcinomas.[10] The process of tumor development has been conceptualized with a classic stepwise evolution of malignancy in three phases: initiation, promotion, and progression.[97] In initiation, normal cells accumulate genetic changes that cannot be repaired, such as point mutations, deletions, chromosomal rearrangements, and genetic methylation. Mediators of inflammation, including cytokines, reactive oxygen species (ROS), and prostaglandins, can initiate DNA mutations. Cells with minor DNA damage can often be repaired, and if the damage is irreparable, cellular death pathways are typically initiated so that these cells die via apoptosis. In some cases, however, cells with permanent mutations persist, and predispose cells to additional genetic alterations, leading to a selective cell growth advantage.[97] Activation of oncogenes, deactivation of tumor suppressor genes, and regulators of cellular proliferation during initiation lead to tissue microenvironment alterations that help promote the expansion of initiated cells. Once a clone of neoplastic cells is established, they can induce and elaborate a pro-inflammatory microenvironment via recruitment of leukocytes and may promote genetic instability via release of ROS, leading to further genetic instability within the tumor microenvironment.[20,148] Progression is the substantial growth and/or metastasis (distant spread) of cancer from its original site.[97]

Constitutively active NF-kB is implicated in diseases that are associated with inappropriate inflammatory responses (such as asthma and autoimmune diseases) or unnatural survival (cancer).[120] The mechanisms that lead to NF-kB overactivation in tumor cells can be due to upstream activation of NF-kB signaling, direct alteration of NF-kB signaling pathway members (for example, mutation of IkBa, enhanced

proteasomal activity), genetic alterations leading to the decoupling of NF-kB factors from their regulators, and autocrine and paracrine production of inflammatory cytokines.[66,3,34] Some members of the NF-kB family are directly oncogenic, including c-Rel, which consistently transforms cells in culture and is amplified in lymphomas[47] and v-Rel protein, which leads to rapidly fatal lymphoma/leukemia in birds.[46] Other known oncogenes that signal through NF-kB and lead to its overactivation include Ras, myc, Pim-2 (a transcriptionally regulated oncogenic kinase), and various viral proteins, including Kaposi's sarcoma-associated herpesvirus, hepatitis B virus protein HBx, EBV-latent membrane protein, and human T lymphocytic leukemia virus (HTLV-1).[3,98]

There are several examples of work that demonstrate a link between inflammation and the perpetuation or development of cancer. For example, Taketomi et al. demonstrated that inflammation in a nontumorous part of the liver was a risk factor for recurrence of hepatocellular carcinoma following surgery.[135] In a study by Pidgeon et al., Balb/c mice received mammary carcinoma cells via tail vein injection; some of these mice experienced surgical trauma or LPS injection, while controls received anesthesia only. Those that were exposed to surgical trauma or LPS had increased evidence of lung metastasis, as well as increased tumor cell proliferation and decreased apoptotic activity in tumor cells.[112] Recently, in the evaluation of somatic mutagenesis in hematopoietic stem/progenitor cells in patients with cardiovascular disease, NF-kB overactivation was directly tied to the pro-inflammatory shift induced by clonal hematopoiesis (CH).[2,61,26] Finally, modern mathematical evaluation of early B cell differentiation includes several biological perturbations with NF-kB signaling, and predicts that 1) constant but intermediate NF-kB signaling during B cell differentiation

promotes the emergence of a CXCR7+ B cell precursor that has a phenotype compatible with leukemia-initiating cells, and 2) constitutively overactive NF-kB signaling can potentially lead to a blockage in lineage commitment.[36]

NF-kB signaling in cancer

There are several distinctive and complementary capabilities that allow tumors to grow and spread in the body, known as the "hallmarks" of cancer.[52] NF-kB is able to induce several of these cellular alterations, including evasion of apoptosis, self-sufficiency in growth signaling, induction of angiogenesis, and induction of invasion and metastasis.

Evasion of apoptosis: Cellular apoptosis is a programmed cell death pathway that is designed to activate following periods of significant physiologic stress or after the cell experiences irreparable damage. Despite exposure to many typically lethal cellular stresses, cancer cells are not only able to survive, but can gain new mutations and continue to evolve, ultimately becoming more aggressive. Some typically apoptosis-inducing scenarios to which cancer cells are immune include cellular signaling imbalances that result from elevated levels of oncogene activation, DNA damage secondary to rapid, unchecked proliferation, and exposure to antineoplastic drugs or radiation.

Apoptotic signaling partners are divided into two major pathways: the intrinsic pathway, which is involved in sensing intracellular signals, and the extrinsic pathway,

which is involved in processing extracellular death-inducing signals. Following initiation, the apoptotic cascade involves a sequence of caspase enzyme activation; ultimately, the cascade results in activation of key executioner caspases that disassemble the cell so that it can be consumed by phagocytic cells. The “trigger” that initiates the intrinsic apoptotic pathway is controlled by counterbalancing pro- and anti-apoptotic members of the Bcl2 family of proteins. Pro-apoptotic Bak and Bax are embedded in the mitochondrial outer membrane (MOM), and when relieved of inhibition by anti-apoptotic relatives, they create a pore within the MOM, allowing the release of cytochrome c, initiating apoptosis.

Tumor cells have evolved a number of mechanisms to prevent or limit apoptotic activity, including loss of function of the TP53 tumor suppressor (a DNA damage sensor), increased expression of anti-apoptotic proteins such as Bcl2 or Bcl-xl, downregulating pro-apoptotic factors, or preventing binding of ligands that can induce extrinsic apoptosis.

NF-kB was the first oncogenic transcription factor whose functional regulation was found to depend on its cellular localization rather than its level of transcription. Constitutive activation of NF-kB is seen in many different cancer types, and its activation, as mentioned previously, results in pro-survival signaling in most cells, inducing expression of at least 26 survival genes such as c-IAP1, caspase-8/FADD, (FAS-associated death domain)-like-IL-1B-converting enzyme (FLICE), TRAF, c-FLIP, and members of the BCL2 family, such as Bcl-xl.[66,67,34] Most agents that experimentally induce apoptosis also activate NF-kB, consistent with NF-kB acting as part of the cell’s defensive machinery that can mediate chemoresistance and radioresistance.[149,150] In

addition to mediating resistance to anticancer therapies, NF-kB has an important role in the emergence of neoplastic cells by preventing the death of cells that have undergone significant DNA damage; there is evidence for transcriptional antagonism between active NF-kB signaling and TP53, a checkpoint control colloquially known as the "guardian of the genome."[153,34]

Inappropriate constitutive activation of NF-kB can lead to unnatural survival of cells, promoting tumorigenesis. For example, the NF-kB target c-IAP1 can directly block caspase functions or indirectly induce their ubiquitination and degradation. TRAF proteins amplify NF-kB signaling activation and interfere with the caspase cascade. c-FLIP, once activated, associates with TNFR to compete with and block caspase-8 activation. Finally, as previously mentioned, mitochondrial cytochrome-c release into cytosol leads to activation of the intrinsic apoptotic program, and this pathway is controlled at the mitochondrial membrane level by proteins of the Bcl2 family that are either pro or anti-apoptotic. NF-kB activation leads to transcription of several genes coding for anti-apoptotic proteins of the Bcl2 family, all of which act to prevent cytochrome c release. NF-kB can also prevent programmed necrosis by induction of genes that encode for antioxidant proteins.[86]

NF-kB can also play a key role in regulating oxidative stress in cells. For example, when it is acutely expressed, it can induce nitric oxide (NO) synthesis, which has been described as a pro-apoptotic function;[27,68] however, when there is chronic production of NO via constitutively active NF-kB signaling, apoptosis is inhibited.[14,30] NF-kB also regulates activation of heme oxygenase-1 (HO1), which enhances free heme catabolism and protects the cell from damaging effects to lipid bilayer cell

membranes.[63,30] Upregulation of HO1 has been correlated with resistance to TNFa-mediated apoptosis as well as resistance to chemotherapy-induced apoptosis.[54,116,30]

Acquisition of limitless replicative potential: Overactive NF-kB can induce transcription of the gene for cyclin D1, which is involved in the G1/S transition of the cell cycle and therefore promotes cellular proliferation.[66] Several inflammatory cytokines that are downstream of NF-kB activation can serve as growth factors for tumor cells, including IL-2, granulocyte macrophage colony stimulating factor (GM-CSF), IL-1B (AML), TNFa (Hodgkin's lymphoma), and IL-6 (multiple myeloma).[66,104,3] In addition, telomerase reverse transcriptase (TERT) protects the telomeres of neoplastic cells from shortening, which ultimately prevents normal cellular senescence or cell death. Because NF-kB overactivation can lead to TERT-dependent transcription and induction of telomerase activity, this is another means by which cells can acquire limitless replicative potential.[83,45,9]

Induction of angiogenesis: Cytokines that are enhanced by NF-kB activity can also lead to constitutive expression of angiogenic chemokines and growth factors (such as IL-8 and vascular endothelial growth factor [VEGF]), which affect tumor vessel growth and ultimately, lead to tumor dissemination.[66,59]

Induction of invasion and metastasis: Metastasis is mediated in part via the expression of various adhesion molecules, including ICAM-1, VCAM-1, and ELAM-1, which are in turn mediated by NF-kB.[146,34] Tumor invasion is also regulated, in part, by NF-kB-regulated gene products, including matrix metalloproteinases (MMP), urokinase plasminogen activator (uPA), and IL-8.[66] Inducible nitric oxide synthase (iNOS) has also been linked with metastatic activity of neoplastic cells.[139]

From these available data, it is tempting to conclude that NF-kB activation is always connected with tumorigenesis, but there are some scenarios in which the opposite is true. Interestingly, NF-kB blockade has been experimentally associated with the spontaneous development of squamous cell carcinomas and other cutaneous neoplasms.[147,29] Work by Nakagawa et al. attempted to discern the role of constitutively active NF-kB signaling in leukemogenesis by studying mice that express constitutively active IKK2. These mice demonstrated a reduced pool of hematopoietic stem cells (HSCs), and the functions of the remaining HSCs were compromised. Mice demonstrated a hyper-proliferative phenotype of HSCs with loss of quiescence.[101] Interestingly, increased HSC turnover and impaired HSC function are also seen in mice that have a deficiency of RelA.[130] While it is unclear as to why both loss and gain of NF-kB function would lead to a similar phenotype, Nakagawa et al. speculate that "fine-tuning" of NF-kB signaling is necessary for HSC biology.[101] Thus, while several NF-kB inhibitory drugs are being developed for cancer treatment, caution is warranted, as the activation or inactivation of NF-kB may lead to tumorigenesis, depending on the specific circumstances.[3]

NF-kB inhibition in cancer therapy

Because NF-kB activation requires the activation of multiple steps in signaling, there are numerous ways in which signaling can be interrupted at various points in the process. Examples of anticancer therapeutics that have been explored in human medicine include those that interfere with IKK activity (anti-inflammatory drugs and natural compounds such as curcumin), those that bind NF-kB and prevent its nuclear

translocation, and proteasome inhibitors that prevent NF-kB activation by blocking degradation of inhibitory molecules like IkB.[34,43,160,136,44,123] As previously mentioned, our group has been investigating the therapeutic potential of PTL, a sesquiterpene lactone originally purified from the shoots of feverfew (*Tanacetum parthenium*) to treat various canine cancers. This is a drug that appears effective for several types of human cancer, and mechanistically, exerts its anticancer effects in part via NF-kB inhibition.[43] Many different canine cancer cell lines are sensitive to parthenolide and exhibit NF-kB inhibition following treatment (see Chapter 2).

NF-kB overactivation in canine cancers

Leukemias and lymphomas

Gene expression profiling (GEP) of human diffuse large B cell lymphomas (DLBCL) distinguishes two primary neoplastic subtypes: those that arise from cells within germinal centers (GC) and those that are immediately post-germinal center and differentiating toward plasma cells (ABC).[7,5] Although these two types of cancer are histologically identical, the chromosomal aberrations and pathways that drive their differentiation are different, and most notably, NF-kB activation is characteristic of ABC DLBCL but not GC DLBCL.[31,162] By comparison, GEP of canine DLBCL reveals a gene expression pattern typically most similar to ABC DLBCL, in part because of constitutively active NF-kB signaling and activation of downstream anti-apoptotic genes in most cases.[115,6,7]

Constitutive activation of both the classical and alternative NF-kB signaling pathways has been documented in dogs with DLBCL.[42,119,99] Inactivating mutations in TRAF3 were first identified in canine DLBCL, then in some human DLBCL samples.[16] TRAF3 encodes a negative regulator of the non-canonical NF-kB pathway, leading to upregulation of NF-kB. In addition, mutations that lead to constitutively active canonical NF-kB signaling (in TNFAIP3 and CD79b) were observed in low numbers of canine DLBCL cases.[7,16] These studies provide convincing evidence that NF-kB overactivation is important in the pathogenesis of canine DLBCL.

The importance of NF-kB signaling in canine lymphoma and leukemia has also been documented during the evaluation of multiple investigational anticancer compounds, discussed below.

Intracellular transport between nuclear and cytoplasmic compartments is regulated by importins and exportins, and of the seven known exportins, most tumor suppressor proteins and IkB are transported out of the cell nucleus by exportin 1 (XPO1/CRM1). Stabilization of IkB within the cell nucleus may neutralize constitutively active NF-kB activity in canine lymphoma. KPT-335 is a selective inhibitor of nuclear export (SINE) that has shown biological activity *in vitro* and *in vivo* in dogs with previously progressive non-Hodgkin's lymphoma.[121,85,117]

In a study evaluating PTL in inhibition of NF-kB activity in human leukemic stem cells, Guzman et al. also evaluated cells from dogs with acute leukemia. They found that most acute leukemia cells from dogs (7/8 samples) exhibited constitutive activation of NF-kB and that exposure to PTL *in vitro* led to decreased NF-kB activity and decreased survival. Three dogs with acute leukemia also received PTL therapy, and

peripheral blood from these animals demonstrated a rapid and consistent reduction in immature CD34+ cells in these animals following treatment, consistent with differentiation and/or death of primitive leukemia cells.[51] In this manuscript, the authors demonstrated active NF-kB signaling in part by demonstrating nuclear p65 immunofluorescence that was inhibited by PTL therapy. This experiment was repeated in several types of hematopoietic tumors in dogs, with similar results (data to follow).

Bortezomib is a proteasome inhibitor that has been utilized for treatment of human multiple myeloma and other hematological malignancies. A primary mechanism of action for this drug is via NF-kB inhibition, which was investigated in canine leukemia and lymphoma cell lines by Kojima et al. This study demonstrated constitutive activation of NF-kB in some cell lines, and showed that treatment with bortezomib prevented nuclear translocation of NF-kB and inhibited the growth of several cell lines.[74]

Methotrexate (MTX) is an antimetabolite used as an anticancer therapeutic in various types of canine and feline cancer, including lymphoma. Pawlak et al investigated MTX-induced cell death in canine lymphoma and leukemia cell lines. Their data suggest that apoptotic cell death is mediated via inhibition of NF-kB, leading to decreased expression of Bcl2, and enabling activation of the intrinsic apoptotic cascade.[107]

Finally, work by Matsuda et al. showed that inhibition of NF-kB by the synthetic compound IMD-0354 in canine lymphoma cells could increase glucocorticoid receptor expression, sensitizing cells to dexamethasone.[89] This work implies that combination therapy with glucocorticoids and NF-kB inhibitors may be beneficial for some dogs with lymphoma.

Hemangiosarcoma

As previously discussed, angiosarcomas (AS) are rare vascular tumors of endothelial origin, comprising approximately 1-2% of sarcomas in humans, and shared mutations in both species imply a shared pathogenesis for this disease.

Yunnan Baiyao is a Chinese herbal medication that has been used in people for its hemostatic properties and is used anecdotally in dogs with visceral HSA. A study by Wirth et al. demonstrated that *Yunnan Baiyao* induces both time and dose-dependent apoptotic cell death in canine HSA cell lines *in vitro*. Intriguingly, they noted that wild yam root, a component of this medication, contains a plant phytosterol estrogen known as diosgenin, which induces anti-proliferative and pro-apoptotic effects, in part via downregulation of NF-kB.[155,90,4]

Mammary cancer

Building evidence in the literature suggests a role for overexuberant NF-kB signaling in canine mammary cancer. In neoplastic mammary tissues from dogs, several researchers have found molecular evidence consistent with NF-kB overactivation. In a canine model of breast ductal carcinoma in situ (DCIS), Mohammed et al. evaluated the transcriptome of mammary lesions along the continuum of cancer progression in the mammary gland, and found that NF-kB was differentially overexpressed in canine DCIS and cancer as compared to samples from normal tissues and dogs with atypical ductal hyperplasia.[94] Zhang et al. reported relative miR-497

downregulation in canine mammary cancer tissue and discovered that restoration of miR-497 inhibits active NF-kB signaling *in vitro*.[163] Protein phosphatase 2A (PP2A) is an evolutionarily conserved serine/threonine protein phosphatase that functions as a tumor suppressor that can be inhibited by SET; increased SET protein levels in canine mammary cancer and osteosarcoma (OS) leads to a decrease in PP2A activity, which in turn positively regulates mTOR, B-catenin, and NF-kB signaling in these cells.[143,64]

Lee et al. evaluated the secreted frizzled protein 2 (sFRP2) overexpression in canine mammary tumor cells, which they documented as key to resistance to apoptosis. Using electrophoretic mobility shift assays (EMSAs), they found that the UV-induced level of active NF-kB in mammary gland cells expressing sFRP2 was significantly increased relative to NF-kB activity in control cells, suggestive of NF-kB-mediated apoptotic resistance.[79]

There is some evidence suggesting that NF-kB overactivation is correlated with a poorer prognosis. A study evaluating immunohistochemical staining of NF-kB p65 in canine mammary tumors found that higher nuclear expression of NF-kB was correlated with larger tumor size, lymph node metastasis, and higher mitotic index (MI), while a correlation with distant metastasis nor cyclin D1 expression was not observed.[92] Martins et al. also observed an association between increased NF-kB activation and poorer prognosis in dogs with mammary cancer.[87]

Malignant Melanoma

In a study comparing the transcriptome of canine oral malignant melanoma in comparison with human disease, there was > 80% homology in upregulation of significant oncogenes, with activation of the JAK-STAT pathway being the most frequently upregulated pathway in both species. In addition, several target genes of NF-kB were upregulated, consistent with NF-kB activation, and binding motifs for NF-kB were observed in the highest number of upregulated differentially expressed genes (DEGs) in canine melanoma.[113]

Glioma

During transcriptome evaluation of canine oligodendroglioma tissues, Mitchell et al. found that IRX5, important for cancer cell survival, was among the top 10 upregulated genes relative to normal brain tissue.[91] While IRX5 has not been characterized in glioma, its overexpression has been found to contribute to NF-kB overactivation and interactions with osteopontin in (human) tongue squamous cell carcinoma.[58]

Osteosarcoma

Osteosarcoma is a malignant mesenchymal tumor affecting bones and soft tissues of dogs and humans; in dogs, it is the most common primary bone tumor and shares clinical and biological similarities to human cancer.[158,156]

As previously stated, increased SET protein levels in canine OS positively regulate NF-kB signaling secondary to decreased PP2A activity.[143,64]

Iyer et al. performed genome-wide RNAi screening in canine OS cells to identify genes correlated with aggressive features (growth and survival in anchorage-independent conditions) and found that TMIFGD3 (transmembrane and immunoglobulin domain containing 3) expression decreased cell sphere formation and downregulated NF-kB activity.[60]

Additionally, there is some interesting work demonstrating the effect of NF-kB overactivation within the tumor microenvironment in canine OS. Avnet et al. found that interstitial acidosis in canine OS is a microenvironmental condition that mimics wound healing and contributes to tumor cell proliferation via the release of mitogenic and chemotactic factors from reactive mesenchymal cells.[12] In subsequent work, this group evaluated the role of mesenchymal stem cells (MSC) in OS, and determined that co-culture with MSC previously incubated for 10 hours in an acidic environment enhanced OS tumorigenicity, mediated largely via MSC-stimulated activation of NF-kB.[8]

Prostate Cancer

The only non-human animal known to spontaneously develop prostate cancer is the dog, which makes dogs a good large animal model for this human disease.[129,82] AR-42 is a histone deacetylase inhibitor (HDACi) that inhibits the proliferation of several different cancer types. AR-42 upregulated PTEN and downregulated PI3K and NF-kB

expression in canine prostate cancer cells, leading to resistance to anoikis and repression of pro-apoptotic proteins.[35]

Studies including multiple cancer cell types

CIGB-552 is an anticancer peptide that induces expression of copper metabolism domain-containing protein 1 (COMMD), leading to ubiquitination of NF-kB RelA and cell death in cancer cell lines.[145,37] In a pilot clinical trial of CIBG-552, dogs with lymphoma (3), malignant melanoma (1), and mast cell tumor (1) experienced clinical benefit.[145]

Specific Aims and Project Rationale

The overarching goals of this project are to determine whether PTL may be a viable therapeutic for disseminated neoplasms in dogs and humans. Because some of these cancers are relatively more common in some dog breeds than in humans, this study may lay the groundwork for future clinical trials for PTL or other therapeutics that can exploit alteration of NF-kB activity in both species. To this end, the specific aims of this research are the following:

1. Characterize changes in NF-kB activity and redox balance in canine cell lines with PTL therapy.
2. Characterize NF-kB expression in spontaneous tumors in dogs, using both archived, formalin-fixed, paraffin-embedded tissues and primary lymphoma cells isolated from lymph node aspirates of dogs.

3. Characterize PTL's antitumor activity, both as a single agent, and in combination with other standard-of-care chemotherapeutics, in canine cell lines.
4. Develop a murine xenograft model of disseminated canine HS, then evaluate PTL alone, and in combination with lomustine/CCNU in this model.

References

1. Chapter 20 - Hematopoietic Cancers. In: Mak TW, Saunders ME, Jett BD, eds. *Primer to the Immune Response (Second Edition)*. Boston: Academic Cell; 2014:553-585.

2. Abegunde SO, Buckstein R, Wells RA, Rauh MJ. An inflammatory environment containing TNFα favors Tet2-mutant clonal hematopoiesis. *Exp Hematol*. 2018;59**:** 60-65.

3. Aggarwal BB. Nuclear factor-kappaB: the enemy within. *Cancer Cell*. 2004;6**:** 203-208.

4. Aggarwal BB, Shishodia S. Molecular targets of dietary agents for prevention and therapy of cancer. *Biochem Pharmacol*. 2006;71**:** 1397-1421.

5. Alizadeh AA, Eisen MB, Davis RE, et al. Distinct types of diffuse large B-cell lymphoma identified by gene expression profiling. *Nature*. 2000;403**:** 503-511.

6. Aresu L, Ferraresso S, Marconato L, et al. New molecular and therapeutic insights into canine diffuse large B-cell lymphoma elucidates the role of the dog as a model for human disease. *Haematologica*. 2019;104**:** e256-e259.

7. Avery AC. The Genetic and Molecular Basis for Canine Models of Human Leukemia and Lymphoma. *Front Oncol*. 2020;10. Review.

8. Avnet S, Di Pompo G, Chano T, et al. Cancer-associated mesenchymal stroma fosters the stemness of osteosarcoma cells in response to intratumoral acidosis via NF-κB activation. *Int J Cancer*. 2017;140**:** 1331-1345.

9. Bajaj S, Kumar MS, Peters GJ, Mayur YC. Targeting telomerase for its advent in cancer therapeutics. *Med Res Rev*. 2020;40**:** 1871-1919.

10. Balkwill F, Mantovani A. Inflammation and cancer: back to Virchow? *Lancet*. 2001;357**:** 539-545.

11. Bjelakovic G, Nikolova D, Gluud LL, Simonetti RG, Gluud C. Mortality in randomized trials of antioxidant supplements for primary and secondary prevention: systematic review and meta-analysis. *JAMA*. 2007;297**:** 842-857.

12. Bonuccelli G, Avnet S, Grisendi G, et al. Role of mesenchymal stem cells in osteosarcoma and metabolic reprogramming of tumor cells. *Oncotarget*. 2014;5**:** 7575-7588.

13. Bos JL. Ras oncogenes in human cancer: a review. *Cancer Res*. 1989;49**:** 4682-4689.

14. Brandão MM, Soares E, Salles TS, Saad ST. Expression of inducible nitric oxide synthase is increased in acute myeloid leukaemia. *Acta Haematol*. 2001;106**:** 95-99.

15. Buehler D, Rice SR, Moody JS, et al. Angiosarcoma outcomes and prognostic factors: a 25-year single institution experience. *Am J Clin Oncol*. 2014;37**:** 473-479.

16. Bushell KR, Kim Y, Chan FC, et al. Genetic inactivation of TRAF3 in canine and human B-cell lymphoma. *Blood*. 2015;125**:** 999-1005.

17. Cabello CM, Bair WB, 3rd, Lamore SD, et al. The cinnamon-derived Michael acceptor cinnamic aldehyde impairs melanoma cell proliferation, invasiveness, and tumor growth. *Free Radic Biol Med*. 2009;46**:** 220-231.

18. Cannon C, Borgatti A, Henson M, Husbands B. Evaluation of a combination chemotherapy protocol including lomustine and doxorubicin in canine histiocytic sarcoma. *J Small Anim Pract*. 2015;56**:** 425-429.

19. Caoimhe E, Alina N, Justin L, et al. Genomic profiling of primary histiocytic sarcoma reveals two molecular subgroups. *Haematologica*. 2020;105**:** 951-960.

20. Cassim S, Pouyssegur J. Tumor Microenvironment: A Metabolic Player that Shapes the Immune Response. *Int J Mol Sci*. 2020;21**:** 157.

21. Childress MO, Ramos-Vara JA, Ruple A. Retrospective analysis of factors affecting clinical outcome following CHOP-based chemotherapy in dogs with primary nodal diffuse large B-cell lymphoma. *Vet Comp Oncol*. 2018;16**:** E159-E168.

22. Choi J, Liu RM, Forman HJ. Adaptation to oxidative stress: quinone-mediated protection of signaling in rat lung epithelial L2 cells. *Biochem Pharmacol*. 1997;53**:** 987-993.

23. Chowdhury SKR, Gemin A, Singh G. High activity of mitochondrial glycerophosphate dehydrogenase and glycerophosphate-dependent ROS production in prostate cancer cell lines. *Biochem Biophys Res Commun*. 2005;333**:** 1139-1145.

24. Clifford CA, Mackin AJ, Henry CJ. Treatment of Canine Hemangiosarcoma: 2000 and Beyond. *J Vet Intern Med*. 2000;14**:** 479-485.

25. Cohen SM, Storer RD, Criswell KA, et al. Hemangiosarcoma in rodents: mode-of-action evaluation and human relevance. *Toxicol Sci*. 2009;111**:** 4-18.

26. Cook EK, Luo M, Rauh MJ. Clonal hematopoiesis and inflammation: Partners in leukemogenesis and comorbidity. *Exp Hematol*. 2020;83**:** 85-94.

27. Crowell JA, Steele VE, Sigman CC, Fay JR. Is Inducible Nitric Oxide Synthase a Target for Chemoprevention? *Mol Cancer Ther*. 2003;2**:** 815-823.

28. da Silva EZM, Jamur MC, Oliver C. Mast Cell Function: A New Vision of an Old Cell. *J Histochem Cytochem*. 2014;62**:** 698-738.

29. Dajee M, Lazarov M, Zhang JY, et al. NF-κB blockade and oncogenic Ras trigger invasive human epidermal neoplasia. *Nature*. 2003;421**:** 639-643.

30. Darwish NHE, Sudha T, Godugu K, et al. Novel Targeted Nano-Parthenolide Molecule against NF-kB in Acute Myeloid Leukemia. *Molecules*. 2019;24.

31. Davis RE, Brown KD, Siebenlist U, Staudt LM. Constitutive Nuclear Factor κB Activity Is Required for Survival of Activated B Cell–like Diffuse Large B Cell Lymphoma Cells. *J Exp Med*. 2001;194**:** 1861-1874.

32. Dervisis NG, Kiupel M, Qin Q, Cesario L. Clinical prognostic factors in canine histiocytic sarcoma. *Vet Comp Oncol*. 2017;15**:** 1171-1180.

33. Dickerson EB, Thomas R, Fosmire SP, et al. Mutations of Phosphatase and Tensin Homolog Deleted from Chromosome 10 in Canine Hemangiosarcoma. *Vet Pathol*. 2005;42**:** 618-632.

34. Dolcet X, Llobet D, Pallares J, Matias-Guiu X. NF-kB in development and progression of human cancer. *Virchows Arch*. 2005;446**:** 475-482.

35. Elshafae SM, Kohart NA, Altstadt LA, Dirksen WP, Rosol TJ. The Effect of a Histone Deacetylase Inhibitor (AR-42) on Canine Prostate Cancer Growth and Metastasis. *Prostate*. 2017;77**:** 776-793.

36. Enciso J ML, Álvarez-Buylla ER, Pelayo R. Dynamical modeling predicts an inflammation-inducible CXCR7+ B cell precursor with potential implications in lymphoid blockage pathologies. *PeerJ*. 2020.

37. Fernández Massó JR, Oliva Argüelles B, Tejeda Y, et al. The Antitumor Peptide CIGB-552 Increases COMMD1 and Inhibits Growth of Human Lung Cancer Cells. *J Amino Acids*. 2013;2013**:** 251398.

38. Galdiero MR, Marone G, Mantovani A. Cancer Inflammation and Cytokines. *Cold Spring Harb Perspect Biol*. 2018;10.

39. García-Piñeres AJ, Castro V, Mora G, et al. Cysteine 38 in p65/NF-kappaB plays a crucial role in DNA binding inhibition by sesquiterpene lactones. *J Biol Chem*. 2001;276**:** 39713-39720.

40. Garden OA, Volk SW, Mason NJ, Perry JA. Companion animals in comparative oncology: One Medicine in action. *Vet J*. 2018;240**:** 6-13.

41. Gardner HL, Fenger JM, London CA. Dogs as a Model for Cancer. *Annu Rev Anim Biosci*. 2016;4**:** 199-222.

42. Gaurnier-Hausser A, Patel R, Baldwin AS, May MJ, Mason NJ. NEMO-Binding Domain Peptide Inhibits Constitutive NF-κB Activity and Reduces Tumor Burden in a Canine Model of Relapsed, Refractory Diffuse Large B-Cell Lymphoma. *Clin Cancer Res*. 2011;17**:** 4661-4671.

43. Ghantous A, Sinjab A, Herceg Z, Darwiche N. Parthenolide: from plant shoots to cancer roots. *Drug Discov Today*. 2013;18**:** 894-905.

44. Ghasemi F, Shafiee M, Banikazemi Z, et al. Curcumin inhibits NF-kB and Wnt/β-catenin pathways in cervical cancer cells. *Pathol Res Pract*. 2019;215**:** 152556.

45. Ghosh A, Saginc G, Leow SC, et al. Telomerase directly regulates NF-κB-dependent transcription. *Nat Cell Biol*. 2012;14**:** 1270-1281.

46. Gilmore TD. Multiple mutations contribute to the oncogenicity of the retroviral oncoprotein v-Rel. *Oncogene*. 1999;18**:** 6925-6937.

47. Gilmore TD. The Re1/NF-kappa B/I kappa B signal transduction pathway and cancer. *Cancer Treat Res*. 2003;115**:** 241-265.

48. Griffin GK, Sholl LM, Lindeman NI, Fletcher CD, Hornick JL. Targeted genomic sequencing of follicular dendritic cell sarcoma reveals recurrent alterations in NF-κB regulatory genes. *Mod Pathol*. 2016;29**:** 67-74.

49. Guan J, Lo M, Dockery P, et al. The xc−cystine/glutamate antiporter as a potential therapeutic target for small-cell lung cancer: use of sulfasalazine. *Cancer Chemother Pharmacol*. 2008;64**:** 463.

50. Gustafson DL, Duval DL, Regan DP, Thamm DH. Canine sarcomas as a surrogate for the human disease. *Pharmacol Ther*. 2018;188**:** 80-96.

51. Guzman ML, Rossi RM, Neelakantan S, et al. An orally bioavailable parthenolide analog selectively eradicates acute myelogenous leukemia stem and progenitor cells. *Blood*. 2007;110**:** 4427-4435.

52. Hanahan D, Weinberg RA. Hallmarks of cancer: the next generation. *Cell*. 2011;144**:** 646-674.

53. Hawk MA, McCallister C, Schafer ZT. Antioxidant Activity during Tumor Progression: A Necessity for the Survival of Cancer Cells? *Cancers (Basel)*. 2016;8**:** 92.

54. Heasman SA, Zaitseva L, Bowles KM, Rushworth SA, Macewan DJ. Protection of acute myeloid leukaemia cells from apoptosis induced by front-line chemotherapeutics is mediated by haem oxygenase-1. *Oncotarget*. 2011;2**:** 658-668.

55. Hedan B, Thomas R, Motsinger-Reif A, et al. Molecular cytogenetic characterization of canine histiocytic sarcoma: A spontaneous model for human histiocytic cancer

identifies deletion of tumor suppressor genes and highlights influence of genetic background on tumor behavior. *BMC Cancer*. 2011;11**:** 201.

56. Hernández-Suárez B, Gillespie DA, Pawlak A. DNA damage response proteins in canine cancer as potential research targets in comparative oncology. *Vet Comp Oncol*. 2022;20**:** 347-361.

57. Hibi T, Nii H, Nakatsu T, et al. Crystal structure of gamma-glutamylcysteine synthetase: insights into the mechanism of catalysis by a key enzyme for glutathione homeostasis. *Proc Natl Acad Sci USA*. 2004;101**:** 15052-15057.

58. Huang L, Song F, Sun H, Zhang L, Huang C. IRX5 promotes NF-κB signalling to increase proliferation, migration and invasion via OPN in tongue squamous cell carcinoma. *J Cell Mol Med*. 2018;22**:** 3899-3910.

59. Huang S, Robinson JB, DeGuzman A, Bucana CD, Fidler IJ. Blockade of Nuclear Factor-κB Signaling Inhibits Angiogenesis and Tumorigenicity of Human Ovarian Cancer Cells by Suppressing Expression of Vascular Endothelial Growth Factor and Interleukin 8. *Cancer Res*. 2000;60**:** 5334-5339.

60. Iyer SV, Ranjan A, Elias HK, et al. Genome-wide RNAi screening identifies TMIGD3 isoform1 as a suppressor of NF-κB and osteosarcoma progression. *Nat Commun*. 2016;7**:** 13561.

61. Jaiswal S, Fontanillas P, Flannick J, et al. Age-Related Clonal Hematopoiesis Associated with Adverse Outcomes. *N Engl J Med*. 2014;371**:** 2488-2498.

62. Jamal R, Gale RE, Shaun N, Thomas B, Wheatley K, Linch DC. The retinoblastoma gene (rb1) in acute myeloid leukaemia: analysis of gene rearrangements, protein expression and comparison of disease outcome. *Br J Haematol*. 1996;94**:** 342-351.

63. Jeney V, Balla J, Yachie A, et al. Pro-oxidant and cytotoxic effects of circulating heme. *Blood*. 2002;100**:** 879-887.

64. Kake S, Tsuji S, Enjoji S, et al. The role of SET/I2PP2A in canine mammary tumors. *Sci Rep*. 2017;7**:** 4279-4279.

65. Kamiguti AS, Serrander L, Lin K, et al. Expression and Activity of NOX5 in the Circulating Malignant B Cells of Hairy Cell Leukemia. *J Immunol*. 2005;175**:** 8424-8430.

66. Karin M, Cao Y, Greten FR, Li Z-W. NF-κB in cancer: from innocent bystander to major culprit. *Nat Rev Cancer*. 2002;2**:** 301-310.

67. Karin M, Lin A. NF-κB at the crossroads of life and death. *Nat Immunol*. 2002;3**:** 221-227.

68. Kielbik M, Szulc-Kielbik I, Klink M. The Potential Role of iNOS in Ovarian Cancer Progression and Chemoresistance. *Int J Mol Sci*. 2019;20**:** 1751.

69. Kim J-H, Graef AJ, Dickerson EB, Modiano JF. Pathobiology of Hemangiosarcoma in Dogs: Research Advances and Future Perspectives. *Vet Sci*. 2015;2**:** 388-405.

70. Kim Y, Sengupta S, Sim T. Natural and Synthetic Lactones Possessing Antitumor Activities. *Int J Mol Sci*. 2021;22**:** 1052.

71. Kirpensteijn J, Kik M, Teske E, Rutteman GR. TP53 Gene Mutations in Canine Osteosarcoma. *Vet Surg*. 2008;37**:** 454-460.

72. Kleih M, Böpple K, Dong M, et al. Direct impact of cisplatin on mitochondria induces ROS production that dictates cell fate of ovarian cancer cells. *Cell Death Dis*. 2019;10**:** 851.

73. Knudsen ES, Nambiar R, Rosario SR, Smiraglia DJ, Goodrich DW, Witkiewicz AK. Pan-cancer molecular analysis of the RB tumor suppressor pathway. *Commun Biol*. 2020;3**:** 158.

74. Kojima K, Fujino Y, Goto-Koshino Y, Ohno K, Tsujimoto H. Analyses on activation of NF-κB and effect of bortezomib in canine neoplastic lymphoid cell lines. *J Vet Med Sci*. 2013;75**:** 727-731.

75. Kommalapati A, Tella SH, Durkin M, Go RS, Goyal G. Histiocytic sarcoma: a population-based analysis of incidence, demographic disparities, and long-term outcomes. *Blood*. 2018;131**:** 265-268.

76. Kumar B, Koul S, Khandrika L, Meacham RB, Koul HK. Oxidative Stress Is Inherent in Prostate Cancer Cells and Is Required for Aggressive Phenotype. *Cancer Res*. 2008;68**:** 1777-1785.

77. Kumar R, Khan SP, Joshi DD, Shaw GR, Ketterling RP, Feldman AL. Pediatric histiocytic sarcoma clonally related to precursor B-cell acute lymphoblastic leukemia with homozygous deletion of CDKN2A encoding p16INK4A. *Pediatr Blood Cancer*. 2011;56**:** 307-310.

78. Lamerato-Kozicki AR, Helm KM, Jubala CM, Cutter GC, Modiano JF. Canine hemangiosarcoma originates from hematopoietic precursors with potential for endothelial differentiation. *Exp Hematol*. 2006;34**:** 870-878.

79. Lee JL, Chang CJ, Chueh LL, Lin CT. Secreted frizzled related protein 2 (sFRP2) decreases susceptibility to UV-induced apoptosis in primary culture of canine mammary gland tumors by NF-kappaB activation or JNK suppression. *Breast Cancer Res Treat*. 2006;100**:** 49-58.

80. Lenardo MJ, Baltimore D. NF-κB: A pleiotropic mediator of inducible and tissue-specific gene control. *Cell*. 1989;58**:** 227-229.

81. Lenehan PF, Gutiérrez PL, Wagner JL, Milak N, Fisher GR, Ross DD. Resistance to oxidants associated with elevated catalase activity in HL-60 leukemia cells that

overexpress multidrug-resistance protein does not contribute to the resistance to daunorubicin manifested by these cells. *Cancer Chemother Pharmacol*. 1995;35**:** 377-386.

82. Leroy BE, Northrup N. Prostate cancer in dogs: comparative and clinical aspects. *Vet J*. 2009;180**:** 149-162.

83. Li Y, Zhou Q-L, Sun W, et al. Non-canonical NF-κB signalling and ETS1/2 cooperatively drive C250T mutant TERT promoter activation. *Nat Cell Biol*. 2015;17**:** 1327-1338.

84. Ling YH, Liebes L, Zou Y, Perez-Soler R. Reactive oxygen species generation and mitochondrial dysfunction in the apoptotic response to Bortezomib, a novel proteasome inhibitor, in human H460 non-small cell lung cancer cells. *J Biol Chem*. 2003;278**:** 33714-33723.

85. London CA, Bernabe LF, Barnard S, et al. Preclinical Evaluation of the Novel, Orally Bioavailable Selective Inhibitor of Nuclear Export (SINE) KPT-335 in Spontaneous Canine Cancer: Results of a Phase I Study. *PLoS One*. 2014;9**:** e87585.

86. Luo J-L, Kamata H, Karin M. IKK/NF-kappaB signaling: balancing life and death--a new approach to cancer therapy. *J Clin Invest*. 2005;115**:** 2625-2632.

87. Martins GR, Gelaleti GB, Moschetta MG, Maschio-Signorini LB, Zuccari DAPdC. Proinflammatory and Anti-Inflammatory Cytokines Mediated by NF-κB Factor as Prognostic Markers in Mammary Tumors. *Mediators Inflamm*. 2016;2016**:** 9512743.

88. Massoth LR, Hung YP, Ferry JA, et al. Histiocytic and Dendritic Cell Sarcomas of Hematopoietic Origin Share Targetable Genomic Alterations Distinct from Follicular Dendritic Cell Sarcoma. *Oncologist*. 2021;26**:** e1263-e1272.

89. Matsuda A, Tanaka A, Muto S, et al. A novel NF-κB inhibitor improves glucocorticoid sensitivity of canine neoplastic lymphoid cells by up-regulating expression of glucocorticoid receptors. *Res Vet Sci*. 2010;89**:** 378-382.

90. Mazzio EA, Soliman KF. In vitro screening for the tumoricidal properties of international medicinal herbs. *Phytother Res*. 2009;23**:** 385-398.

91. Mitchell D, Chintala S, Fetcko K, et al. Common Molecular Alterations in Canine Oligodendroglioma and Human Malignant Gliomas and Potential Novel Therapeutic Targets. *Front Oncol*. 2019;9. Original Research.

92. Mkaouar L, Endo Y, Jun HX, et al. Relationship between NF-kappaB Expression and Malignancy of Canine Mammary Gland Tumor Tissues. *J Vet Med Sci*. 2012;74**:** 713-718.

93. Mobaraki M, Faraji A, Zare M, Manshadi H. Molecular Mechanisms of Cardiotoxicity: A Review on Major Side-effect of Doxorubicin. *Indian J Pharm Sci*. 2017;79.

94. Mohammed SI, Utturkar S, Lee M, et al. Ductal Carcinoma In Situ Progression in Dog Model of Breast Cancer. *Cancers (Basel)*. 2020;12**:** 418.

95. Moirano SJ, Lima SF, Hume KR, Brodsky EM. Association of prognostic features and treatment on survival time of dogs with systemic mastocytosis: A retrospective analysis of 40 dogs. *Vet Comp Oncol*. 2018;16**:** E194-E201.

96. Moore PF. A Review of Histiocytic Diseases of Dogs and Cats. *Vet Pathol*. 2014;51**:** 167-184.

97. Morrison WB. Inflammation and Cancer: A Comparative View. *J Vet Intern Med*. 2012;26**:** 18-31.

98. Mosialos G. The role of Rel/NF-κB proteins in viral oncogenesis and the regulation of viral transcription. *Semin Cancer Biol*. 1997;8**:** 121-129.

99. Mudaliar M, Haggart R, Miele G, et al. Comparative Gene Expression Profiling Identifies Common Molecular Signatures of NF-κB Activation in Canine and Human Diffuse Large B Cell Lymphoma (DLBCL). *PLoS One*. 2013;8**:** e72591.

100. Murai A, Asa SA, Kodama A, Hirata A, Yanai T, Sakai H. Constitutive phosphorylation of the mTORC2/Akt/4E-BP1 pathway in newly derived canine hemangiosarcoma cell lines. *BMC Vet Res*. 2012;8**:** 128.

101. Nakagawa MM, Chen H, Rathinam CV. Constitutive Activation of NF-κB Pathway in Hematopoietic Stem Cells Causes Loss of Quiescence and Deregulated Transcription Factor Networks. *Front Cell Dev Biol*. 2018;6. Original Research.

102. Neelakantan S, Nasim S, Guzman ML, Jordan CT, Crooks PA. Aminoparthenolides as novel anti-leukemic agents: Discovery of the NF-κB inhibitor, DMAPT (LC-1). *Bioorg Med Chem Lett*. 2009;19**:** 4346-4349.

103. Ortega AL, Mena S, Estrela JM. Glutathione in cancer cell death. *Cancers (Basel)*. 2011;3**:** 1285-1310.

104. Pahl HL. Activators and target genes of Rel/NF-κB transcription factors. *Oncogene*. 1999;18**:** 6853-6866.

105. Panieri E, Santoro MM. ROS homeostasis and metabolism: a dangerous liason in cancer cells. *Cell Death Dis*. 2016;7**:** e2253-e2253.

106. Pardanani A. Systemic mastocytosis in adults: 2013 update on diagnosis, risk stratification, and management. *Am J Hematol*. 2013;88**:** 612-624.

107. Pawlak A, Kutkowska J, Obmińska-Mrukowicz B, Rapak A. Methotrexate induces high level of apoptosis in canine lymphoma/leukemia cell lines. *Res Vet Sci*. 2017;114**:** 518-523.

108. Pei S, Minhajuddin M, Callahan KP, et al. Targeting Aberrant Glutathione Metabolism to Eradicate Human Acute Myelogenous Leukemia Cells. *J Biol Chem*. 2013;288**:** 33542-33558.

109. Pelicano H, Carney D, Huang P. ROS stress in cancer cells and therapeutic implications. *Drug Resist*. 2004;7**:** 97-110.

110. Perez-Lanzon M, Zitvogel L, Kroemer G. Failure of immunosurveillance accelerates aging. *Oncoimmunology*. 2019;8**:** e1575117.

111. Perillo B, Di Donato M, Pezone A, et al. ROS in cancer therapy: the bright side of the moon. *Exp Mol Med*. 2020;52**:** 192-203.

112. Pidgeon GP, Harmey JH, Kay E, Costa MD, Redmond HP, Bouchier-Hayes DJ. The role of endotoxin/lipopolysaccharide in surgically induced tumour growth in a murine model of metastatic disease. *Br J Cancer*. 1999;81**:** 1311-1317.

113. Rahman MM, Lai YC, Husna AA, et al. Transcriptome analysis of dog oral melanoma and its oncogenic analogy with human melanoma. *Oncol Rep*. 2020;43**:** 16-30.

114. Ren X, Zhao B, Chang H, Xiao M, Wu Y, Liu Y. Paclitaxel suppresses proliferation and induces apoptosis through regulation of ROS and the AKT/MAPK signaling pathway in canine mammary gland tumor cells. *Mol Med Rep*. 2018;17**:** 8289-8299.

115. Richards KL, Motsinger-Reif AA, Chen H-W, et al. Gene Profiling of Canine B-Cell Lymphoma Reveals Germinal Center and Postgerminal Center Subtypes with Different Survival Times, Modeling Human DLBCL. *Cancer Res*. 2013;73**:** 5029-5039.

116. Rushworth SA, MacEwan DJ. HO-1 underlies resistance of AML cells to TNF-induced apoptosis. *Blood*. 2008;111**:** 3793-3801.

117. Sadowski AR, Gardner HL, Borgatti A, et al. Phase II study of the oral selective inhibitor of nuclear export (SINE) KPT-335 (verdinexor) in dogs with lymphoma. *BMC Vet Res*. 2018;14**:** 250.

118. Schiffman JD, Breen M. Comparative oncology: what dogs and other species can teach us about humans with cancer. *Philos Trans R Soc Lond B Biol Sci*. 2015;370**:** 20140231.

119. Seelig DM, Ito D, Forster CL, et al. Constitutive activation of alternative nuclear factor kappa B pathway in canine diffuse large B-cell lymphoma contributes to tumor cell survival and is a target of new adjuvant therapies. *Leuk Lymphoma*. 2017;58**:** 1702-1710.

120. Serasanambati M, Chilakapati SR. Function of Nuclear Factor Kappa B (NF-kB) in human diseases- A Review. *South Indian J Biol Sci*. 2016;2**:** 368.

121. Shacham S, Barnard S, Kisseberth W, et al. Results of a Phase I Dose Escalation Study of the Novel, Oral CRM1 Selective Inhibitor of Nuclear Export (SINE) KPT-335 in Dogs with Spontaneous Non-Hodgkin's Lymphomas (NHL). *Blood*. 2012;120**:** 161-161.

122. Shearin AL, Hedan B, Cadieu E, et al. The MTAP-CDKN2A locus confers susceptibility to a naturally occurring canine cancer. *Cancer Epidemiol Biomarkers Prev*. 2012;21**:** 1019-1027.

123. Shimizu K, Konno S, Ozaki M, et al. Dehydroxymethylepoxyquinomicin (DHMEQ), a novel NF-kappaB inhibitor, inhibits allergic inflammation and airway remodelling in murine models of asthma. *Clin Exp Allergy*. 2012;42**:** 1273-1281.

124. Shin H-J, Kwon H-K, Lee J-H, Anwar MA, Choi S. Etoposide induced cytotoxicity mediated by ROS and ERK in human kidney proximal tubule cells. *Sci Rep*. 2016;6**:** 34064.

125. Siwak DR, Shishodia S, Aggarwal BB, Kurzrock R. Curcumin-induced antiproliferative and proapoptotic effects in melanoma cells are associated with suppression of IkappaB kinase and nuclear factor kappaB activity and are independent of the B-Raf/mitogen-activated/extracellular signal-regulated protein kinase pathway and the Akt pathway. *Cancer*. 2005;104**:** 879-890.

126. Skorupski KA, Clifford CA, Paoloni MC, et al. CCNU for the Treatment of Dogs with Histiocytic Sarcoma. *J Vet Intern Med*. 2007;21**:** 121-126.

127. Smith PS, Zhao W, Spitz DR, Robbins ME. Inhibiting catalase activity sensitizes 36B10 rat glioma cells to oxidative stress. *Free Radic Biol Med*. 2007;42**:** 787-797.

128. Sorenmo KU, Baez JL, Clifford CA, et al. Efficacy and Toxicity of a Dose-Intensified Doxorubicin Protocol in Canine Hemangiosarcoma. *J Vet Intern Med*. 2004;18**:** 209-213.

129. Staal J, Beyaert R. Inflammation and NF-κB Signaling in Prostate Cancer: Mechanisms and Clinical Implications. *Cells*. 2018;7.

130. Stein SJ, Baldwin AS. Deletion of the NF-κB subunit p65/RelA in the hematopoietic compartment leads to defects in hematopoietic stem cell function. *Blood*. 2013;121**:** 5015-5024.

131. Strickland I, Ghosh S. Use of cell permeable NBD peptides for suppression of inflammation. *Ann Rheum Dis*. 2006;65 Suppl 3**:** iii75-iii82.

132. Sun S-C. Non-canonical NF-κB signaling pathway. *Cell Res*. 2011;21**:** 71-85.

133. Szatrowski TP, Nathan CF. Production of large amounts of hydrogen peroxide by human tumor cells. *Cancer Res*. 1991;51**:** 794-798.

134. Takada M, Smyth LA, Thaiwong T, et al. Activating Mutations in PTPN11 and KRAS in Canine Histiocytic Sarcomas. *Genes*. 2019;10**:** 505.

135. Taketomi A, Takenaka K, Matsumata T, et al. Circulating intercellular adhesion molecule-1 in patients with hepatocellular carcinoma before and after hepatic resection. *Hepatogastroenterology*. 1997;44**:** 477-483.

136. Taromi S, Lewens F, Arsenic R, et al. Proteasome inhibitor bortezomib enhances the effect of standard chemotherapy in small cell lung cancer. *Oncotarget*. 2017;8**:** 97061-97078.

137. Tate G, Suzuki T, Mitsuya T. Mutation of the PTEN gene in a human hepatic angiosarcoma. *Cancer Genet Cytogenet*. 2007;178**:** 160-162.

138. Thamm DH, Weishaar KM, Charles JB, Ehrhart III EJ. Phosphorylated KIT as a predictor of outcome in canine mast cell tumours treated with toceranib phosphate or vinblastine. *Vet Comp Oncol*. 2020;18**:** 169-175.

139. Thomsen LL, Miles DW. Role of nitric oxide in tumour progression: lessons from human tumours. *Cancer Metastasis Rev*. 1998;17**:** 107-118.

140. To MD, Rosario RD, Westcott PMK, Banta KL, Balmain A. Interactions between wild-type and mutant Ras genes in lung and skin carcinogenesis. *Oncogene*. 2013;32**:** 4028-4033.

141. Trachootham D, Alexandre J, Huang P. Targeting cancer cells by ROS-mediated mechanisms: a radical therapeutic approach? *Nat Rev Drug Discov*. 2009;8**:** 579-591.

142. Trachootham D, Zhou Y, Zhang H, et al. Selective killing of oncogenically transformed cells through a ROS-mediated mechanism by beta-phenylethyl isothiocyanate. *Cancer Cell*. 2006;10**:** 241-252.

143. Tsuji S, Ohama T, Nakagawa T, Sato K. Efficacy of an anti-cancer strategy targeting SET in canine osteosarcoma. *J Vet Med Sci*. 2019;81**:** 1424-1430.

144. Vail DM, Macewen EG. Spontaneously Occurring Tumors of Companion Animals as Models for Human Cancer. *Cancer Invest*. 2000;18**:** 781-792.

145. Vallespi MG, Rodriguez JC, Seoane LC, et al. The first report of cases of pet dogs with naturally occurring cancer treated with the antitumor peptide CIGB-552. *Res Vet Sci*. 2017;114**:** 502-510.

146. van de Stolpe A, Caldenhoven E, Stade BG, et al. 12-O-tetradecanoylphorbol-13-acetate- and tumor necrosis factor alpha-mediated induction of intercellular adhesion molecule-1 is inhibited by dexamethasone. Functional analysis of the human intercellular adhesion molecular-1 promoter. *J Biol Chem*. 1994;269**:** 6185-6192.

147. van Hogerlinden M, Rozell BL, Ahrlund-Richter L, Toftgård R. Squamous cell carcinomas and increased apoptosis in skin with inhibited Rel/nuclear factor-kappaB signaling. *Cancer Res*. 1999;59**:** 3299-3303.

148. Vilchis-Ordoñez A, Ramírez-Ramírez D, Pelayo R. The triad inflammation-microenvironment-tumor initiating cells in leukemia progression. *Curr Opin Physiol*. 2021;19**:** 211-218.

149. Wang C-Y, Cusack JC, Liu R, Baldwin AS. Control of inducible chemoresistance: Enhanced anti-tumor therapy through increased apoptosis by inhibition of NF-κB. *Nat Med*. 1999;5**:** 412-417.

150. Wang C-Y, Mayo MW, Baldwin AS. TNF- and Cancer Therapy-Induced Apoptosis: Potentiation by Inhibition of NF-κB. *Science*. 1996;274**:** 784-787.

151. Wang G, Wu M, Durham AC, et al. Molecular subtypes in canine hemangiosarcoma reveal similarities with human angiosarcoma. *PLoS One*. 2020;15**:** e0229728.

152. Wang G, Wu M, Maloneyhuss MA, et al. Actionable mutations in canine hemangiosarcoma. *PLoS One*. 2017;12**:** e0188667.

153. Webster GA, Perkins ND. Transcriptional Cross Talk between NF-κB and p53. *Mol Cell Biol*. 1999;19**:** 3485-3495.

154. Willmann M, Hadzijusufovic E, Hermine O, et al. Comparative oncology: The paradigmatic example of canine and human mast cell neoplasms. *Vet Comp Oncol*. 2019;17**:** 1-10.

155. Wirth KA, Kow K, Salute ME, Bacon NJ, Milner RJ. In vitro effects of Yunnan Baiyao on canine hemangiosarcoma cell lines. *Vet Comp Oncol*. 2016;14**:** 281-294.

156. Withrow SJ, Powers BE, Straw RC, Wilkins RM. Comparative Aspects of Osteosarcoma: Dog Versus Man. *Clin Orthop Relat Res*. 1991;270**:** 159-168.

157. Wondrak GT. Redox-Directed Cancer Therapeutics: Molecular Mechanisms and Opportunities. *Antioxid Redox Signal*. 2009;11**:** 3013-3069.

158. Wycislo KL, Fan TM. The Immunotherapy of Canine Osteosarcoma: A Historical and Systematic Review. *J Vet Intern Med*. 2015;29**:** 759-769.

159. Xu X, Sutak R, Richardson DR. Iron chelation by clinically relevant anthracyclines: alteration in expression of iron-regulated genes and atypical changes in intracellular iron distribution and trafficking. *Mol Pharmacol*. 2008;73**:** 833-844.

160. Yamamoto Y, Yin MJ, Lin KM, Gaynor RB. Sulindac inhibits activation of the NF-kappaB pathway. *J Biol Chem*. 1999;274**:** 27307-27314.

161. Yang J, Kantrow S, Sai J, et al. Ikk4a/Arf Inactivation with Activation of the NF-κB/IL-6 Pathway Is Sufficient to Drive the Development and Growth of Angiosarcoma. *Cancer Res*. 2012;72**:** 4682-4695.

162. Young RM, Phelan JD, Wilson WH, Staudt LM. Pathogenic B-cell receptor signaling in lymphoid malignancies: New insights to improve treatment. *Immunol Rev*. 2019;291**:** 190-213.

163. Zhang T, Feng X, Zhou T, et al. miR-497 induces apoptosis by the IRAK2/NF-κB axis in the canine mammary tumour. *Vet Comp Oncol*. 19(1):69-78

CHAPTER 2: PARTHENOLIDE AS A THERAPEUTIC IN CANINE NEOPLASIA

Overview

This study provides a unique translational research opportunity to help both humans and dogs diagnosed with diseases that carry dismal prognoses in both species: histiocytic sarcoma (HS), hemangiosarcoma (HSA), and disseminated mastocytosis (MCT). Although disseminated HS, MCT and visceral HSA are exceedingly rare diseases in humans, they are relatively more common in some dog breeds, giving us the opportunity to study this disease in a larger population than would otherwise be available. Because lymphoma is a common cancer affecting both dogs and humans and there is significant cross-species similarity, dogs are also an excellent model for lymphoma. Therapeutics evaluated in dogs with these diseases stand to benefit both canine and human patients.

Assays were performed to assess the therapeutic potential of parthenolide (PTL), a known canonical NF-kB signaling inhibitor with additional mechanisms of antineoplastic activity, including alteration of cellular redox balance. Growth inhibition assays were performed with canine cell lines and primary lymphoma cells isolated from canine patients, using PTL alone or in combination with redox-perturbing standard-of-care therapeutics. Cell death was assessed using flow cytometry. Immunofluorescence was used to assess NF-kB localization, western blot was used to assess NF-kB activity with and without PTL, and canine cells were transfected with a reporter gene cassette containing the NF-kB consensus sequence followed by firefly luciferase gene to study the effect of PTL on NF-kB-related luminescence. PTL's effects on glutathione and

reactive oxygen species generation were assessed with a colorimetric assay and a fluorescent H2DCFDA assay, respectively. Genetic expression changes were assessed with RNA sequencing of HS cells, with and without PTL treatment. A mouse model of disseminated HS was created with NF-kB luminescent cells to study the effect of PTL on this disease *in vivo*.

Canine cell lines and primary cells are sensitive to PTL and undergo dose-dependent apoptosis following exposure to drug. PTL exposure also leads to glutathione depletion, reactive oxygen species generation, and NF-kB inhibition in canine cells. Standard-of-care therapeutics broadly synergize with PTL. In two canine HS cell lines, genetic expression of NF-kB pathway signaling partners is downregulated with PTL therapy. Preliminary data suggest that PTL inhibits NF-kB activity of cells in a mouse model of disseminated HS.

Overall, these data support further investigation of compounds that can antagonize canonical and alternative NF-kB pathway signaling, which are overactivated in canine lymphoma, HS, HSA, and MCT disease. PTL is one promising therapeutic that acts, in part, via canonical NF-kB antagonism in canine neoplasms. Further investigation of this compound *in vivo* is underway in a mouse model of disseminated HS, and if this study is successful, it will provide strong justification for clinical trials with this compound in dogs.

Introduction

Parthenolide (PTL), a sesqueterpine lactone, is a secondary metabolite produced by many plants, but originally isolated from the aerial parts (shoots and leaves) of the

Feverfew plant (*Tanacetum parthenium*).[8] In the plant, it serves a defensive mechanism, and prevents predation by insects and animals by imparting a bitter flavor, and by compromising the cell walls of fungi and bacteria. Initially, this compound was used medicinally to treat a variety of inflammatory conditions, including osteoarthritis.[2] Its use is documented as early as 3,000 years ago in the Balkans.[23,8] Beginning in the 1970s, PTL began to gain recognition as an antineoplastic compound, and has been evaluated in a variety of hematopoietic and solid human tumors.[8,36] There are multiple ways in which PTL can selectively target cancer cells, while sparing normal cells from negative effects of the drug. These include NF-kB inhibition, altered cellular redox balance, tubulin carboxypeptidase inhibition, and DNA methyltransferase-1 (DNMT1) inhibition.[8]

As discussed in the first chapter, the NF-kB family of inducible transcription factors controls cytokine production, cell survival, and other important cell events, and especially plays a key role in regulating the innate immune response to infection. It is commonly overactive in cancer cells, leading to key features involved in tumorigenesis. Although many human tumors have been documented as having constitutively active NF-kB activity, this is less documented in dogs, although there is some literature (as reviewed in Chapter 1) that suggests constitutive NF-kB is also common in canine cancer. While evaluating PTL as an anti-leukemic drug in people, a small group of dogs with acute leukemia were treated with an orally bioavailable fumarate salt of PTL (dimethylamino-PTL, or DMAPT), and their cells demonstrated inhibition of constitutively active NF-kB signaling. This initial experiment laid the foundation for additional investigation of PTL's activity in dogs with cancer.

Dogs, as previously mentioned, are uniquely positioned as a natural animal of various human cancers, since pathology is often conserved between species and dogs share our environments. If comparative oncologic research is successful, its lessons can be used to improve therapeutic approaches and outcomes for both species. There are several hematopoietic neoplasms that are relatively more common in some dog breeds as compared to humans, and therefore, the opportunity to study natural populations with these diseases is greater in dogs. These include mast cell neoplasia, histiocytic sarcoma, and hemangiosarcoma. When these diseases are disseminated throughout the body, they are uniformly lethal in both dogs and humans. Objectives with this research were to 1) assess the sensitivity of canine cancer cell lines to PTL and determine whether this may be due to NF-kB inhibition and/or redox perturbation, 2) evaluate the potential sensitivity to PTL in patient-derived samples, and 3) evaluate PTL's effects in a canine xenograft *in vivo* model of disseminated histiocytic sarcoma.

Materials and methods

Cell lines and conditions

The canine cancer cell lines utilized in this study were generously provided by researchers at other institutions, purchased from the American Type Culture Collection (ATCC), or established from tumor samples in-house (**Table 2.1**). Cells were maintained in appropriate media for the cell line (RPMI 1640 for lymphoma, leukemia, and mast cell lines, and DMEM – or Dulbecco's minimum essential medium for all other cell lines). Media was supplemented with 1x MEM vitamin solution (Cellgro, Henderson,

VA), 2 mM L-glutamine (Cellgro), 1 mM sodium pyruvate (Cellgro), and 10% heat-inactivated fetal bovine serum (FBS) (Atlas, Fort Collins, CO). When cells reached 75% or greater confluency, they were passaged appropriately (with a sterile cell scraper for non-adherent cell lines or with trypsinization for adherent cells). Cells were incubated in a humidified atmosphere with 5% CO_2 at 37 degrees Celsius. Cell lines were authenticated via short tandem repeat analysis and a multispecies multiplex PCR assay (as previously described),[22] and confirmed to be mycoplasma-free prior to use in assays, except for primary HS cells derived from lung tissue (Lacy).

Table 2.1*:* Canine cell lines evaluated in this study.

CELL LINE NAME	CANCER TYPE	SOURCE	BREED
ANGUS	Bladder Transitional Cell Carcinoma	Tufts (E. McNiel)	Scottish Terrier
BLILEY	Bladder Transitional Cell Carcinoma	CSU (S. Dow)	Shetland Sheepdog
KINSEY	Bladder Transitional Cell Carcinoma	Tufts (E. McNiel)	Australian Shepherd
TYLER1	Bladder Transitional Cell Carcinoma	Tufts (E. McNiel)	Beagle
TYLER2	Bladder Transitional Cell Carcinoma	Tufts (E. McNiel)	Beagle
CH52	Hemangiosarcoma	CSU (D. Duval)	
CH58	Hemangiosarcoma	CSU (D. Duval)	
CINDY	Hemangiosarcoma		
DEN-HSA	Hemangiosarcoma	UWM (D. Thamm)	Golden Retriever
SB	Hemangiosarcoma	UWM (E. Dickerson)	German Shepherd
BD	Histiocytic Sarcoma	MSU (V. Yuzbasiyan-Gurkan)	
CSYN27	Histiocytic Sarcoma	CSU (D. Duval)	
DH82	Histiocytic Sarcoma	ATCC	Golden Retriever
NIKE / MH	Histiocytic Sarcoma	MSU (B. Kitchell)	Not collected
LACY LUNG	Histiocytic Sarcoma (Dendritic APC)	CSU (D. Thamm)	Bernese Mountain Dog
LACY BLOOD	Histiocytic Sarcoma (Dendritic APC)	CSU (D. Thamm)	Bernese Mountain Dog
MH588	Histiocytic Sarcoma	CSU (S. Dow)	
CLL1390	Leukemia	UCD (P. Moore)	Not collected
1771	Lymphoma	UPENN (K.A. Jeglum)	Not collected
CLBL1	Lymphoma	Aus (B. Rutgen)	Bernese Mountain Dog
OSW	Lymphoma	OSU (W. Kisseberth)	Not collected
CMT12	Mammary Carcinoma	AU (L. Wolfe)	Not collected

BRMCT	Mast Cell	UCSF (W. Gold)	Not collected
C2	Mast Cell	UCSF (W. Gold)	Not collected
17CM98	Melanoma	UWM (G. Hogge)	Not collected
CML-10C2	Melanoma	AU (L. Wolfe)	Not collected
CML-6M	Melanoma	AU (L. Wolfe)	Mixed Breed
JONES	Melanoma	CSU	Not collected
PARKS	Melanoma	CSU	Not collected
ABRAMS	Osteosarcoma	CSU/UWM	Not collected
D-17	Osteosarcoma	ATCC	Poodle
GRACIE	Osteosarcoma	UWM(E.G. MacEwen)	Not collected
HMPOS	Osteosarcoma	Tokyo	Mixed Breed
MACKINLEY	Osteosarcoma	CSU	Not collected
MORESCO	Osteosarcoma	UWM (E.G. MacEwen)	Not collected
OS2.4	Osteosarcoma	WSU (D. Kochevar)	Not collected
OSA8	Osteosarcoma	UM (J. Modiano)	Not collected
VOGEL	Osteosarcoma	CSU	Not collected
STSA-1	Soft Tissue sarcoma	UI (A. MacNeill)	Golden Retriever
CTAC	Thyroid Carcinoma	OSU	Boxer

AU: Auburn University. Aus: Veterinary University of Austria. CSU: Colorado State University. MSU: Michigan State University. OSU: The Ohio State University. Tokyo: University of Tokyo. UCSF: University of California San Francisco. UI: University of Illinois at Urbana-Champaign. UM: University of Minnesota. UPENN: University of Pennsylvania. UWM: University of Wisconsin-Madison. WSU: Washington State University.

Primary cells

Primary lymphoma cells were collected from lymph node aspirates of patients in the Flint Animal Cancer Center (FACC) at Colorado State University under an approved Colorado State University Veterinary Teaching Hospital Clinical Review Board protocol and with signed informed owner consent. Following collection, aspirated cells were placed in cell media. Following centrifugation of cells, any erythrocytes in suspension were lysed with ACK (Ammonium-Chloride-Potassium) buffer (Thermo-Fisher Scientific, Waltham, MA) prior to placement in RPMI 1640 C/10 media with 20% FBS and 50 ng/mL megaCD40L (Enzo Life Science, Plymouth Meeting, PA).[11]

Peripheral blood was collected from FACC patients, with approval by Colorado State University's IACUC. Peripheral blood mononuclear cells (PBMCs) were isolated using Lymphocyte Separation Medium (Sigma-Aldrich, St. Louis, MO) and standard methods. Briefly, peripheral blood was diluted with one volume of PBS and 2.5 mM EDTA in a 15 mL conical tube. LSM was gently added to the bottom of tube, and was centrifuged, without braking, for 15 minutes at 1,400 rpm. Following centrifugation, most plasma was gently removed using a serological pipette, and the PBMC layer was removed and placed in a new conical tube. Remaining blood components were discarded. The conical holding the PBMC layer was centrifuged at 1,400 rpm for 5 minutes, and the supernatant was discarded. If erythrocytes were evident in the remaining cell pellet (imparting a grossly pink to red color), they were lysed with 5 minutes of incubation with ACK lysis buffer.

With permission from animal owners, primary HS cells were collected from pleural effusion fluid, peripheral blood, and in one case, post-mortem lung tissue, following cytologic diagnosis of disease by the author. The effusion fluid and blood specimens were treated in the same fashion as primary lymphoma cells (with lysis of erythrocytes in ACK buffer for 5 minutes at room temperature prior to placement in C/10 media with 20% FBS). Immunocytochemistry was performed by the Leukocyte Antigen Laboratory at the University of California-Davis, to determine that cells of interest were of dendritic antigen presenting cell (APC) origin. Following initial documentation of HS cell sensitivity to PTL, cells were maintained in culture for four months from one patient to create two new canine HS cell lines.

Chemicals and antibodies

Parthenolide was obtained from Cayman Chemicals (Ann Arbor, MI) and was prepared as a 0.4 M stock solution, dissolved in dimethylsulfoxide (DMSO). Lomustine and toceranib were obtained from Selleck Chemicals (Houston, TX) and were prepared as a 50 mg/mL and 0.5 mg/mL stock solutions, respectively, dissolved in DMSO. Doxorubicin was obtained in a 2 mg/mL aqueous solution from the Veterinary Teaching Hospital pharmacy. Drug stocks were aliquoted and stored at -20 degrees Celsius, except for doxorubicin, which was stored in a -4-degree Celsius refrigerator. Antibodies used in this study are outlined in **Table 2.2**.

Table 2.2: Antibodies used in this study.

ANTIBODY CATALOG NUMBER	SOURCE	TARGET	NF-KB PATHWAY	DILUTION(S) USED
AB16502	Abcam	p65/RelA	Canonical	0.5 ug/mL (WB, ICC), 1:5,000 (IHC)
AB76302	Abcam	phospho p65/RelA	Canonical	1:10,000 (WB)
NB100-82063	Novus Biologics	p100/p52	Alternative	1:1,000 (WB), 1:200 (IHC)
AB133462	Abcam	phospho IKBa	Canonical	1:10,000 (WB)
AB76429	Abcam	IKBa	Canonical	1:2,500 (WB)
AB8227	Abcam	Beta-Actin	N/A	1:2,500 (WB)

Growth inhibition

For single agent evaluation with PTL, cells were plated in C10 at either 10,000 cells/well (non-adherent lymphoma and leukemia cell lines) or 2,000 cells/well in 100 µL of C/10 medium and allowed to adhere for 24 hours. Cells were then treated with 100 µL of media containing 2x of progressively decreasing PTL concentrations. After 72 hours, relative cell viability was determined using a fluorometric assay that detects

metabolically active cells (Alamar Blue™, Promega, Madison, WI), according to manufacturer instructions. Relative cell viability was expressed as a percentage of vehicle control-treated cells. Cellular viability was normalized to the mean of four vehicle control wells containing DMSO equivalent to the maximum concentration of PTL used in the assay. The IC50 was determined mathematically using non-linear curve fitting with the “log(inhibitor) vs. response” function in Prism v9 software (GraphPad, La Jolla, CA).

Immunocytochemistry

Cells were grown to near confluence in (~90%) in T25 culture flasks and were treated with DMSO (vehicle control) or 7.5 μM PTL for 6 hours. Cells were harvested (via cell scraping or trypsinization, as appropriate), then washed with PBS. Following this, cells were suspended in PBS at a concentration of 400,000 cells/0.4 mL and were cytocentrifuged in Cytofuge Stat Spinfor 5 minutes at 1,400 RPM. Extraneous PBS was discarded, and slides were allowed to air dry for five minutes prior to fixation with 4% paraformaldehyde. Cells were permeabilized in 1% Triton X-100 in PBS, then were blocked with 10% fetal bovine serum (FBS) and 1% bovine serum albumin (BSA) in PBST (PBS + 0.01% Tween 20). Antibodies were diluted in PBST + 0.1% BSA. Slides were incubated overnight with primary antibody at 4 degrees Celsius in a humidified environment. The following day, slides were incubated with secondary antibody for 1 hour at room temperature in the dark. Slides were kept in a dark, 4-degree Celsius environment prior to imaging with an Olympus IX83 confocal microscope. Slides with an isotype control antibody and without primary antibody were used as negative controls for the experiment.

NF-kB reporter cell line assays

Hygromycin resistance was determined experimentally for three HS cell lines: DH82, NIKE, and MH588. Cell lines were transfected using electroporation (Electro Square Porator™ 830, BTX, Holliston, MA) and the pGL4.32[*luc2P*/NF-κB-RE/Hygro] Vector, which contains five copies of an NF-κB response element (NF-κB-RE) that drives transcription of the luciferase reporter gene *luc2P* (*Photinus pyralis*). Following selection with hygromycin (150-250 ug/mL, depending on the cell line) for 2 weeks, cells were grown to 75% confluency in black-bottomed, 96-well plates (Corning), then treated in triplicate with serially diluted concentrations of PTL. Cells were treated with 1:200, 30 mg/mL luciferin, followed by imaging with the IVIS. Luminescence of each well was measured as a percentage of the luminescence observed in vehicle control (DMSO-treated wells). Experiments were repeated three times to generate the luminescence-inhibition curves that are shown in this work.

Differential expression of genes in cell lines that are relatively sensitive or resistant to PTL

RNA sequencing gene expression data (counts and relative $\log_2$-FPKM) for 32 canine cancer cell lines were generously provided by Drs. Sunetra Das and Dawn Duval, and R code to determine differentially expressed genes was provided by Dr. Kathryn E. Cronise. Differentially expressed genes associated with PTL sensitivity were identified with DESeq2. Correlation with PTL logIC50 values was determined using Pearson correlations between z-score normalized CPM expression and PTL logIC50

values, requiring a Benjamini and Hochberg false discovery rate less than 0.05. **Table 2.3** below defines the most sensitive (IC50 < 5 μM PTL) or resistant cell lines (IC50 > 50 μM PTL), for the purposes of this analysis.

Table 2.3: Cell lines defined as sensitive and resistant for differential expression analysis.

CELL LINE	TYPE	PTL	IC50
OS2.4	Osteosarcoma	Sensitive	1.19
CTAC	Thyroid	Sensitive	1.89
CINDY	Hemangiosarcoma	Sensitive	3.16
DEN-HSA	Hemangiosarcoma	Sensitive	3.18
CLBL1	Lymphoma	Sensitive	3.89
CML-10C2	Melanoma	Sensitive	4.23
JONES	Melanoma	Sensitive	4.29
CMT12	Mammary Tumor	Resistant	79.39
MORESCO	Osteosarcoma	Resistant	94.73
STSA-1	Soft Tissue Sarcoma	Resistant	106.93
D-17	Osteosarcoma	Resistant	130.24

RNA Sequencing

DH82 HS cells were plated to 50% confluency in T75 culture flasks and allowed to adhere overnight. Cells were treated with 10 μM PTL or vehicle in triplicate for 24 hours, then washed and trypsinized. Following a wash with PBS, RNA was extracted from cells using the RNEasy Mini Kit (Qiagen, Germantown, MD). Sequencing was performed by Novogene (Sacramento, CA). Data analysis was performed with assistance from Dr. Sunetra Das. Briefly, low quality reads were removed with trimmomatic, and hisat2 was used to align reads to the canine reference genome. featureCounts was used to tabulate the number of reads per gene, then DESeq2 was used to identify differentially expressed genes.

RT-qPCR

Primers were designed using Primer-BLAST. Primers were designed to generate amplicons between 70-200 bp, intron-spanning, with 50-60% GC content, and to have melting temperatures between 57 and 63 degrees Celsius. Primers were ordered from Integrated DNA Technologies (IDT, Coralville, IA, **Table 2.4**).

Table 2.4: Primers used for RT-qPCR experiments. HO = heme oxygenase.

NAME	SEQUENCE	PRIMER PAIR EFFICIENCY	TM (DEGREES CELSIUS)	GC CONTENT
HO_1F	CAG CAG AGC ACA AGA CTC GAC	94.70%	58.0	57.1
HO_1R	CAC CGT TGC CAC CAA AAA GC		58.0	55.0
TNFAIP6_3F	GCT ACA ACC CAC ATG CAA AGG	99.36%	56.9	52.4
TNFAIP6_3R	ACA TAG TCA GCC AAG CAG GC		57.7	55.0
HPRT_F	ACT TTG CTT TCC TTG GTC AGG CAG	97.74%	59.9	50.0
HPRT_R	GGC TTA TAT CCA ACA CTT CGT GGG		57.6	50.0

Primers were centrifuged briefly to ensure the lyophilized primer was at the bottom of the tube. Primers were dissolved in nuclease-free water to achieve an end concentration of 100 μM. Primers were stored at -20 degrees Celsius when not in use. RNA was isolated using the RNeasy Mini Kit, as previously described. RNA quantity was measured using the Nanodrop, and quality was verified prior to cDNA synthesis. cDNA synthesis was performed using the QuantiTect Reverse Transcription Kit (Qiagen, Valencia, CA), and a no reverse transcriptase (no RT) control was made for each sample. cDNA quantity and quality were determined with the Nanodrop, and cDNA was diluted to a concentration of 12.5 ng/μL in nuclease-free water. Primer pairs were validated using serially diluted cDNA (50-0.04 ng) in addition to no RT controls. qPCR was performed with duplicate samples with denaturation at 95 degrees Celsius for 10 minutes, followed by 40 cycles of 30 seconds at 95 degrees Celsius (melting) and 60

seconds at 60 degrees Celsius (annealing and elongation) using the iQ SYBR Green Supermix kit (Bio-Rad, Hercules, CA) with 100 nM forward primer and 300 nM reverse primer in 25 µL reactions on the Stratagene Mx3000P instrument. Validated primers were defined as having an amplification efficiency of 90-110% with a standard curve R^2 value of >0.98 and replicates within 0.5 C_T. Dissociation curves were evaluated to determine whether the amplicon was likely to be a single product. qPCR was run using 50 ng of RNA and one primer pair for HPRT (housekeeping gene) for normalization. Relative gene expression was determined using the delta delta CT (or ddCT) method, as previously described.[18]

nCounter Canine IO (Immuno-oncology) Panel

DH82 and MH588 HS cells were treated (four technical replicates) with 10 µM PTL for 6 hours. Cells were harvested and RNA was extracted with an RNEasy Mini Kit (Qiagen, Germantown, MD). RNA quantity and quality were evaluated with a Nanodrop analyzer. Three samples from each group were selected (based on RNA quantity and quality) for downstream analysis. Nanostring sequencing for the 800-gene Canine Immuno-oncology panel (Canopy Biosciences, St. Louis, MO) was performed at the University of Arizona (Tucson, AZ). Data were analyzed with nCounter software (Canopy Biosciences, St. Louis, MO), using the Advanced Analysis module, and standard normalization methods included with the software

Flow cytometry

Apoptosis was assessed using the Pacific Blue™ Annexin V Apoptosis Detection Kit with PI (BioLegend, San Diego, CA). Flow cytometry was performed using a Beckman Coulter Gallios flow cytometer. Analysis was performed with FlowJo software (FlowJo LLC, Ashland, OR).

Electrophoretic Mobility Shift assay (EMSA)

Cells were grown to ~75% confluence in T175 culture flasks, then were incubated for 6 hours with vehicle control (DMSO) or 7.5 μM PTL. Following treatment, cells were collected (via scraping for BrMCT and Osw, and via trypsinization for DH82 HS cells), washed, and pelleted. Cells were snap frozen with liquid nitrogen, then shipped on dry ice to Dr. Craig Jordan's laboratory at CU Anschutz for performance of the EMSA, as previously described.[25,10]

H2DCFDA (ROS) assay

Cells were collected (via cell scraping or trypsinization, as appropriate), counted, and resuspended in 8 mL of 10% PBS with 10% FBS (X concentration of cells used). Five replicate wells of unstained cells from each cell line, or from PBMCs, were pipetted into a 96-well, black-bottomed plate. The remaining cells were treated with 5 μM H2DCFDA at 37 degrees Celsius in the dark for 45 minutes. Following incubation, cells were washed with PBS, and then resuspended at original concentration in PBS with 10% FBS. Most cells were incubated for an additional hour in the dark while one aliquot of cells was pre-treated with 2 mM N-Acetylcysteine. This aliquot of cells was washed with PBS three times prior to treatment with 15 μM PTL. The remaining cell aliquots

were then treated with vehicle control (0.26% DMSO, to mirror the 15 μM PTL concentration that was used), various doses of PTL, or Luperox (a positive control for the assay at 10 μL/1 mL). Cells were plated in five replicate wells in the aforementioned 96-well black-bottomed plate. Fluorescence of the DCF (2',7'-dichlorofluorescein) was detected with a Biotek synergy HT plate reader (Santa Clara, CA) over five hours (excitation 485 nm / emission 535 nm).

Glutathione quantification assay

A glutathione reductase-DTNB recycling microtiter plate assay was performed as previously described to measure total glutathione and glutathione disulfide (GSSG).[34] Briefly, cells treated with various concentrations of PTL, 2 mM NAC pretreatment followed by PTL, or Buthionine sulphoximine (BSO, a positive control for the assay). Diluted HCl (10 mmol/L) was used to lyse cells, followed by protein measurement (BCA assay) and subsequent protein removal via centrifugation in 1.3% sulfosalicylic acid. Lysed cell supernatant was combined with a reaction mixture (0.7 mmol/L DTNB or Ellman's reagent, 1.2 IU/mL GSSG-reductase, and 0.24 mmol/L NADPH) prior to mixing and kinetic measurement of absorbance at 415 nm over 2 minutes. For measurement of GSSG, cell lysates were treated with 2-vinypyridine for GSH derivatization, and the procedure was largely the same as for GSH, except that 2x concentrations of blanks, standards, and samples were used for measurement.

Migration and Invasion assays

0.1 x 10^6 HS cells were plated in 100 µL of serum-free DMEM media in a 24-well Boyden chamber plate with 3 µL pore diameter cell culture inserts (Falcon, Corning, NY). Following adherence of cells to the well overnight, cells were treated in duplicate with DMSO vehicle control, 7.5 µM PTL, or 15 µM PTL. Two control wells were left untreated as cell viability controls. Cells were allowed to migrate for 20 hours post-treatment. At experiment completion, cells that had not migrated were removed, wells were washed, and lower compartment wells were fixed with 4% paraformaldehyde for 10 minutes on ice, stained with 3% crystal violet (Sigma-Aldrich, St. Louis, MO), rinsed with distilled water, and allowed to air-dry overnight. Membranes were then cut from the cell culture inserts, then mounted on Superfrost Plus glass slides with immersion oil. Five 400x fields per membrane were counted, and the mean number of cells per field was determined for each membrane.

Western blot

CLBL1 (Lym), C2 (MCT), DH82 (HS), and SB cells were plated at ~50% confluency in T25 flasks with C/10 media 24 hours prior to treatment. The following day, cells were washed with PBS, and treated with vehicle control for 15 µM PTL (0.013% DMSO in C/10 media), 7.5 µM PTL, or 15 µM PTL for 6 hours. Following treatment, cells were collected either via cell scraping (CLBL1, C2 cells) or trypsinization (DH82, SB), as appropriate. For DH82 and SB, cells were washed with PBS and then exposed to 1 mL trypsin for 5 minutes to detach them from the culture plate. 2 mL C/10 media were added to neutralize trypsin. Collected cells were centrifuged at 1,400 rpm for 5 minutes. The trypsin/media supernatant was removed from pelleted cells, and cell

pellets were resuspended in 1 mL PBS in a 1.5 mL Eppendorf tube. Cells were then centrifuged at 10,000 rpm at 4 degrees Celsius for 5 minutes. After discarding the PBS supernatant, cells were homogenized with 150 µL of buffer containing M-PER protein extraction reagent (Pierce), 1 mM $NaVO_4$, 1 mM PMSF, Complete Mini Protease Inhibitor (Roche), and 1% SDS. The cell homogenate was placed on ice for 10 minutes, and lysates were passed through a 25-gauge needle 5 times. Following centrifugation at 10,000 rpm at 4 degrees Celsius for 5 minutes, the supernatant was used to measure cellular protein concentrations, using the BCA protein kit (Bichinchoninic Acid kit, Pierce, Rockford, IL). For evaluation of NF-kB p65 and IKBa expression, 25-30 ug samples of cells were electrophoresed into a denaturing 4-12% Bis-Tris gel (Invitrogen, Carlsbad, CA), and were transferred electrophoretically to a polyvinylidene difluoride (PVDF) membrane. Membranes were blocked with SuperBlock™ (PBS) Blocking Buffer (Thermo Fisher Scientific, Waltham, MA) for one hour at room temperature, followed by incubation of primary antibody (as indicated in **Table 2.2**) overnight on a rocker, in blocking solution at 4 degrees Celsius. After three washes in TBST, membranes were incubated in a 1:20,000 dilution of HRP-conjugated goat anti-rabbit IgG for 1 hour at room temperature. Immunoreactive proteins were detected using SuperSignal® West Pico Chemiluminescent Substrate (Pierce) and was analyzed via autoradiography. In between evaluation for phospho-proteins and total protein/loading control expression, blots were stripped for ten minutes on a rocker at room temperature, with Restore™ Stripping Buffer, followed by three washes in TBST. Antibodies for total NF-kB p65 and IKBa were incubated overnight at 4 degrees Celsius, followed by incubation with secondary antibody, as previously described. Beta-Actin was used as a loading control;

this antibody was incubated for 1 hour at room temperature followed by incubation with secondary antibody, as previously described. Relative band intensity was measured in ImageLab computer software (Bio-Rad Laboratories, Hercules, CA).

Xenograft model creation

6–8-week-old, female nude mice were purchased from Envigo Laboratories (Indianapolis, IN), and 6–8-week-old, female Balb/c-scid, NOD/scid, and NOD/scid-gamma mice were purchased from Jackson Laboratory (Bar Harbor, ME). All animals were housed in microisolator cages in Colorado State University's laboratory animal housing facilities, and all procedures were approved by the Institutional Animal Care and Use Committee (IACUC) at Colorado State University. Prior to experimentation, mice were allowed to adjust to their new environment for one week. Mice were identified with ear tags. Prior to imaging involving tumor luminescence, mice were injected with 3 mg (0.1 mL of 30 mg/mL) luciferin subcutaneously in the scruff and were anesthetized with 3% isoflurane in an induction box. Mice were imaged five minutes post-injection in the IVIS® 200 Spectrum Imager (PerkinElmer, Akron, OH). When relevant, DMAPT was delivered at 100 mg/kg in ddH_2O via oral gavage, as has been done previously. Pharmacokinetically, this dose achieves a maximum concentration (C_{max}) of 25 μM, with a half-life of 0.63 hours in serum.[10] Mouse were weighed 3 times weekly. Criteria for humane euthanasia, as outlined in our IACUC protocol, included growth of subcutaneous tumors >10 mm in maximal diameter, >15% body weight loss, weakness, ascites, and/or dyspnea.

Statistical analysis

All data are expressed as means +/- SD, unless otherwise noted. Statistical analyses were performed using Prism v9 software.

Results

1. Sensitivity of canine tumor cell lines to parthenolide

1a: Broad characterization of PTL's effects across all cell lines in the FACC collection

Initially, eight hematopoietic cell lines were tested for their sensitivity to PTL, which were evaluated following analysis of 72-hour growth inhibition curves. Following promising results on this initial study, with inhibitory concentration 50 (IC50) values of 4-23 micromolar. Based on previous pharmacokinetic studies of the drug in dogs, in which oral dosing of 100 mg/kg dimethyl-aminoparthenolide (DMAPT) yielded a C_{max} of 61 μM and a serum half-life of 1.9 hours,[10] the biologically achievable dose of PTL in dogs is thought to be ~15 μM. Most of these initially screened cell lines had IC50s that were below or near his biologically relevant dose. Based on these promising data, the study was expanded to include a larger number of cell lines from Colorado State University (CSU) and from other sources. Most cell lines (30/40 or 75%) were sensitive to PTL at single-agent doses, and only 4/40 or 10% of cell lines appeared resistant to this drug (79-130 micromolar; **Figures 2.1, 2.2, and 2.3**).

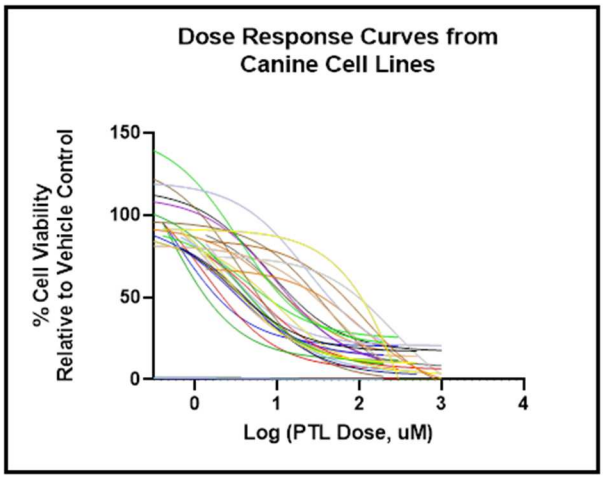

Figure 2.1 - Dose response curves for canine cell lines treated with PTL (Prism software).

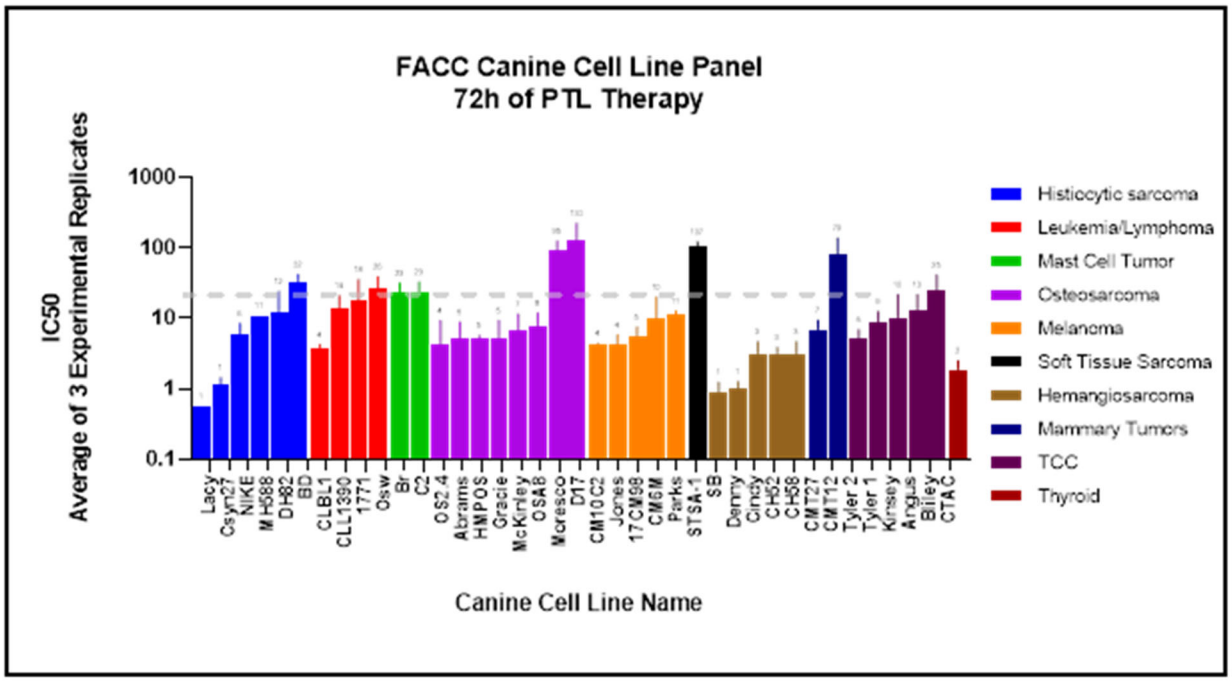

Figure 2.2: Bar graph showing the IC50 (determined using Prism software from dose response curves above) for canine cell lines. The dotted, gray line represents the biologically achievable concentration of PTL in a canine patient (15 μM). Error bars are the standard deviation of the IC50, as determined over three experimental replicates.

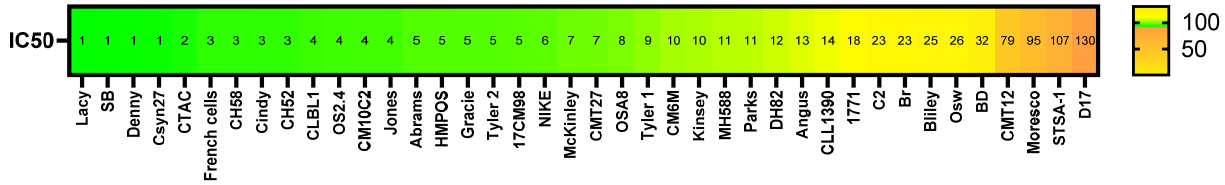

Figure 2.3: An alternative summary graphic that highlights the sensitivity of most canine cell lines to PTL. Cell lines with green coloration are sensitive at single agent dose concentrations. Less sensitive cell lines are in yellow, and the most resistant cell lines are colored in orange.

To determine potential drivers of PTL resistance versus sensitivity in canine cell lines, whole exome data were analyzed. Cells with an IC50 of >20 μM were designated "resistant," while those with an IC50 of <5 μM were designated "sensitive." Differentially expressed genes between these data sets were determined (**Table 2.5**). 2/13 differentially expressed genes are known downstream targets of NF-kB signaling.[35,33] This list of differentially expressed genes was then evaluated with the "Investigate Gene Sets" module from Gene Set Enrichment Analysis (GSEA), for which the "Hallmark" set of genes was most informative (**Table 2.6**). Several genes in the Epithelial to mesenchymal transition set are downstream of NF-kB signaling, as is one gene in the estrogen response pathways.[31]

Table 2.6: GSEA Hallmarks pathways that are upregulated in canine cell lines that are more sensitive to PTL. Although only low numbers of canine genes were differentially expressed in this analysis, their concurrent differential expression was statistically significant, as shown below. All pathways do contain genes that are known targets of NF-kB signaling.

Gene set name	*# of genes*	*p-value*	*FDR q-value*
Estrogen Response – Late	5	$8.91\ e^{-5}$	$4.45\ e^{-3}$
Epithelial to mesenchymal transition	4	$1.07\ e^{-3}$	$1.79\ e^{-2}$
Estrogen Response – Early	4	$1.07\ e^{-3}$	$1.79\ e^{-2}$

1b: Further characterization of canine cell line responses to PTL

In selecting tumor cell lines for further characterization, those of hematopoietic origin were prioritized, since these have been shown, in human medicine, to commonly have constitutively active NF-kB activity.[3,29] In addition, if these experiments were successful and PTL was deemed a promising anti-neoplastic compound for canine diseases, some of the neoplasms selected (MCT, HS) would be excellent candidates as models of deadly, orphan diseases in humans.[9,12,16] To this end, in noting that hemangiosarcoma (HSA) is exquisitely sensitive to PTL, and since canine HSA has the potential to be an excellent model of visceral angiosarcoma in humans, an HSA cell line was also included in downstream analyses.

To ascertain whether growth inhibition was due to apoptosis or cell cycle inhibition, dual color flow cytometry for Annexin V and PI was performed, as well as cell cycle analysis (**Figure 2.4**). All hematopoietic cell lines evaluated underwent dose-dependent apoptosis over 24 hours. To assess whether some cellular apoptosis could be prevented by pre-treatment with an antioxidant, cells were treated for 1-hour prior to drug with 2 mM N-Acetylcysteine. All cells pre-treated with antioxidant, followed by PTL, demonstrated a decreased proportion of cells undergoing apoptosis, to varying degrees. CLBL1 exhibited G1 cell cycle arrest, while other cell lines exhibited only an increase in the Sub-G1 fraction, indicative of cellular fragmentation/apoptosis.

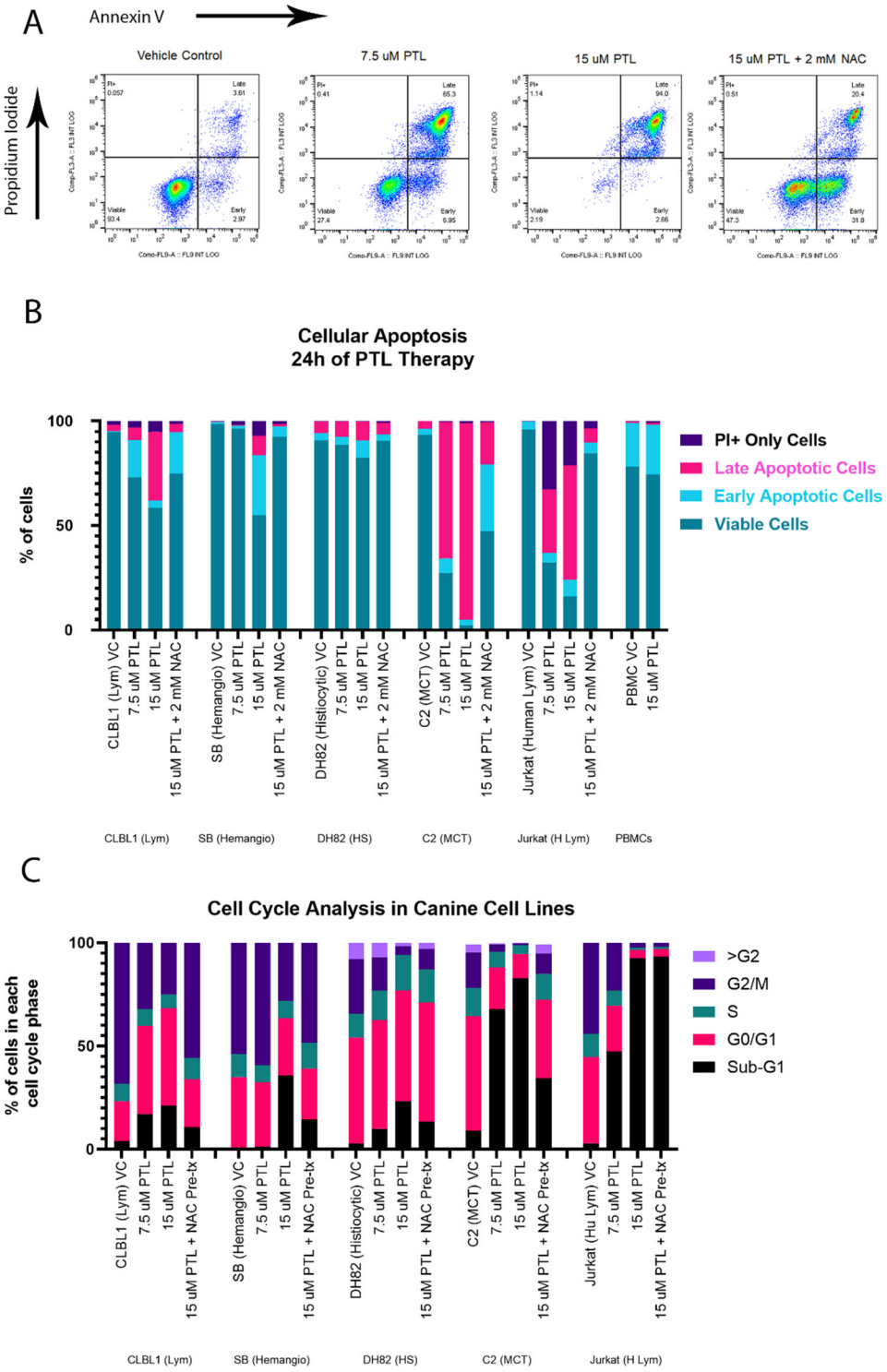

Figure 2.4: A: Dot plots showing raw flow cytometer output from the dual-color apoptosis assay. The signal for Annexin V is on the X axis, while signal for propidium iodide (nuclear stain) is on the Y axis. Viable cells are in the lower left corner, cells experiencing early apoptosis are in the bottom right, and late apoptotic cells are in the upper right-hand corner. In this example cell line (C2 MCT), there is a dose-dependent increase in the number of apoptotic cells following PTL

treatment. Pre-treatment of cells with 2 mM N-Acetylcysteine decreases the numbers of apoptotic cells. B: Assays were performed twice, and the output shown is a representative summary from one experiment. Stacked column graph showing that all cell lines experience dose-dependent apoptosis with PTL, but that normal, mononuclear cells isolated from dogs without hematopoietic cancer undergo only slight apoptosis with PTL therapy. C: Assays were performed twice, and the output shown is a representative summary from one experiment. Stacked column graph showing percentages of cells in each cell cycle with PTL treatment. Most cell lines have a significant increase in the Sub-G1 population with PTL treatment, consistent with apoptosis. Only CLBL1 (Lym) also exhibits G1 cell cycle arrest.

1c: NF-kB signaling in selected canine cells treated with parthenolide

Following the documentation of PTL-induced apoptosis in several canine cell lines, evaluation for cellular NF-kB activity was performed. With aid from a collaborator at the University of Colorado (Dr. Mohammad Minhajuddin), Anschutz campus, an EMSA (electrophoretic mobility shift assay) was performed, which demonstrated constitutive NF-kB activity in the DH82 HS cell line **(Figure 2.5).** Two other cell lines tested, Osw (a T cell lymphoma), and BrMCT (a mast cell tumor), did not demonstrate constitutive NF-kB activity. Based on a copyright issue in using the Osw, and some question as to the identity of the BrMCT cell line, we ultimately pursued further characterization of alternative canine hematopoietic cell lines, C2 (mast cell tumor) and CLBL1 (B cell lymphoma).

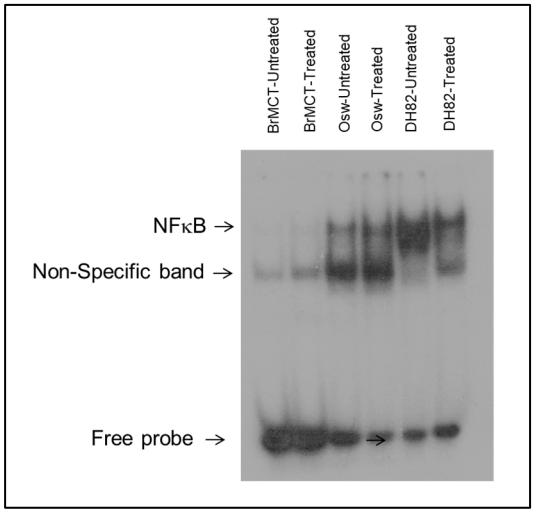

Figure 2.5: Electrophoretic mobility shift assay. Three cell lines of multiple types were included for characterization of NF-kB RelA:DNA binding: BrMCT, Osw (T cell lymphoma), and DH82 (HS). Of these three cell lines, DH82 exhibited strong RelA:DNA binding, consistent with constitutive activation of the canonical signaling pathway. This binding was markedly decreased following treatment with 7.5 μM PTL for 6 hours, as shown. The other two cell lines did not exhibit a marked difference in RelA:DNA binding.

Next, evaluation of NF-kB activity was performed via western blot. Phosphorylation of serine 536 has been associated with transcriptional activation of RelA/p65, but because another study has also shown phosphorylation of serine 536 to ultimately limit NF-kB activity, presumably to prevent subsequent deleterious inflammation,[26,19,21] evaluation of IKBa S36 phosphorylation was also performed. S36 is one of two critical serine residues on IKBa that is necessary for ubiquitination and subsequent degradation of IKBa in the 26S proteasome.[20] Results from these experiments (two replicates per cell line) are shown in **Figure 2.6.**

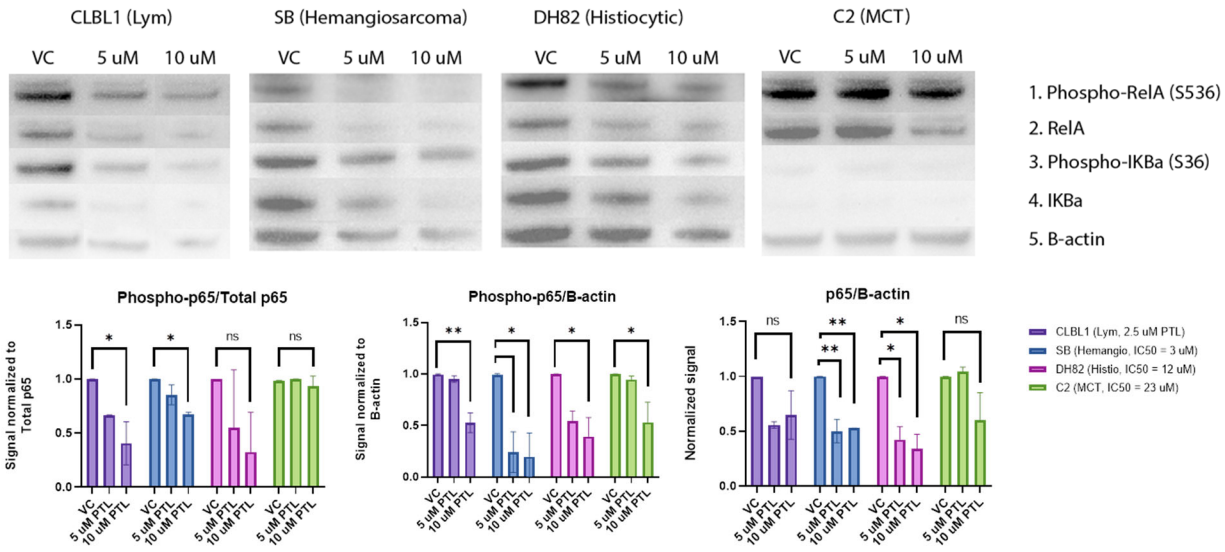

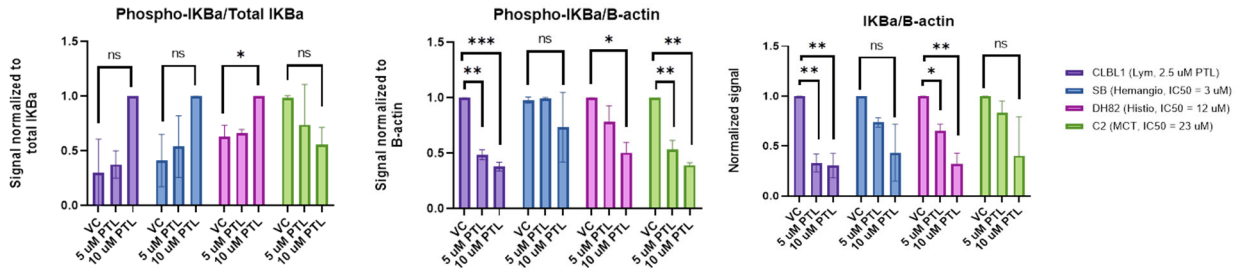

Figure 2.6: Western blots and quantification for phospho-RelA (S536) and phospho-IKBa (S36) in various canine cell lines, normalized to total p65/IKBa protein or B-actin (as indicated). Decreased phosphorylation of RelA is observed all cell lines. Decreased phosphorylation of IKBa is expected with inhibition of NF-kB signaling. This is evident in DH82 HS cells. In the other cell lines, the decreased phosphorylation of IKBa appears to be largely secondary to degradation of IKBa. Error bars = SD determined from two experimental replicates for each condition. Statistical significance was evaluated with a one-way ANOVA and a post-hoc Dunett's test, comparing both PTL treatment conditions with vehicle control.

Relative to total RelA in the cell, the signal from phosphorylated RelA decreased in a dose-dependent manner with PTL treatment in all cell lines (CLBL1 – lymphoma, SB – hemangiosarcoma, DH82 – histiocytic sarcoma, and C2 – mast cell tumor). Total RelA also decreased in a dose-dependent fashion with PTL treatment in all cell lines, which indicates degradation of RelA. Notably, effects were only observed at the highest concentration in the C2 cell line, which has the highest PTL IC50 of the cell lines evaluated. Once RelA translocates into the cell nucleus, repression of NF-kB signaling depends on resynthesis of IKBa, which dissociates NF-kB from binding sites in DNA and exports it to the cell cytosol. After activation, p65 may also be degraded by the proteasome in the nucleus to terminate transcription.[28] Phosphorylated IKBa also decreased in a dose-dependent fashion in most cell lines, and IKBa degradation was evident in some cell lines.

In many cancer types, the metastatic process leads to significant morbidity and mortality. Because NF-kB is documented to aid in tumor promotion and metastasis, migration and invasion assays were performed, using two HS cell lines (**Figure 2.7**).

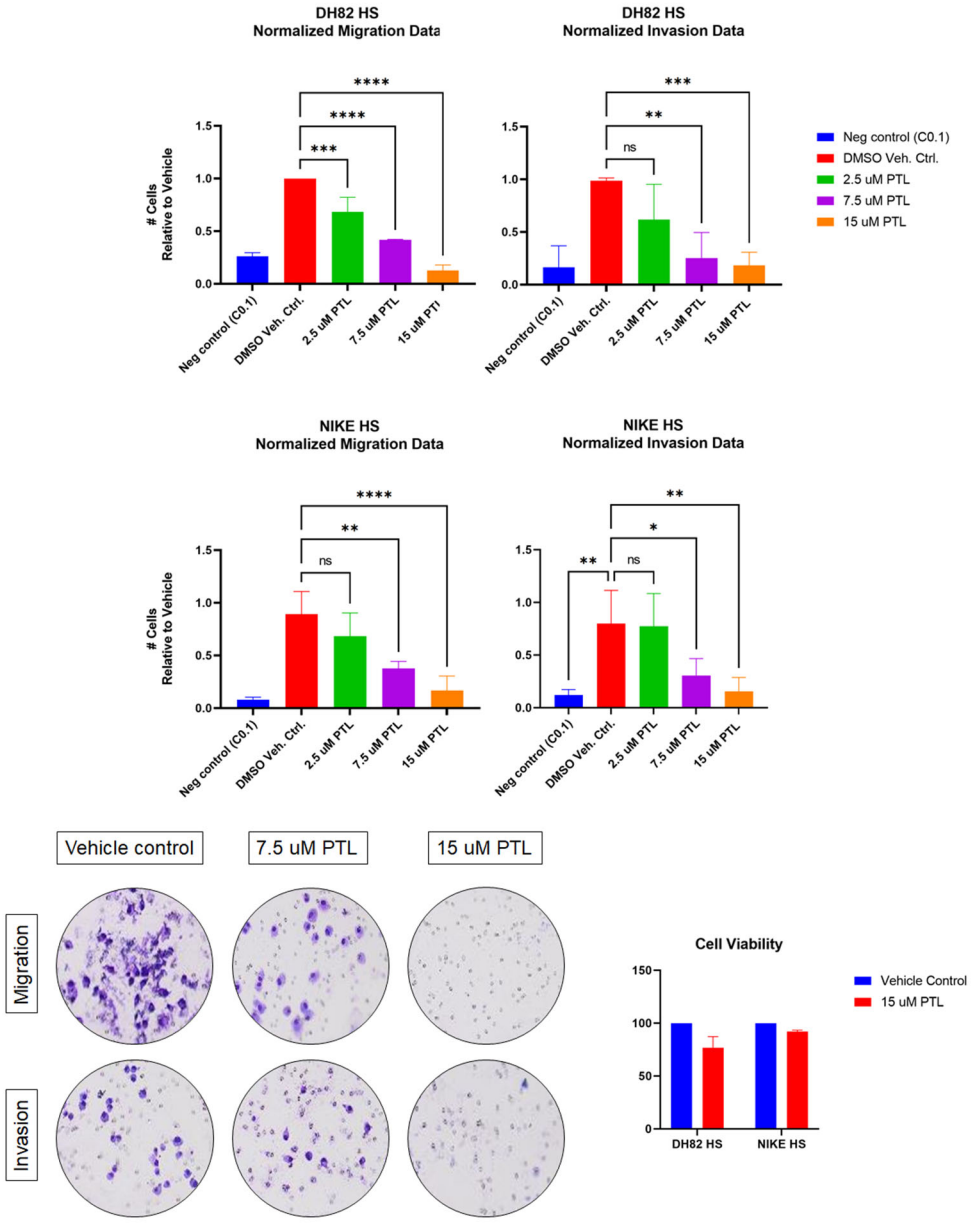

Figure 2.7: Top and middle: Normalized migration (left) and invasion (right) data for two HS cell lines. Error bars are the SD of four measurements (two replicate wells, two experimental

replicates). Bottom left: Selected example images from a migration and invasion assay performed with the NIKE HS cell line, 1000x, crystal violet stain. The small holes are the pores in the membrane (through which cells migrate or invade). Bottom right: Cell viability was determined via the Alamar Blue assay (as previously described). Although there is a decrease in cell viability that may be contributing to the values in the migration and invasion assays for DH82 HS cells, this difference does not account for all of the differences in these data.

Both HS cell lines exhibited a dose-dependent decrease in migration and invasion with PTL treatment. Although there was a mild decrease in cell viability in DH82 cells with 15 μM PTL, the decreased migration and invasion evident in the assay was clearly not all due to decreased cellular viability.

PTL is known to inhibit NF-kB signaling in two ways. The primary means of inhibition is thought to occur at the NF-kB to DNA binding interface, but PTL can also prevent phosphorylation of IKBa, which can prevent nuclear translocation of NF-kB and therefore prevent transcription of downstream target genes.[8] To determine whether inhibition of nuclear translocation is occurring with PTL therapy in canine cancer cell lines, immunocytochemistry for RelA was performed (**Figure 2.8**). CLBL1 (lymphoma) and DH82 (HS) exhibited the most dramatic inhibition of nuclear translocation, consistent with the decreased S36 phosphorylation observed in these cell lines via western blot.

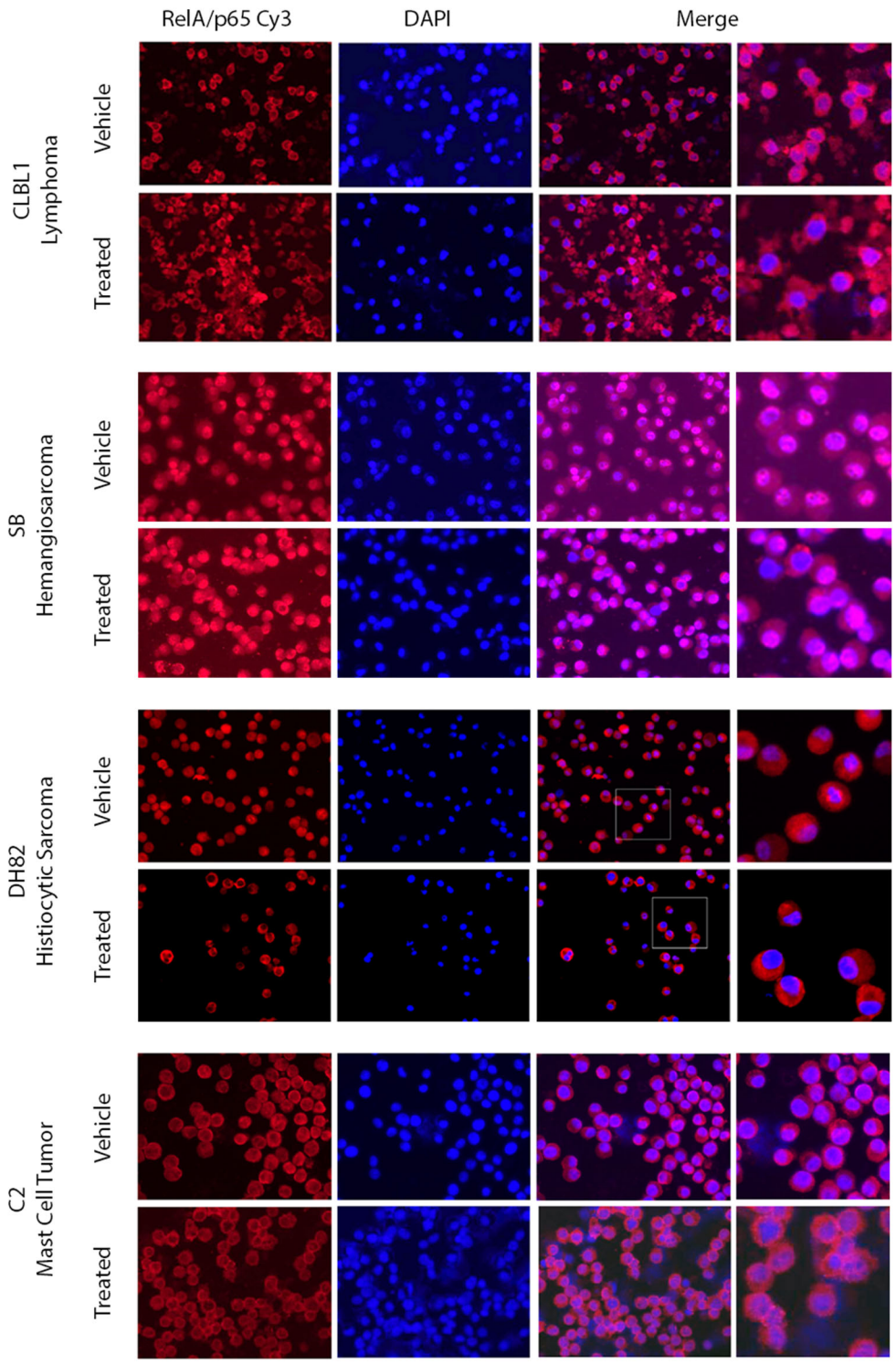

Figure 2.8: Immunocytochemistry (ICC) in four canine cell lines. Cells were treated with 0.02% DMSO (vehicle control for 7.5 μM PTL) or with 7.5 μM PTL for 6 hours. The overlap in blue and red stains creates a hazy purple appearance, which indicates nuclear RelA. Nuclear RelA

activity is most evident in SB (hemangiosarcoma) and DH82 (HS) cell lines. All cell lines exhibit some inhibition of nuclear translocation, to varying degrees.

Because HS seemed like a promising neoplasm to focus on with additional experiments, NF-kB reporter cell lines were created via transfection of a plasmid containing an NF-kB response element that drives transcription of a luciferase reporter gene (luc2P). In each case (**Figure 2.9**), the NF-kB activity of each of these cell lines is decreased with increasing doses of PTL, as expected. The CLBL1 NF-kB luciferase cell line (generously provided by Dr. Jaime Modiano, University of Minnesota) also demonstrated decreased NF-kB signaling with increasing doses of PTL.

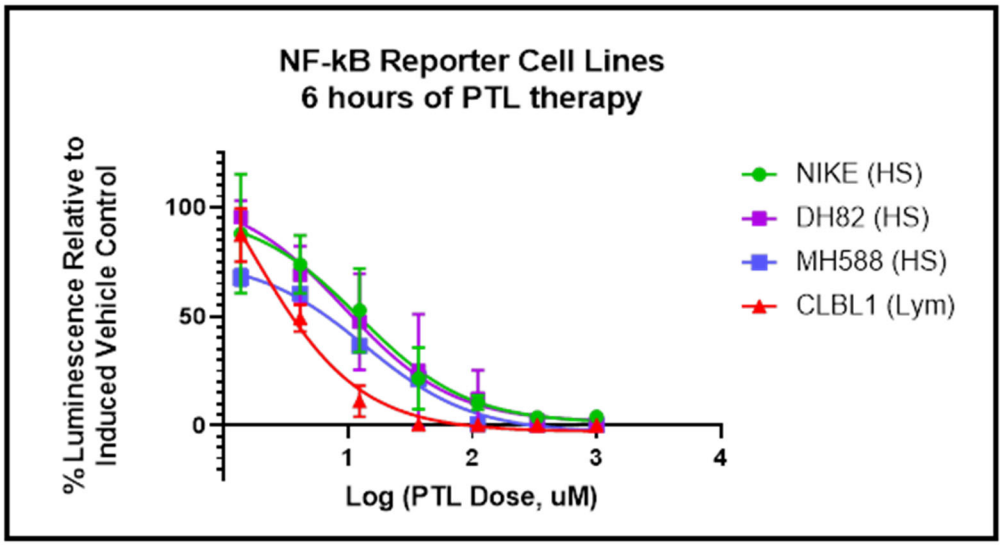

Figure 2.9: Dose-response curves generated for NF-kB reporter cell lines. Data shown are from three experimental replicates; error bars = SD over all experimental replicates.

To evaluate the effect of PTL on gene expression, DH82 HS cells (four biological replicates) were treated with vehicle control or 15 μM PTL for 24 hours, followed by RNA extraction. Following data analysis, 335 genes were identified as being significantly differentially expressed (genes with adjusted p-value <0.05, and log2FC of

<-1.5 or >1.5). A volcano plot shows this selected subset of differentially expressed genes (red, **Figure 2.10**).

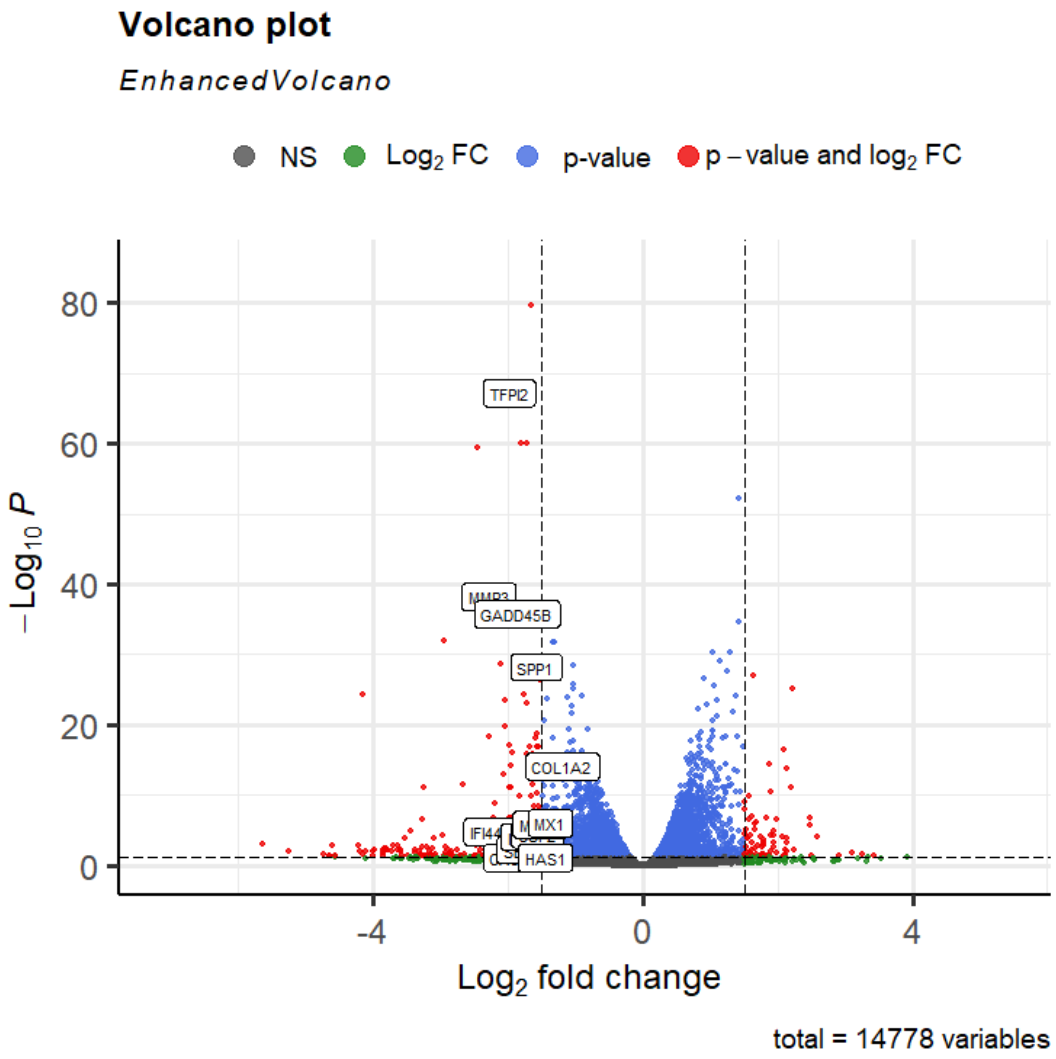

Figure 2.10: Volcano plot showing genes that were defined as differentially expressed. Genes highlighted in red were selected for downstream analysis. These genes have a Log2 fold change <-1.5 or >1.5, and an adjusted p-value of <0.05. Following treatment with PTL, most differentially expressed genes were downregulated. The labeled genes are targets of NF-kB signaling that were down-regulated with PTL treatment (for detail regarding pathways affected by PTL treatment in these cells, see **Table 2.7**).

Differentially expressed genes, as evident in **Figure 2.10,** are predominantly downregulated in DH82 HS cells treated with PTL. A heatmap in **Figure 2.11** shows the

most upregulated and downregulated genes (with Log2FC values of >1.5 or <-1.5, respectively).

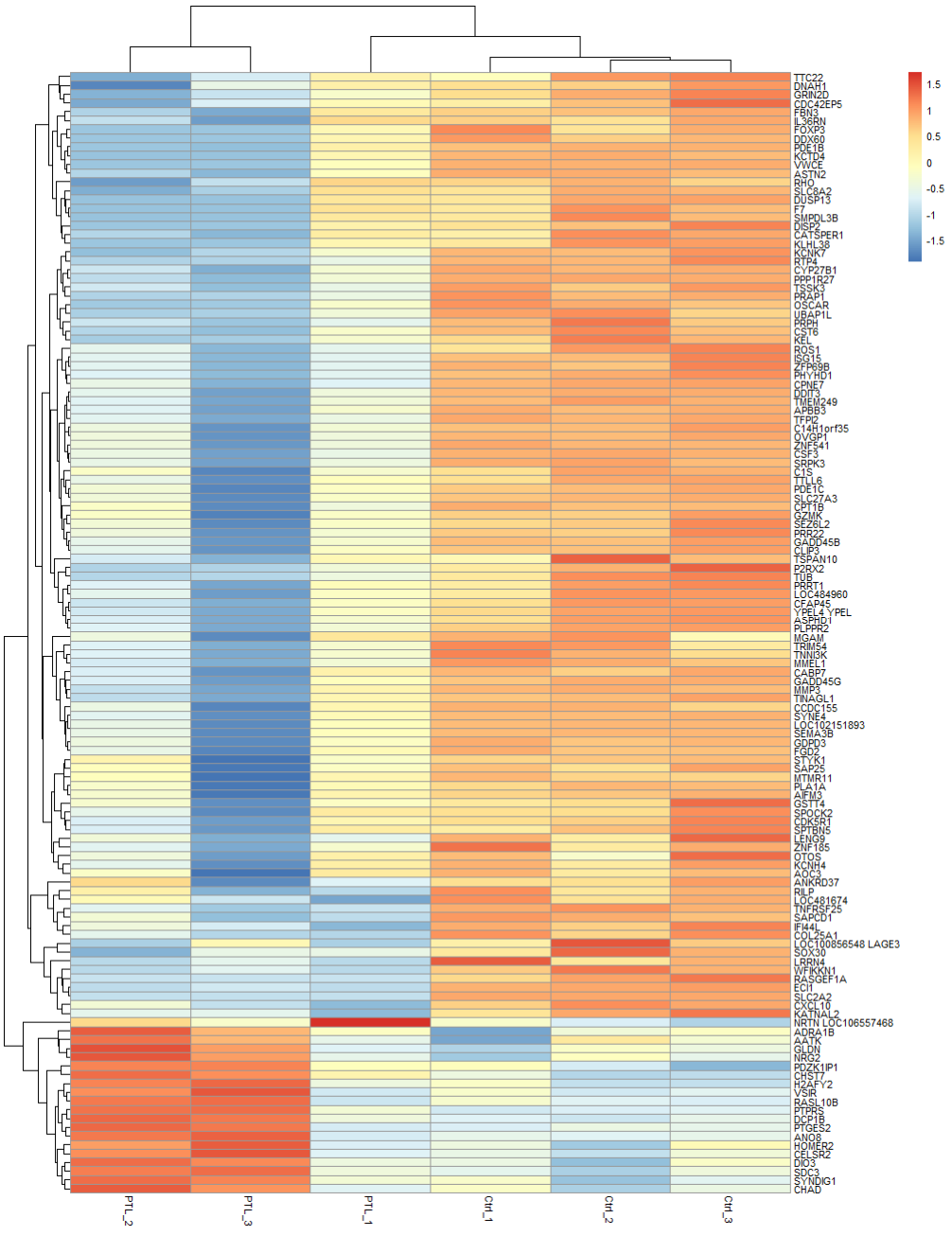

Figure 2.11: Heatmap of differentially expressed genes in PTL-treated (z-score transformed) and vehicle control DH82 HS cells. N = 128 genes, most of which are relatively downregulated with PTL treatment. Interestingly, one drug-treated sample clusters more readily with controls rather than other treated cells, which may indicate that there was an error in drug dosing for this condition, or that drug penetrance/potency was inadequate for this replicate.

RT-qPCR was performed for validation of RNA-Seq results, evaluating TNFAIP6, the promoter of which is most commonly bound by NF-kB RelA. Via RT-qPCR, TNFAIP6 was downregulated to ~0.41 in PTL-treated cells, relative to control, consistent with RT-qPCR results (Log2FC of -1.29). Additionally, because its expression is often increased with PTL therapy in human cell lines, we evaluated heme oxygenase (HO-1), which catalyzes the conversion of heme to carbon monoxide, iron, and biliverdin. It represents a prime cellular defense mechanism against oxidative stress.[38] HO-1 overexpression in human cancers may offer cancer cells a growth advantage and provide cellular resistance against therapy.[7] HO-1 expression increased following 6h of 10 μM PTL in three cell lines evaluated, as shown in **Figure 2.12.** These preliminary data suggest that HS cells evaluated may have increased resistance to PTL-induced oxidative damage as compared to the HSA cell lines evaluated.[32]

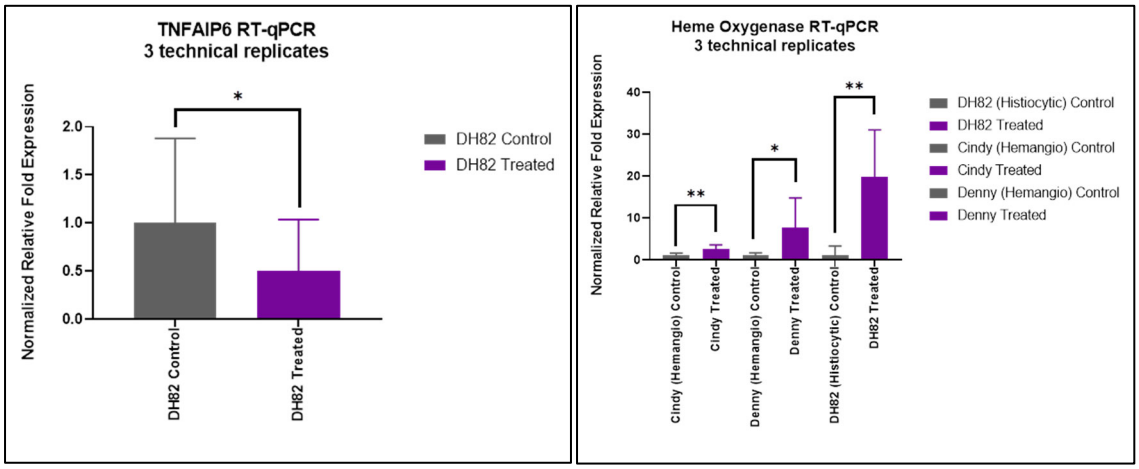

Figure 2.12: Relative fold change expression in RT-qPCR products of heme oxygenase-1, a gene previously demonstrated to have increased expression with PTL therapy, and TNFAIP6, a gene that was downregulated in RNA-seq analysis. Error bars: SD of triplicate measurements. A student's two-tailed t-test was used to evaluate statistical differences between control and treatment groups.

Up and down-regulated genes were further evaluated with the “Investigate Gene Sets” module from Gene Set Enrichment Analysis (GSEA), for which the “Hallmark” set of genes was most informative (**Table 2.7**).

Table 2.7: GSEA Hallmarks pathways that are downregulated in cells treated with 10 μM PTL for 24h. No pathways were identified for upregulated genes in the PTL-treated gene set. All pathways contained documented targets of NF-kB signaling. The # of genes in overlap shows the numbers of genes that overlap with documented genes in the indicated Hallmarks pathway. The k/K value shows the percent overlap between this dataset and the Hallmarks pathway gene dataset. The percentage of downregulated genes that are documented NF-kB signaling targets is also shown.

Gene Set Name	NF-kB targets	# Genes in Overlap (k)	% genes that are NF-kB targets	k/K	p-value	FDR q-value
IFNa Response	3	16	18.8%	16.5%	9.63E-19	4.81E-17
IFNg Response	4	19	21.1%	9.5%	2.26E-17	5.65E-16
TNFa Signaling via NF-kB	3	9	33.3%	4.5%	3.95E-06	6.58E-05
Complement	1	8	12.5%	4.0%	3.19E-05	3.19E-04
KRAS Signaling Up	2	8	25.0%	4.0%	3.19E-05	3.19E-04
Apoptosis	1	6	16.7%	3.7%	4.58E-04	3.81E-03
EMT Transition	5	6	83.3%	3.0%	1.41E-03	7.75E-03
Hypoxia	1	6	16.7%	3.0%	1.41E-03	7.75E-03
KRAS Signaling Down	2	6	33.3%	3.0%	1.41E-03	7.75E-03
Coagulation	2	5	40.0%	3.6%	1.55E-03	7.75E-03

Because there was some incongruity in RNA-Seq data from cells treated with PTL and because it was thought that observed changes may only be represented in PTL-resistant cells at 24h of treatment, this experiment was repeated. Instead of utilizing the same methodology for this second RNA sequencing experiment, data were evaluated using the Nanostring Canine IO (Immuno-oncology) Panel, which evaluates changes in expression of 800 genes that have been identified as important in tumor and immune cell response to treatment in this species. For this experiment, DH82 and MH588 HS cells were treated for 6 hours (a time point at which, experimentally, there is no

evidence of apoptotic cell death). **Figure 2.13** shows normalized gene expression data (z-score) for all 800 genes in the Nanostring Canine IO panel. These data show that all control and drug-treated samples cluster similarly, for both cell lines treated.

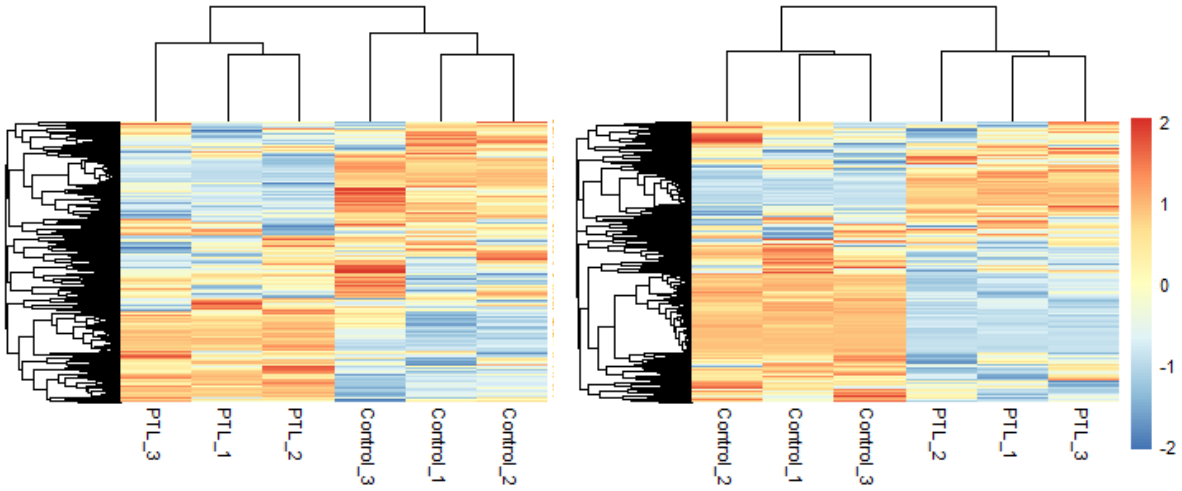

DH82 HS Samples **MH588 HS Samples**

Figure 2.13: Heatmaps of z-score transformed gene expression (all 800 genes) in HS cell lines evaluated with the Nanostring Canine IO panel, made with the pheatmap package in R. Via this method, clustering of control and PTL-treated samples in both cell lines is apparent.

Figure 2.14 shows volcano plots, evaluating differentially expressed genes among the 800 genes in the canine IO panel. Two versions of volcano plots are shown for each cell line: in the first plot, all differentially expressed genes are shown, while in the second plot, genes defined as belonging to the NF-kB signaling pathway by Nanostring are highlighted in yellow. Note that most genes in the panel are downregulated with 6 hours of 10 μM PTL therapy.

DH82 HS cells

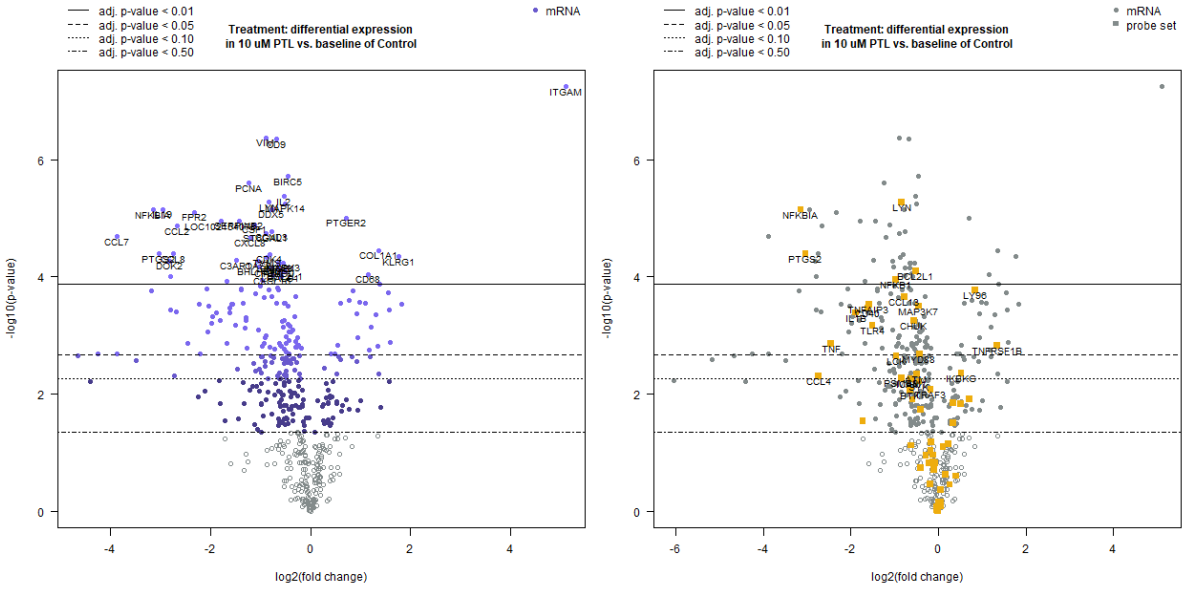

MH588 HS cells

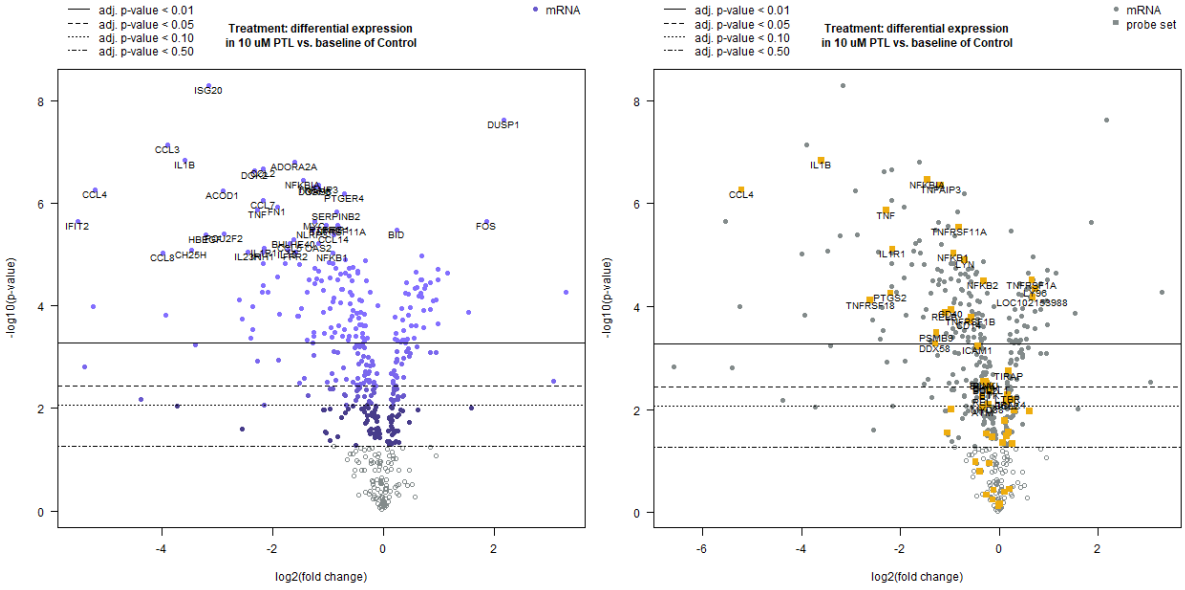

Figure 2.14: Volcano plots showing differentially expressed genes in PTL-treated cells as compared to vehicle control-treated cells. Left: all differentially expressed genes. Right: differentially expressed genes categorized as belonging to the NF-kB signaling pathway (Nanostring).

Tables 2.8 and 2.9 show output from part of the experimental analysis pipeline that was used in the previous RNA-sequencing experiment. First, differentially expressed genes were exported from the Nanostring dataset, and were filtered for significance ($p<0.05$) and a log2FC of <-1.5 or >1.5, as was done previously. Subsets of downregulated and upregulated genes were created from this filtered list, followed by GSEA analysis, as performed for the 24-hour DH82 HS experiment.

Table 2.8: DH82 HS cells. GSEA Hallmarks pathways that are downregulated in DH82 HS cells treated with 10 μM PTL for 6h. No pathways were identified for upregulated genes in the PTL-treated gene set. All pathways contained documented targets of NF-kB signaling. The percentage of downregulated genes in each pathway that are also documented NF-kB signaling targets is shown. The "# of genes in overlap" shows the numbers of genes that overlap with documented genes in the indicated Hallmarks pathway. The k/K value shows the percent overlap between this dataset and the Hallmarks pathway gene dataset.

Gene Set Name	NF-kB targets	# Genes in Overlap (k)	% Genes that are NF-kB targets	k/K	p-value	FDR q-value	Also downregulated in 24h data?
Inflammatory Response	7	15	46.7%	7.5%	1.17E-24	5.87E-23	
TNFa Signaling via NF-kB	10	12	83.3%	6.0%	1.35E-18	3.36E-17	Yes
Allograft Rejection	5	11	45.5%	5.5%	1.12E-16	1.40E-15	
KRAS Signaling Up	7	11	63.6%	5.5%	1.12E-16	1.40E-15	Yes
IFNg Response	6	8	75.0%	4.0%	2.97E-11	2.97E-10	Yes
IL6 JAK STAT3 Signaling	4	6	66.7%	6.9%	3.90E-10	3.25E-09	
IL2 STAT5 Signaling	3	5	60.0%	2.5%	1.93E-06	1.38E-05	
Epithelial to Mesenchymal Transition	4	4	100.0%	2.0%	5.43E-05	3.39E-04	Yes
IFNa Response	1	3	33.3%	3.1%	1.40E-04	7.77E-04	Yes
Complement	1	3	33.3%	1.5%	1.16E-03	5.79E-03	Yes

Table 2.9: MH588 HS cells. GSEA Hallmarks pathways that are downregulated in MH588 HS cells treated with 10 μM PTL for 6h. No pathways were identified for upregulated genes in the PTL-treated gene set. Columns are as previously labeled for Table 2.8, except that there is not a comparison column to 24-hour data (as the 24-hour assay was previously only performed with DH82 HS cells).

Gene Set Name	NF-kB targets	# Genes in Overlap (k)	% Genes that are NF-kB targets	k/K	p-value	FDR q-value
TNFa Signaling via NF-kB	4	4	100.0%	2.0%	8.35E-09	4.18E-07
IL6 JAK STAT 3 Signaling	2	3	66.7%	3.5%	1.87E-07	4.67E-06
Allograft Rejection	3	3	100.0%	1.5%	2.30E-06	3.83E-05
Apoptosis	2	2	100.0%	1.2%	2.30E-04	2.87E-03
Inflammatory Response	1	2	50.0%	1.0%	3.54E-04	2.95E-03
KRAS Signaling Up	1	2	50.0%	1.0%	3.54E-04	2.95E-03

To further explore pathway alterations in differentially expressed genes, KEGG pathway analysis was performed via the Database for Annotation, Visualization, and Integrated Discovery (DAVID). For DH82 HS cells, the most highly represented KEGG pathways were Cytokine-Cytokine Receptor Interaction and TNF signaling; the latter aligns well with downregulation of “TNFa Signaling via NF-kB” in both cell lines. Downregulated genes are starred in two included KEGG Pathway images (**Figure 2.15**). **Figure 2.16** shows another version of the NF-kB signaling pathway. In this version, all genes that were counted as differentially expressed by Nanostring software that were significant ($p<0.05$), without respect to the log2FC value. For MH588 HS cells, the most highly represented KEGG pathways were also Cytokine-Cytokine Receptor interaction and TNFa signaling. **Figure 2.17** shows the KEGG TNF signaling pathway with starred, downregulated genes, while **Figure 2.18** shows NF-kB signaling genes that were identified by the Nanostring algorithm that were significant ($p<0.05$), without respect to the log2FC value. **Tables 2.10** and **2.11** show KEGG signaling-related pathways that were identified and statistically significant for DH82 and MH588 HS cells, respectively.

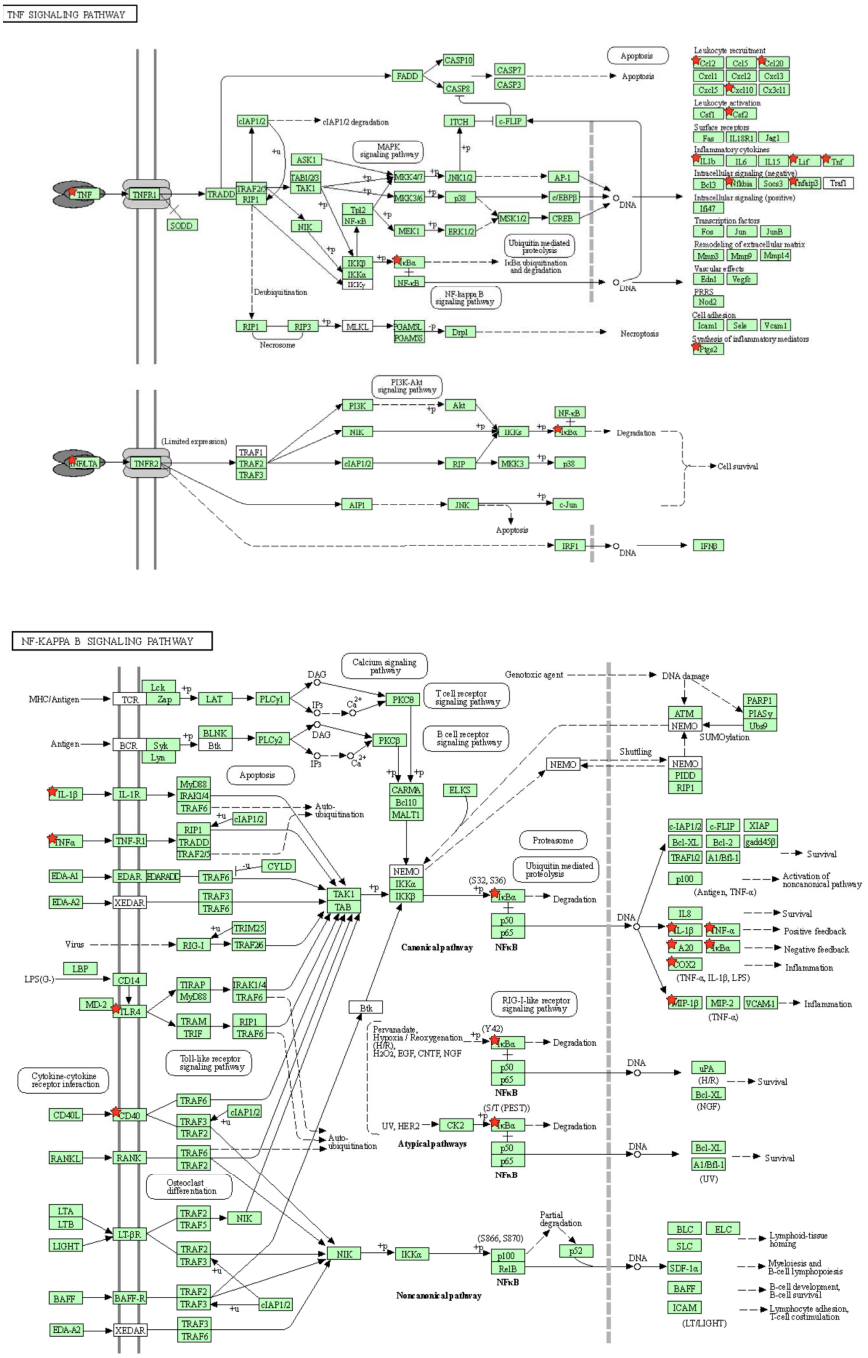

Figure 2.15: Selected KEGG pathway images for DH82 HS cells. Genes that were downregulated by PTL treatment are indicated with red stars.

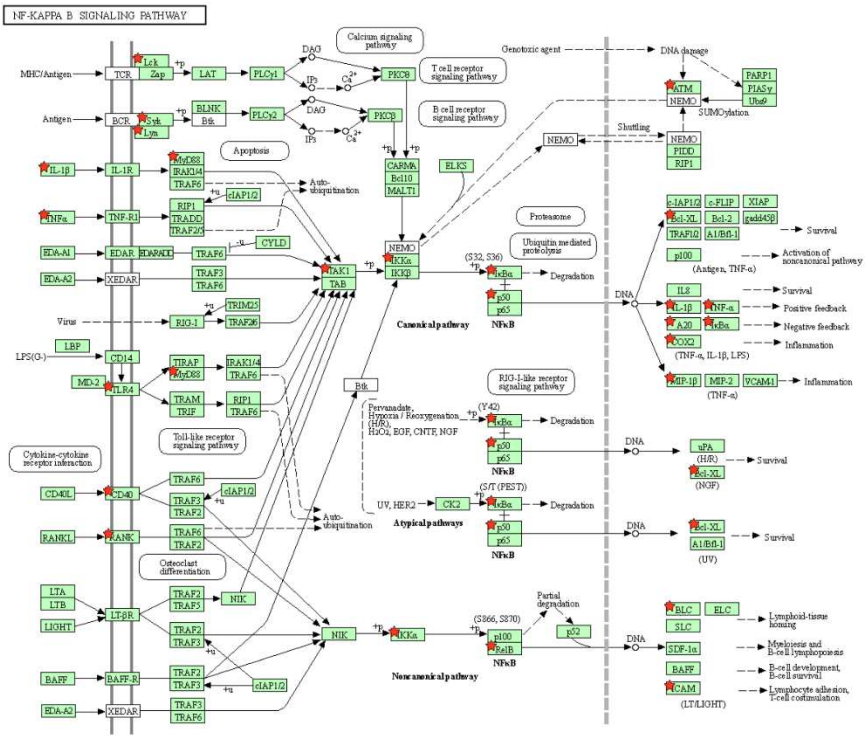

Figure 2.16: DH82 HS cells, NF-kB signaling pathway, showing all genes that were counted as "downregulated" by the Nanostring algorithm ($p < 0.05$, log2FC < 0). Although some gene expression changes are of lower magnitude than our established cutoff, these data support NF-kB signaling as an important target of PTL therapy.

Table 2.10: *Downregulated KEGG Pathways: DH82 HS Cells*

	# Genes	*k/K*	*P-Value*
cfa04060:Cytokine-cytokine receptor interaction	*20*	*47.60%*	*2.60E-19*
cfa04061:Viral protein interaction with cytokine and cytokine receptor	13	31.00%	8.16E-16
cfa04657:IL-17 signaling pathway	12	28.60%	6.37E-14
cfa04620:Toll-like receptor signaling pathway	10	23.80%	2.50E-10
cfa04668:TNF signaling pathway	10	23.80%	6.62E-10
cfa04062:Chemokine signaling pathway	10	23.80%	6.06E-08
cfa04064:NF-kappa B signaling pathway	8	19.00%	1.53E-07
cfa04621:NOD-like receptor signaling pathway	8	19.00%	5.05E-06
cfa04217:Necroptosis	5	11.90%	0.005586
cfa04630:JAK-STAT signaling pathway	5	11.90%	0.004674
cfa05202:Transcriptional misregulation in cancer	5	11.90%	0.008688
cfa04622:RIG-I-like receptor signaling pathway	3	7.10%	0.033329

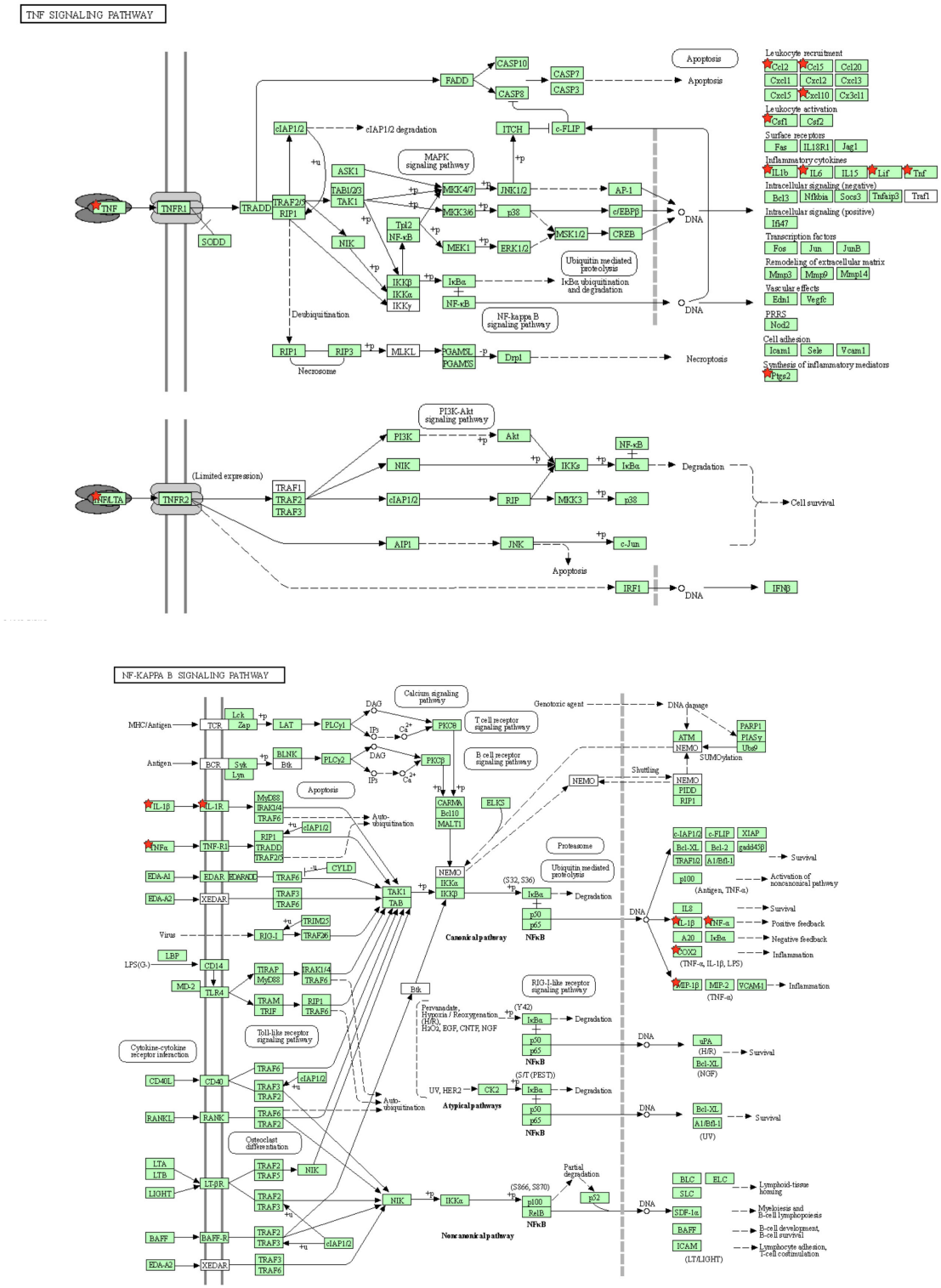

Figure 2.17: Selected KEGG pathway images for MH588 HS cells. Genes that were downregulated by PTL treatment are indicated with red stars.

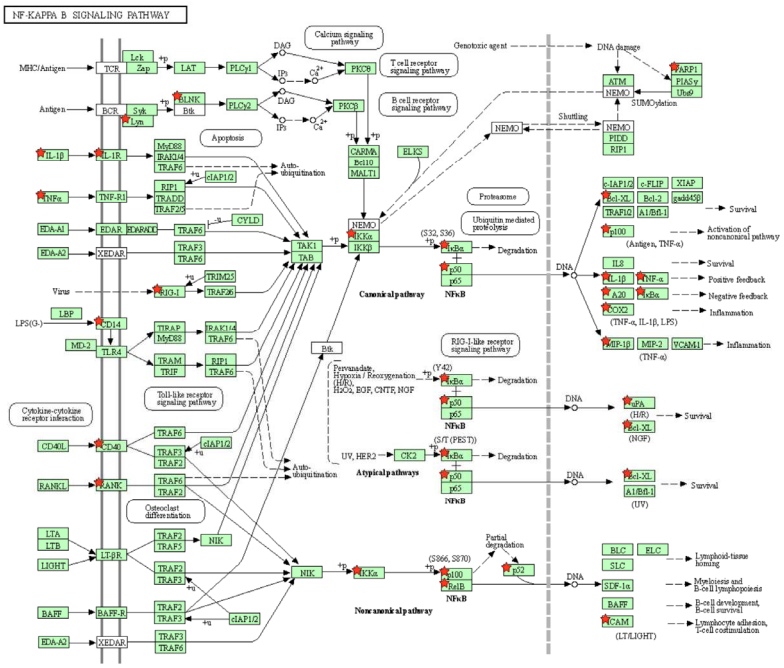

Figure 2.18: MH588 HS cells, NF-kB signaling pathway, showing all genes that were counted as “downregulated” by the Nanostring algorithm ($p < 0.05$, $log2FC < 0$).

***Table 2.11**: Downregulated KEGG Pathways: MH588 HS Cells*	*# Genes*	*k/K*	*P-Value*
cfa04060:Cytokine-cytokine receptor interaction	23	50.0%	2.10E-23
cfa04061:Viral protein interaction with cytokine,cytokine receptor	13	28.3%	1.69E-15
cfa04668:TNF signaling pathway	9	19.6%	2.65E-08
cfa04657:IL-17 signaling pathway	8	17.4%	1.32E-07
cfa04630:JAK-STAT signaling pathway	7	15.2%	7.28E-05
cfa04062:Chemokine signaling pathway	7	15.2%	1.66E-04
cfa04610:Complement and coagulation cascades	7	4.1%	0.003345
cfa04550:Signaling pathways regulating pluripotency of stem cells	7	4.1%	0.042457
cfa04621:NOD-like receptor signaling pathway	6	13.0%	8.00E-04
cfa04370:VEGF signaling pathway	6	3.5%	0.003615
cfa04012:ErbB signaling pathway	6	3.5%	0.016089
cfa04350:TGF-beta signaling pathway	6	3.5%	0.02823
cfa04640:Hematopoietic cell lineage	5	10.9%	7.44E-04
cfa04064:NF-kappa B signaling pathway	5	10.9%	9.51E-04
cfa04622:RIG-I-like receptor signaling pathway	4	8.7%	0.003364
cfa05330:Allograft rejection	3	6.5%	0.007961

In summary, in both the 24h and 6h experiments with canine HS cells, downregulation of pathways containing NF-kB targets is evident, consistent with previous experiments, and with the known activity of PTL as a canonical, NF-kB signaling inhibitor in human and murine cells. Overall, results between GSEA and KEGG pathway analysis are similar. Most downregulated pathways are not surprising in light of expected NF-kB pathway inhibition, including IL6 and TNFa signaling,[1] apoptosis, allograft rejection, interferon responses, and the inflammatory response. KRAS signaling is a pathway that is repeatedly represented in this analysis; activating KRAS mutations often lead to activation of NF-kB, so downregulation of this pathway in HS cells may also be contributing, in turn, to downregulation of NF-kB signaling.[6] Of note, downregulation of the Epithelial to Mesenchymal Transition pathway is conserved in both experiments with DH82 HS cells, which correlates well with migration and invasion data for this cell line.

2: Redox balance in canine cell lines treated with parthenolide

To evaluate reactive oxygen species (ROS) production in canine and human cell lines, fluorogenic H2DCFDA assays were performed with several doses of PTL. To test the effect of antioxidant pre-treatment, one group of cells was pre-treated with 2 mM N-acetylcysteine (NAC) for one hour, followed by washing and treatment with PTL. As a normal cell control condition for lymphocytes and histiocytic-origin cells, peripheral blood mononuclear cells (PBMCs) were isolated form the blood of dogs without hematopoietic cancer, and ROS were measured in the same plate in with DH82 (HS) ROS (**Figure 2.19**).

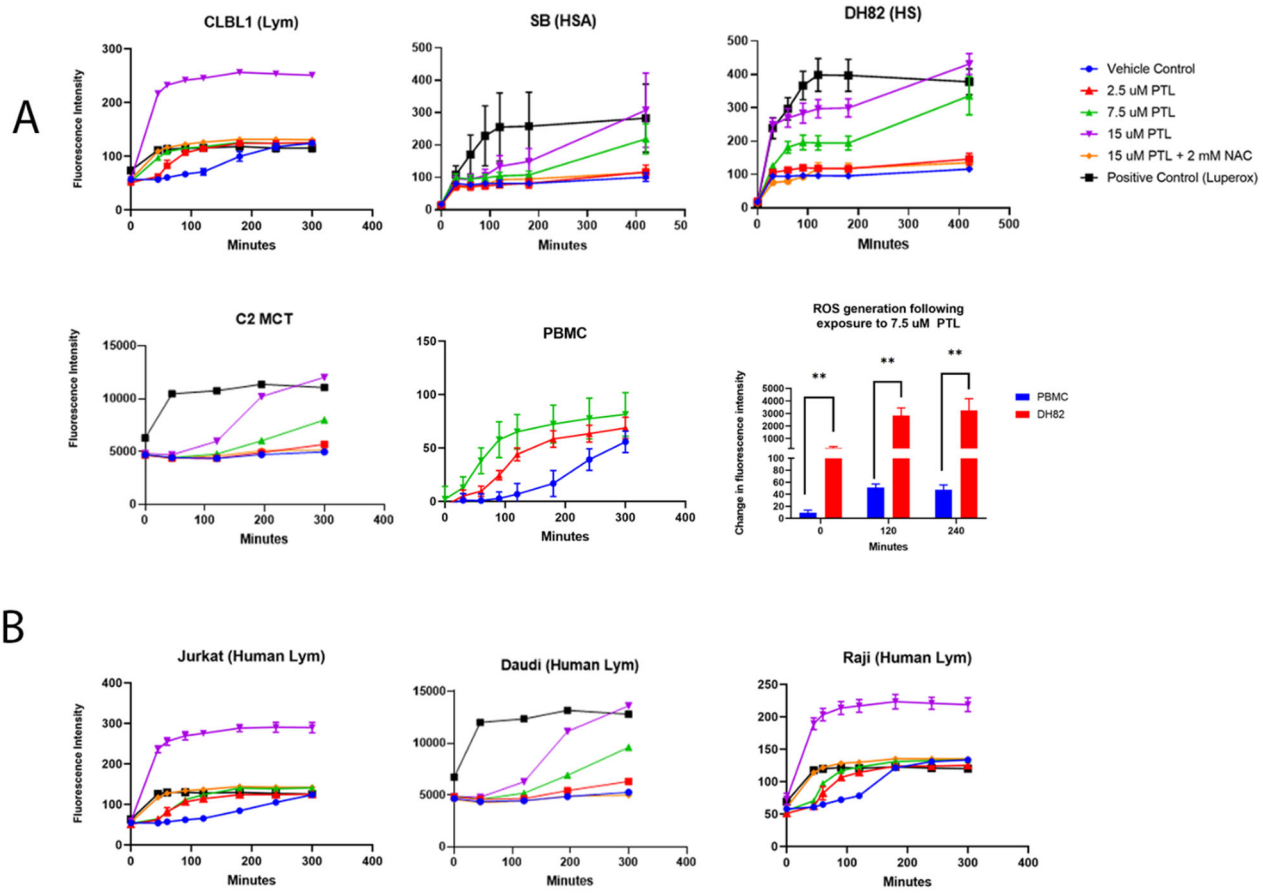

Figure 2.19: ROS generation with PTL treatment. A: Canine cell lines generate dose-dependent ROS with exposure to PTL. ROS generation is blunted, to various degrees, in cells that are pre-treated with 2 mM N-Acetylcysteine. While canine peripheral blood mononuclear cells (PBMCs) do generate ROS with PTL exposure, the effect is not nearly as significant as is seen in DH82 HS cells. To test significance in ROS generation between canine PBMCs and DH82 HS cells, a student's two-tailed t-test was performed (p = <0.01 B: Human lymphoma cell lines generate dose-dependent ROS with PTL exposure as well. Error bars represent the SD for five replicate wells in each experiment. Two experimental replicates were performed for each cell line.

Because PTL has been documented to inhibit glutathione (GSH) synthesis as a reported anti-cancer mechanism, reduced and oxidized glutathione were measured in canine cell lines (**Figure 2.20**). Buthionine sulphoximine, or BSO, is an established inhibitor of gamma-glutamycysteine synthetase, which is critical for synthesis of glutathione, and therefore, BSO treatment results in reduction of intracellular glutathione

over time.[4] BSO was used as a positive control for this assay. As for ROS production, some cells were pre-treated with NAC to determine whether glutathione depletion could be prevented. All canine cell lines evaluated exhibited dose-dependent glutathione depletion over 6 hours, as expected. The C2 (MCT) cell line had a decreased GSH measurement relative to the 2.5 µM PTL treatment condition, which was repeatable across experimental replicates.

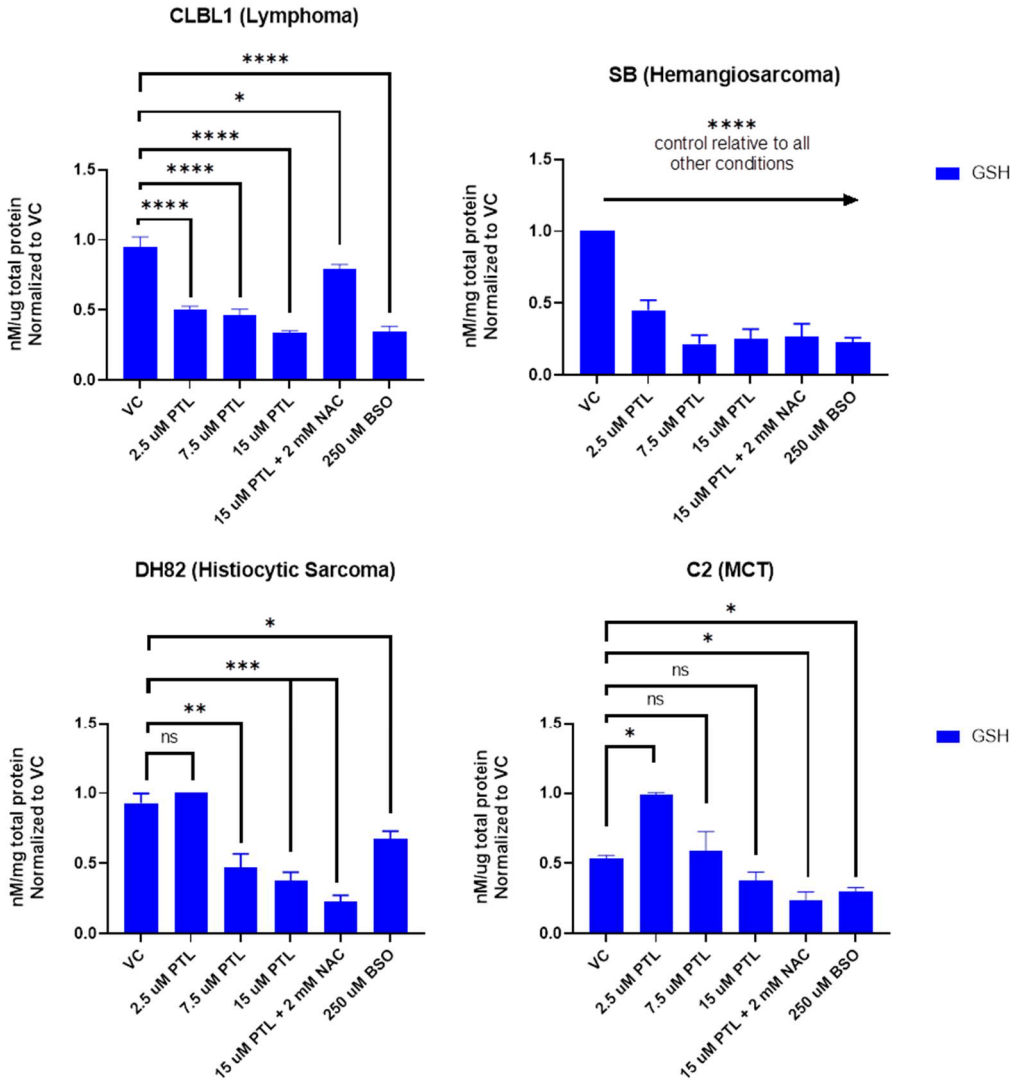

Figure 2.20: All cells evaluated appeared to exhibit dose-dependent depletion of glutathione with PTL treatment, except for C2 (MCT), in which the GSH in the vehicle control-treated set of cells is reliably lower than the 2.5 µM PTL treatment condition. Aside from this anomaly, a trend toward dose-dependent glutathione depletion is observed in all cell lines (variably statistically

significant relative to vehicle control, as shown and evaluated by ANOVA with a post hoc Dunett's test). In the CLBL1 cell line, pre-treatment with 2 mM NAC results in a rescue effect and reduced depletion of GSH. Error bars represent the SD for two experimental replicates.

In a large number of human cell lines evaluating the genes that most strongly predict PTL sensitivity, high expression of GPX2 (glutathione peroxidase 2) was correlated with PTL resistance (unpublished data, courtesy Dr. Craig Jordan and Dr. Jeff Settleman). To determine whether this may be the case in canine cell lines as well, RNA sequencing data from the Flint Animal Cancer Center (FACC) cell line panel, comprising 32 cell lines, was evaluated. None of the glutathione peroxidases had been previously identified as potential drivers of resistance in our canine cell lines. According to the RNA-Seq count data in canine cell lines, GPX1 appears most active, followed by GPX8. In comparing GPX count data with PTL sensitivity, there is a small correlation between GPX1 counts and PTL IC50 ($R^2 = 0.29$), and a slight correlation between GPX8 counts and PTL IC50 ($R^2 = 0.10$). Neither correlation reaches statistical significance ($p = 0.97$). In five canine cell lines (those characterized elsewhere as well as STSA-1, which is a cell line that is more resistant to PTL), total GPX activity did appear relatively low in the most sensitive cell line (SB, IC50 of 3 μM) and higher in cell lines with a higher IC50 (**Figure 2.21)**. Collectively, these data imply that there may potentially be a correlation between GPX activity and PTL IC50, but evaluation across a larger number of cell lines would likely need to be performed for this correlation to reach statistical significance.

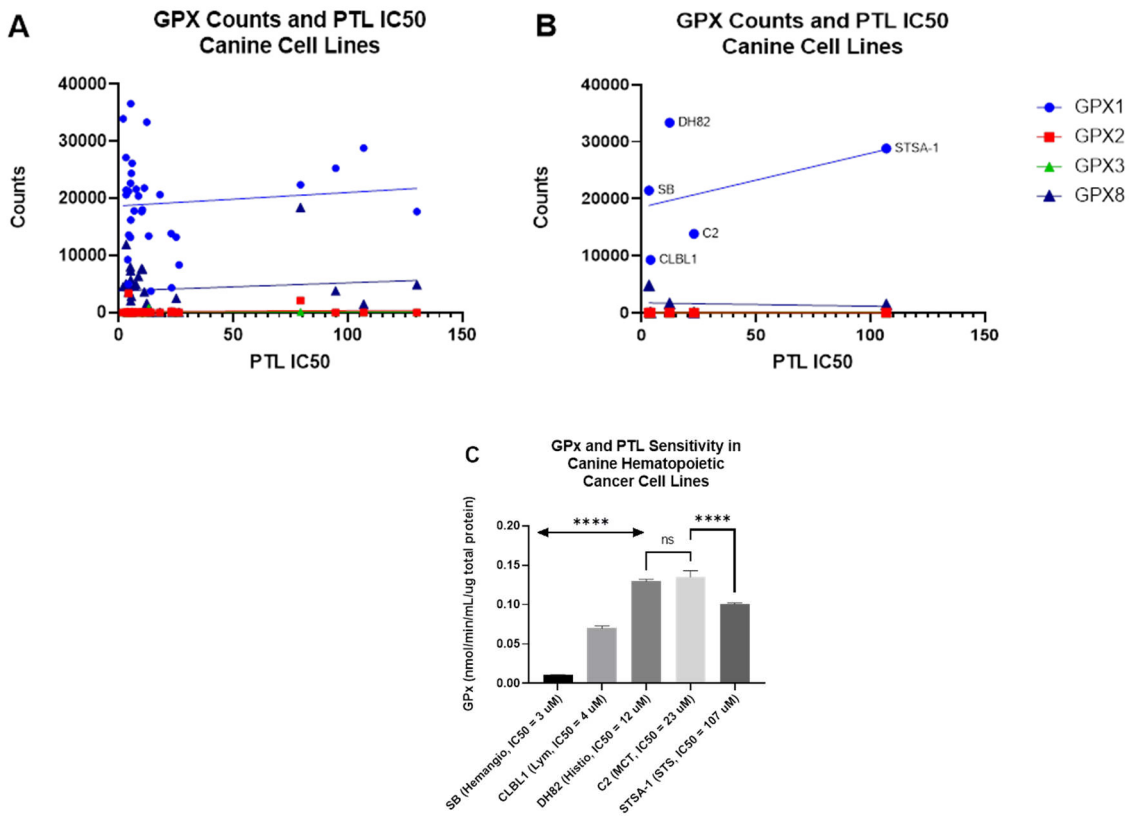

Figure 2.21: A and B: Graphics created from RNA-Seq counts of GPX activity in X canine cell lines. In B, the cell lines selected for GPX measurement are highlighted. In C, measurement of GPx activity was performed. While the GPx enzymatic activity is not exactly as might be predicted by RNA-Seq counts data, the more resistant cell lines do appear to have greater GPx activity as compared to the most sensitive cell lines (SB and CLBL1). Error bars in C are the SD from two experimental replicates (each experiment containing three technical replicates for each condition). The significance of differences between groups was analyzed by one-way ANOVA on ranks with Tukey's post hoc test. **** $p < 0.0001$, ns = not significant.

3. PTL in combination with other therapeutic agents in canine cell lines

To further evaluate PTL's potential efficacy in a canine clinical study, we evaluated PTL alone and in combination with standard-of-care therapeutics for HS: lomustine or CCNU (most commonly used) and doxorubicin. We predicted that these drugs may synergize with PTL because doxorubicin is, itself, a free radical generator, and CCNU is a DNA alkylating agent that also inhibits thioredoxin reductase. Shown in

Figure 2.22 are the combination indices we calculated with Compusyn, software that uses the Chou-Talalay method. A combination index of <1 indicates synergism, meaning that there is greater growth inhibition than would be expected from the additive effects of two agents. With the exception of few dose combinations, there is broad synergism with PTL and either doxorubicin or CCNU, while the effects of combining PTL with toceranib for mast cell tumor cells are generally additive. These results indicate that PTL may be combined with standard-of-care chemotherapeutics for canine patients, but that combination therapy is likely to be most effective when PTL is combined with doxorubicin or CCNU.

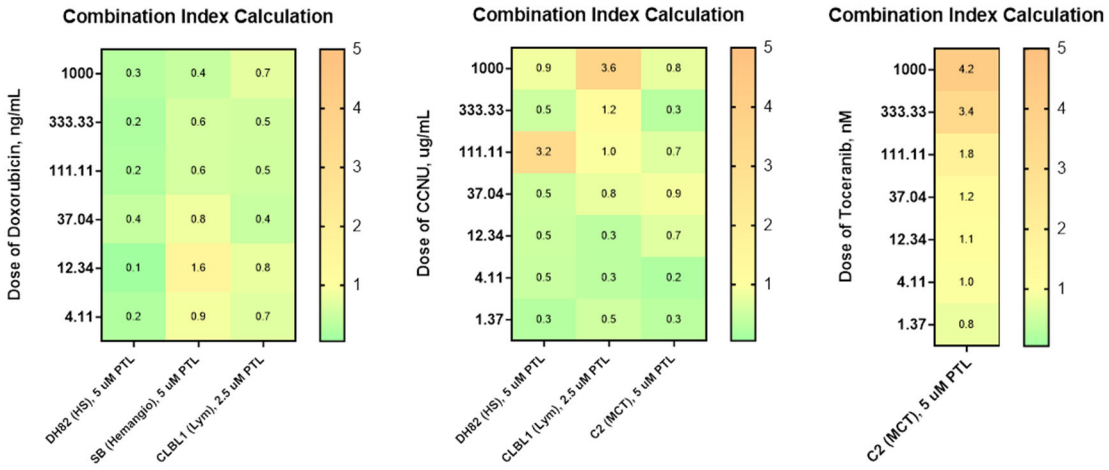

Figure 2.22: Heat maps showing calculated combination indices for cells exposed to 2.5-5 μM PTL. CLBL1 received a lower dose of PTL since in combination with even the smallest doses of doxorubicin and CCNU, 5 μM PTL resulted in cell death of almost all CLBL1 cells.

4. Effects of PTL in patient-derived tumor samples

To determine whether cell line findings were repeatable in primary cells from patients, cells were isolated from patients, maintained in culture for a short time, and cell-based assays were performed. Lymphoma cells were derived from lymph node

aspirates, while HS cells came from effusion or blood (circulating cell) samples. In all cases, cells were sensitive to PTL at concentrations that were similar to those observed in canine cell lines (**Figure 2.23**).

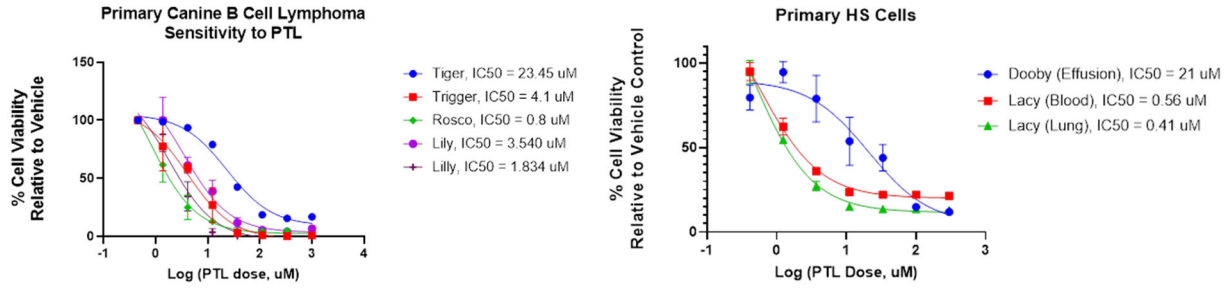

Figure 2.23: Dose response curves for primary cells isolated from canine patients with B cell lymphoma and HS (dendritic APC origin, confirmed via immunocytochemistry). Error bars are the SD from three experimental replicates.

Primary lymphoma cells (of both B and T-cell origin) underwent apoptosis in a dose-dependent fashion. Although only low numbers of cells were available for this assay, in one B cell lymphoma, pre-treatment with 2 mM NAC modestly blunted the apoptotic response, as was observed with canine cell lines (**Figure 2.24**).

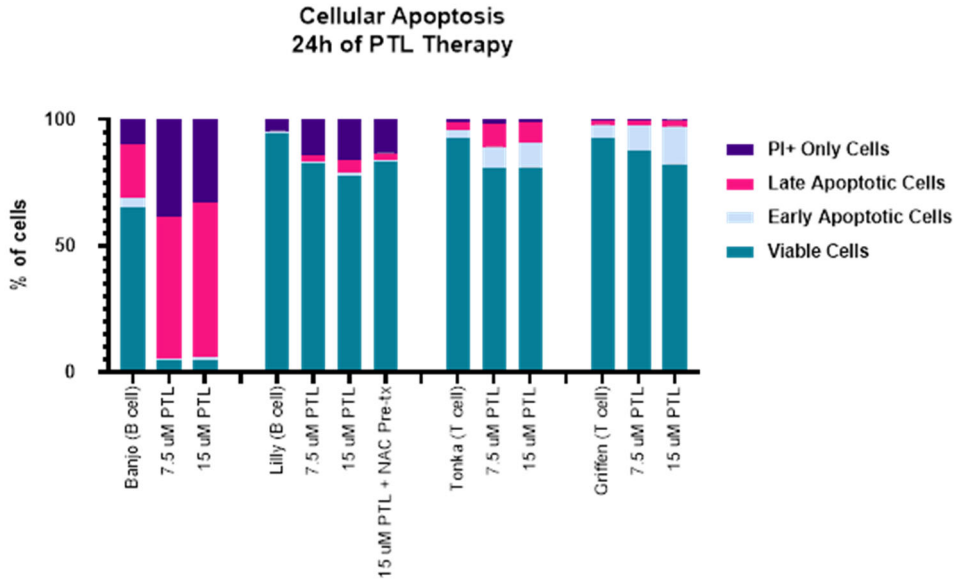

Figure 2.24: Primary lymphoma cells undergo dose-dependent apoptosis with PTL treatment. Only one aliquot of cells contained adequate numbers to evaluate four treatment conditions, including pre-treatment with 2 mM NAC prior to PTL treatment. For this cell aliquot (Lilly, a B cell lymphoma sample), a small rescue effect is observed following NAC pre-treatment.

Because cellular survival of cells from peripheral blood and lung tissue in Lacy HS cells was excellent over time, immunocytochemistry was performed to further document their cellular origin. The patient, an 8 yo FS Bernese mountain dog, was affected by a rare, mixed form of HS, with dendritic antigen presenting cell origin HS (lung) and hemophagocytic histiocytic sarcoma (liver, spleen, bone marrow). Although there were inadequate numbers of cells from peripheral blood for immunocytochemistry, since cells could be expanded in culture and antigens were still present at the time of ICC evaluation, the circulating cells were able to be categorized as of dendritic antigen presenting cell origin (**Figure 2.25**).

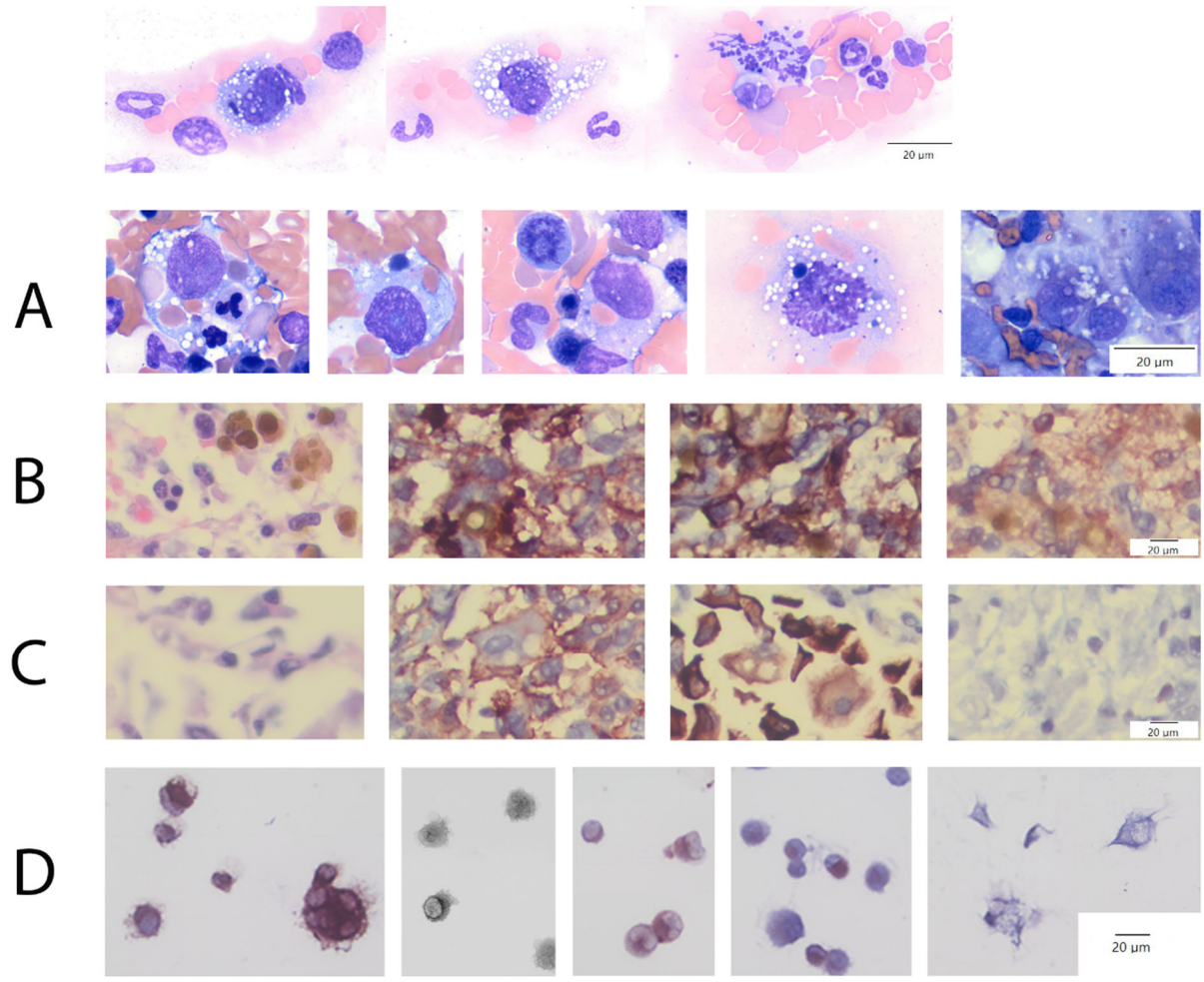

Figure 2.25: Top: Images of circulating, atypical HS cells from the blood of a Bernese Mountain dog. Some of these cells contained erythrocytes and/or dark green pigment, consistent with hemosiderin.
A. 1000x, Modified Wright-Giemsa stain. Images 1-4: Moderately atypical, hemophagocytic, histiocytic cells in splenic aspirate samples; Image 5: Post-mortem bone marrow aspirate, showing large numbers of atypical, hemophagocytic, histiocytic cells.
B: Bone marrow IHC, 400x: from left to right: hematoxylin and eosin; strong, positive, membranous staining of CD18; positive membranous and cytoplasmic staining of Iba1; positive membranous staining of CD11d.
C: Lung IHC, 400x: from left to right: hematoxylin and eosin; positive CD18 staining, positive membranous and cytoplasmic staining of Iba1, negative CD11d staining.
D: Cultured cells from blood, immunocytochemistry, 1000x, from left to right: positive CD11c staining, variable CD1a positivity, positive CD18 staining, positive CD204 staining, and negative CD11d staining.

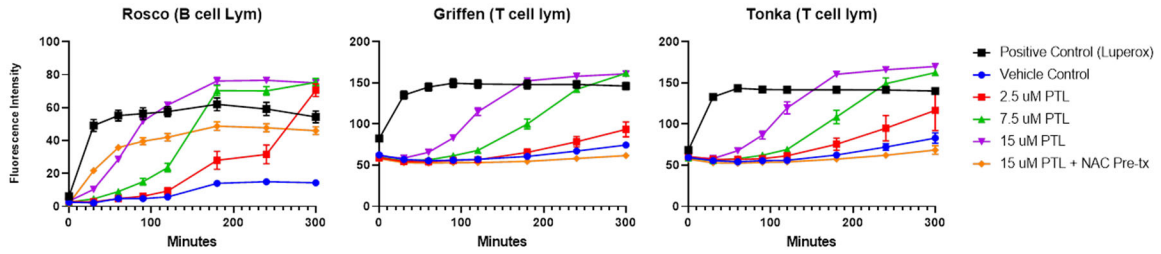

Figure 2.26: H2DCFDA assay in canine primary cells maintained in culture for a short period of time. Multiple primary cells, including those shown this figure, generated dose-dependent ROS with PTL treatment, as has been observed in canine cell lines. Error bars represent the SD for five replicate wells in each experiment. Two experimental replicates were performed for each patient sample.

Primary cells exhibited dose-dependent ROS generation (**Figure 2.26**). Some B cell lymphoma primary cell samples were also evaluated for glutathione depletion over 6 hours of treatment. Because there were fewer viable primary cells available (versus an essentially inexhaustible supply of cells from immortalized cell lines), only three treatment conditions were evaluated in this experiment (**Figure 2.27**). Although two few viable cells were present for an experimental replicate in this case, the data suggest that PTL treatment may deplete GSH in patient-derived tumor samples.

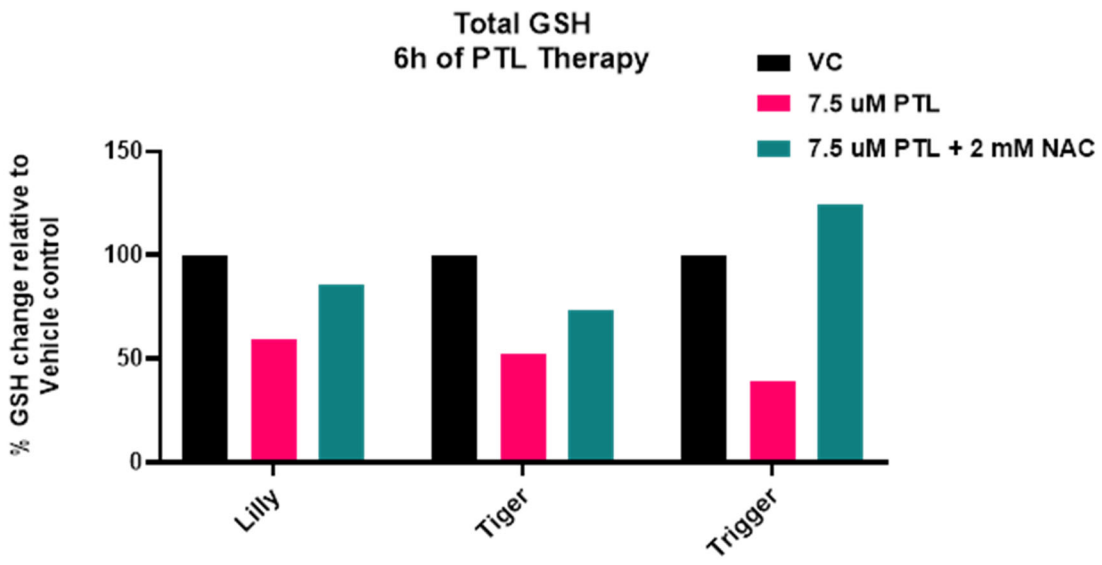

Figure 2.27: Canine primary B cell lymphoma cells experience GSH depletion with PTL therapy. This effect can be "rescued," to varying degrees, with NAC pre-treatment.

5. PTL in a mouse model of disseminated canine HS

To the author's knowledge, at the time of writing, a murine model of truly disseminated canine HS is not described in the literature. One major goal of this study was to develop this mouse model, to further allow additional research on this important and deadly disease in dogs. To mirror the most common clinical presentation of HS in dogs, the ideal model of disseminated HS would result in tumor formation at <30 days, with seeding in one or more abdominal organs, and/or evidence of tumor formation within lung tissue. To this end, injection of canine cells was attempted via three or four routes, depending on the experiment performed: intravenously (IV), intraperitoneally (IP), subcutaneously (SQ, as an experimental control), and in one experiment, intratibially (IT). This latter method was attempted since DH82 cells were originally derived from canine bone marrow, and it was thought that they might better engraft within a more hospitable microenvironment.

In the first experiment, three groups of four immunodeficient nude mice were used, and $1x10^6$ DH82 HS cells with a luciferase reporter were injected IV, IP, and SQ (left flank). Nude mice lack a thymus, and therefore do not have T cells, but have an intact immune system otherwise. Subcutaneous tumor assessment is made easier by the lack of fur. Notably, engraftment of hematopoietic tumors is often not successful in this host. Mice were anesthetized prior to imaging with a Xenogen IVIS imager. **Figure 2.28** shows luminescence of tumor cells 2 days post-injection of cells. Tumor viability (as estimated by luminescent imaging) appeared inconsistent, with two mice demonstrating no signal (one in the IP group, and one in the SQ group). Only one mouse in the IV group demonstrated signal that was not predominantly in the tail area, where cells had been injected. At 35 days post-injection, no appreciable signal was present in the IP or SQ injection groups. In the IV group, there was faint signal near the lung that was interpreted as potentially indicative of tumor development; however, when the tail signal was covered, no signal was evident, even following extended imaging (**Figure 2.29**). Some of the IP mice experienced weight loss, and all mice in these groups were humanely euthanized. There was no gross evidence of tumor development in these animals at necropsy.

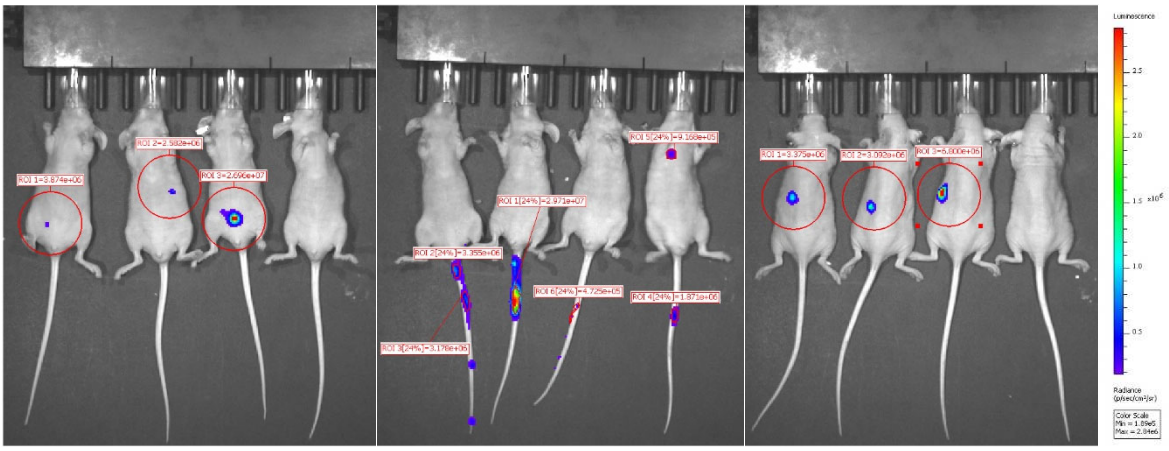

Figure 2.28*:* Mice were imaged 2 days post-injection. Although reasonably strong signal is present in 10/12 mice, the signal that is present appears inconsistent in both the IP and SQ groups of animals.

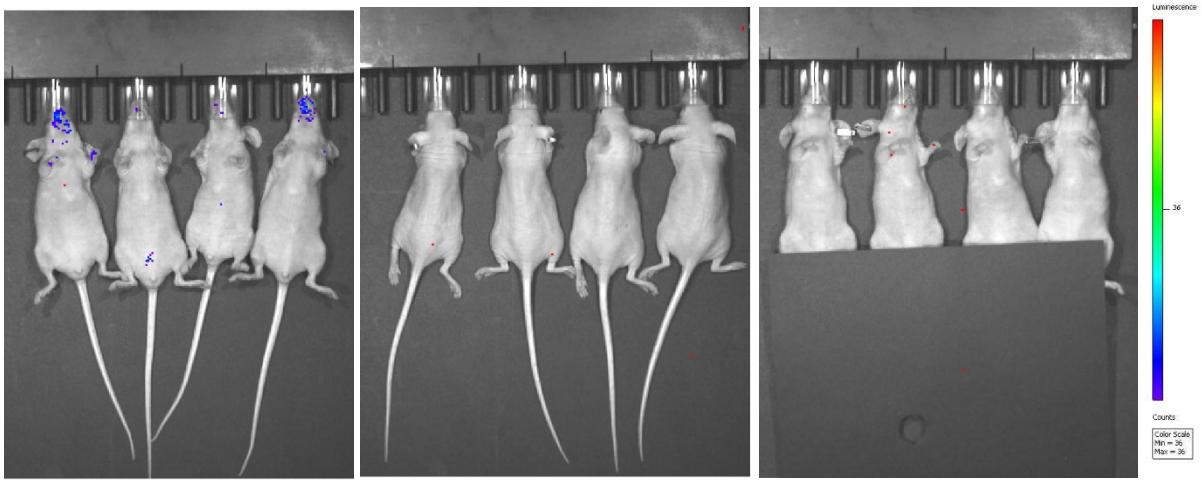

Figure 2.29: Mice were imaged 35 days post-injection. At this time, there was no tumor signal evident in the IP nor SQ groups of animals.

Mice from the original SQ and IV cohorts were re-challenged with DH82 HS cells ($5x10^6$ cells in the R flank of the SQ mice with Matrigel, Fisher Scientific, Hampton, NH; and $1x10^6$ cells in the IV mice). Representative images of luminescent cells in mice 2 days post-injection are shown in **Figure 2.30.**

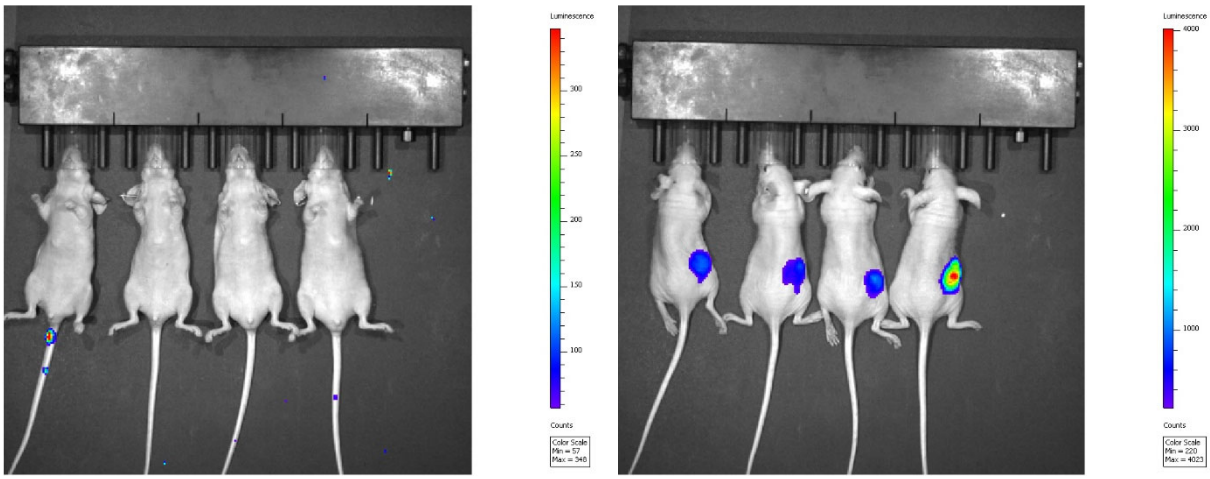

Figure 2.30: Mice re-challenged with DH82 HS luminescent cells, 2 days post-injection. Left: IV injection, in which only a small amount of signal is visible at the site of injection, near the tail vein; Right: SQ injection of 5x cells in Matrigel, using the opposite flank.

Twelve additional nude mice were ordered at this time for injection with NIKE luminescent HS cells ($1x10^6$ cells for IV and IP injections; $5x10^6$ cells for SQ injection with Matrigel). One mouse failed to thrive shortly after arrival, so was ultimately not used in these experiments. **Figure 2.31** shows the luminescence of NIKE HS cells in these mice.

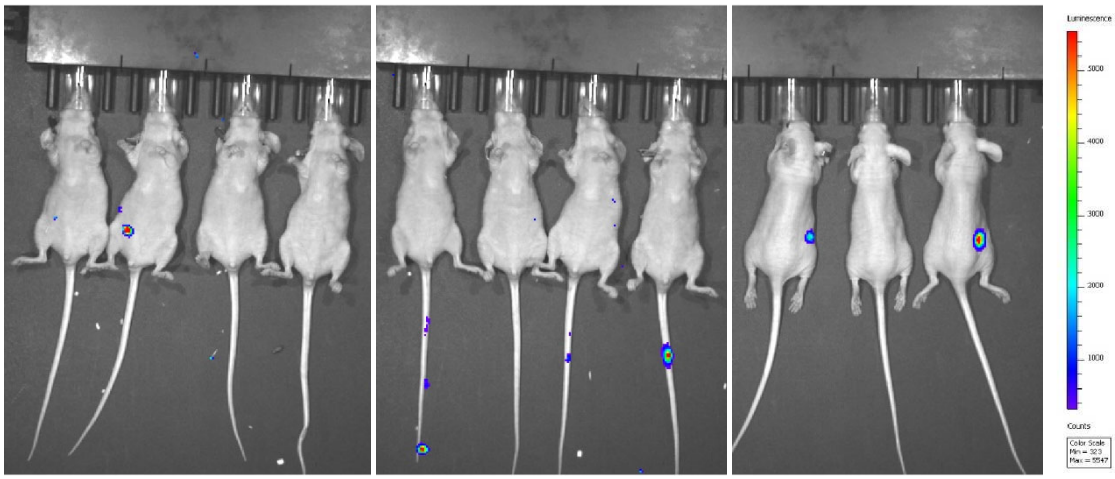

Figure 2.31: Nude mice injected with luminescent NIKE HS cells: from left to right: IP, IV, and SQ with Matrigel.

Although a luminescent signal was not detectable, at day 67, one mouse that had received NIKE cells IP was experiencing weight gain, general malaise, and subtle respiratory difficulty. The abdomen appeared noticeably “full” on visual examination (**Figure 2.32**). On necropsy examination, there was a single, white, firm mass lesion closely associated with the right kidney, which is likely the cause of weight gain in this mouse. Following necropsy, the abdominal mass from Mouse 311 was dissociated mechanically in collagenase, first manually with a scalpel blade, then with sterile metal beads and a stir bar on a magnetic plate at 37 degrees Celsius for 45 minutes. Following lysis of erythrocytes with ACK buffer, as previously described, cells were washed with PBS, then put into DMEM C/10 media for culture. After ~24 hours, these cells bore a physical resemblance to their cells of origin in culture (**Figure 2.32**). Cells passaged through the nude mouse were confirmed to be macrophagic in morphology via light microscopy of cytocentrifuged preparations (not shown).

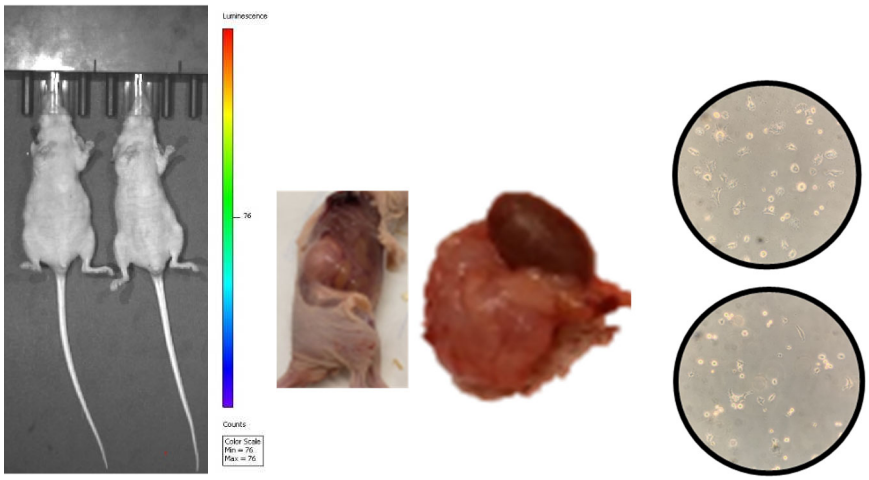

Figure 2.32: From L to R: Mouse 311, the mouse on the left, has a visually “full” abdomen compared to the adjacent mouse. Middle: Gross necropsy images of Mouse 311 showing the large mass lesion associated with the R kidney, which was contributing to palpable and visual abdominal enlargement. Right: cell culture images from a phase contrast microscope, 400x.

Cells on top are NIKE luminescent HS cells in culture, while those on the bottom are from the dissociated mass lesion from Mouse 311.

From this cohort of mice, only two mice ultimately developed tumors, while the remaining mice were euthanized due to weight loss or poor thrift over the course of the experimental period. These mice were DH82 SQ mouse (euthanized 67 and 91 days post-injection due to tumor growth and limited mobility, **Figure 2.33**).

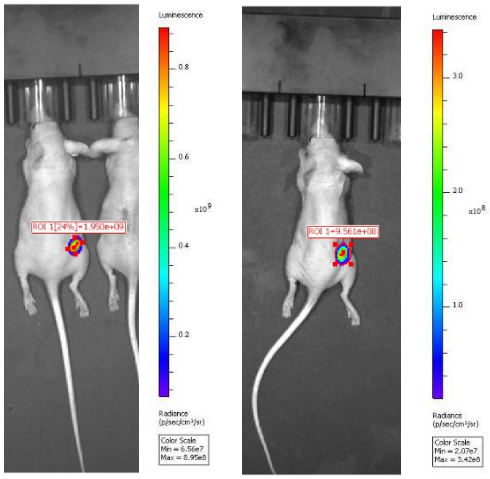

Figure 2.33: DH82 luminescent HS cells that were originally implanted in Matrigel in two immunodeficient nude mice.

Since tumor engraftment had been poor in the nude mouse model (3/29 attempts or ~10%), injection of tumor cells was attempted in a more immunodeficient murine host: the Balb/c scid mouse. Such mice are on a Balb/c genetic background and are homozygous for severe combined immune deficiency spontaneous mutation ($Prkdc^{scid}$ or “scid”). These mice do not have functional T cells or B cells but do have a normal hematopoietic microenvironment. For this experiment, cells with an NF-kB reporter were utilized. As both DH82 and NIKE HS cells have constitutive activity of NF-kB, tumor burden should theoretically be detectable with these cells via IVIS imaging. For these experiments, mice received $1x10^6$ cells IV or $5x10^6$ cells via IP, SQ, and intratibially/IT,

with Matrigel in the IP and SQ injection methods. The intratibial method was attempted in this cohort of mice since DH82 HS cells were originally derived from bone marrow, and it was though that they may prefer the bone marrow niche. **Figure 2.34** shows one of four Balb/c scid mice with luminescent DH82 and NIKE cells at days 4, 13, and 27 post-peritoneal injection. Each of the mice shown was the only one in the group that had detectable signal at day 4 that was maintained by day 27. Following this, signal was no longer detectable. These mice were euthanized due to the coronavirus pandemic.

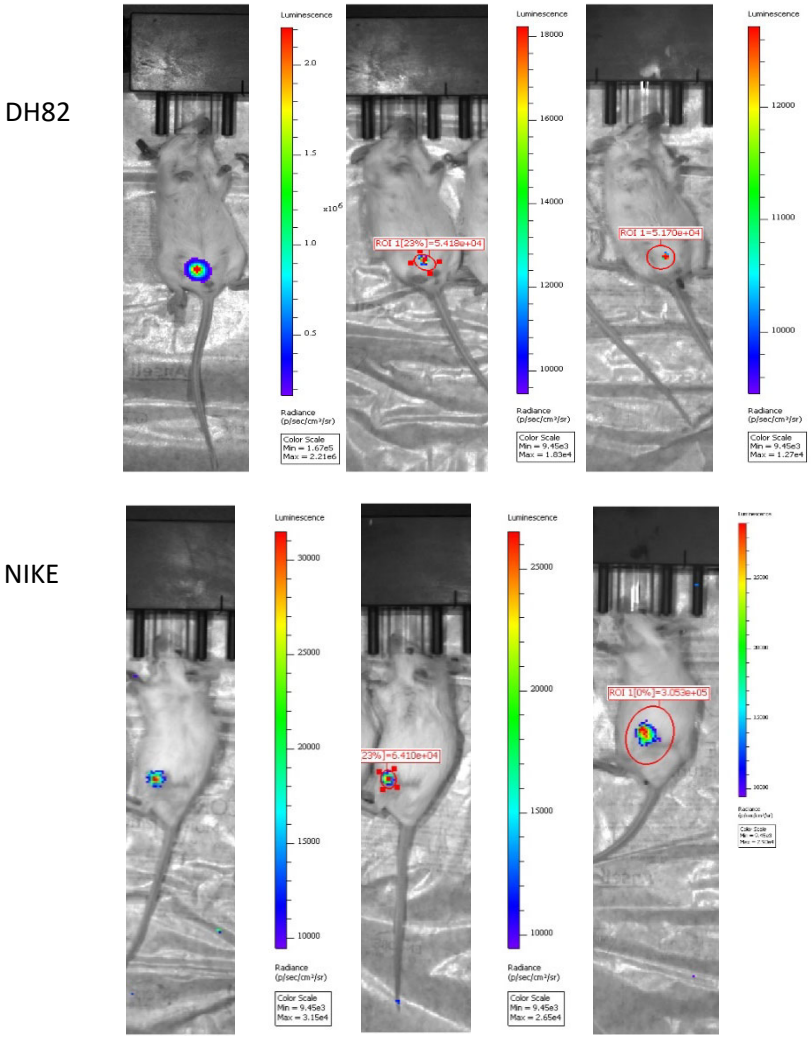

Figure 2.34 shows one of four Balb/c scid mice with luminescent DH82 and NIKE cells at days 4, 13, and 27 (from left to right) post-peritoneal injection. Each of the mice shown was the only one in the group that had detectable signal at day 4 that was maintained by day 27.

In addition, a single mouse with an intratibial injection of DH82 HS cells successfully developed a tumor and was euthanized 113 days after injection (**Figure 2.35**). The remaining mice that did not develop tumors were euthanized due to cessation of additional experiments during the coronavirus pandemic.

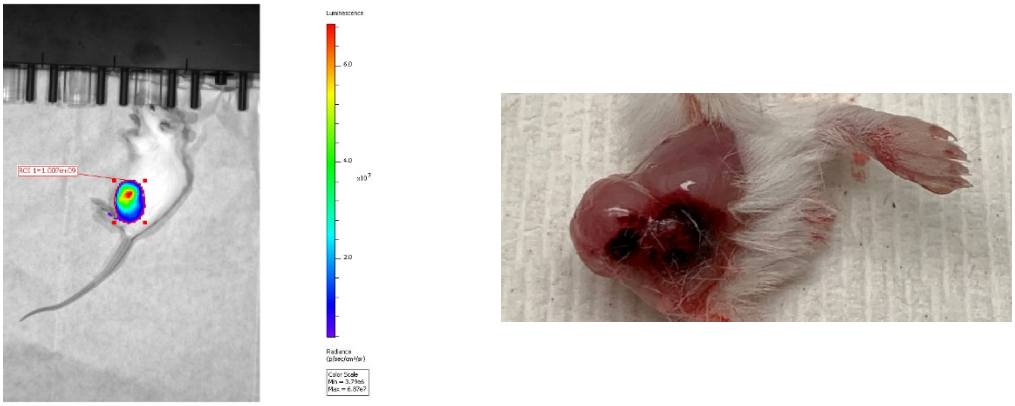

Figure 2.35: Luminescent and gross images from one of four mice that ultimately developed a mass lesion following injection of DH82 HS cells.

Two of four mice with subcutaneous DH82 HS tumors were euthanized due to tumor development. Cells were isolated with dissection and collagenase from one mouse (M353) with a particularly aggressively growing tumor. Around this time, the laboratory acquired another HS cell line from Dr. Steve Dow (MH588) and transfected this cell line with the NF-kB reporter plasmid, as previously described.

Since there was some evidence of increased xenograft success in a more immunocompromised mouse model, NOD SCID mice were used for the next HS cell injection study. These mice have impaired T and B cell development, as well as deficient natural killer (NK) cell function, but have a high incidence of thymic lymphoma, and a relatively shortened lifespan compared to some strains (~36 weeks). Mice were injected with DH82 HS cells (passaged through M353, and therefore referred to

hereafter as “M353” cells), and MH588 HS cells. Both cell lines exhibited strong NF-kB luciferase reporter activity prior to injection into mice intraperitoneally (with Matrigel), intravenously, and subcutaneously (with Matrigel). When injected subcutaneously, both of these cell lines produced small, subcutaneous tumors. This was the first mouse model with successful development of disseminated HS from intraperitoneal injection of M353 (DH82) cells, although tumor development followed a long latency period (>126 days). Both mice developed a malignant effusion with tumor masses in the peritoneal cavity.

Following greater success in the NOD SCID mouse model, and at the recommendation of Dr. Craig Jordan, this experiment was repeated in the NSG mouse model. Relative to NOD SCID mice, NSG mice have no functional NK cells, and have an extended natural lifespan (>89 weeks versus ~36 weeks). All mice in these groups, except for mice in the MH588 intravenous group, ultimately developed tumors. IP mice in both groups developed malignant effusions and exhibited lung tumor formation, while those in the IV group developed many tumors throughout lung tissue. Prior to euthanasia, mice were dosed via oral gavage with 100 mg/kg fumarate salt DMAPT (orally bioavailable PTL) dissolved in water, and luminescent imaging was performed before and after medication administration. Attenuation of luminescent signal, when initially present, was observed in most tumor-bearing mice evaluated (**Figure 2.36**). Intriguingly, the difference in luminescence was less dramatic for mice with subcutaneous tumors, which may be due to differences in tumor distribution (one large, solitary lesion versus many lesions distributed throughout the lungs and peritoneum). Cells from one DH82 HS/M353 mouse (M423) and one MH588 HS (M426) were

harvested from peritoneal effusions and re-expanded in cell culture for future use. Notably, the M423 cells appeared to grow very aggressively in culture, and many large and multinucleated cells were noted (**Figure 2.37**). It was thought that, perhaps, these cells may grow aggressively in an animal model as well.

Table 2.12: Time to tumor development in NSG mice. Each group contained 3 mice.

CELL LINE	MODEL	NUMBER OF CELLS USED	DAYS TO TUMOR DEVELOPMENT	ST DEV
MH588	IP	7.0E+06	69.0	29.4
	IV	1.0E+06	N/A	N/A
	SQ	7.0E+06	64.0	0.0
M353	IP	7.0E+06	67.7	16.2
	IV	1.0E+06	117.0	6.1
	SQ	7.0E+06	70.0	0.0

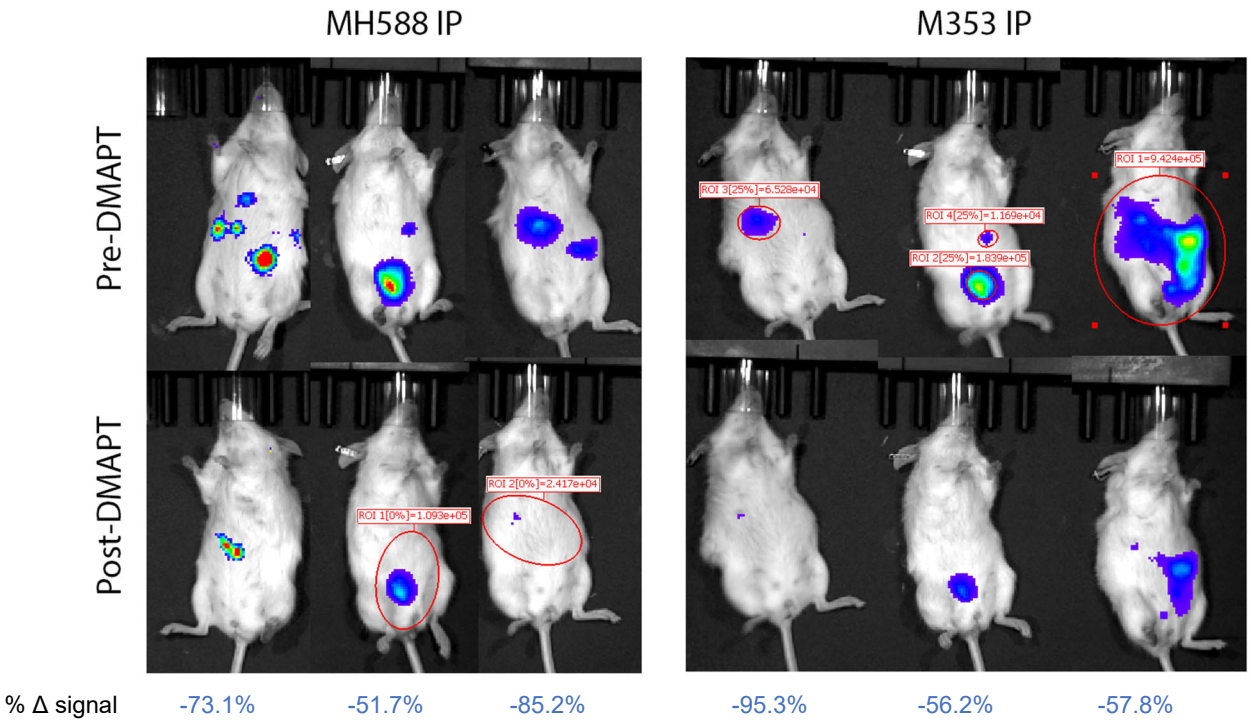

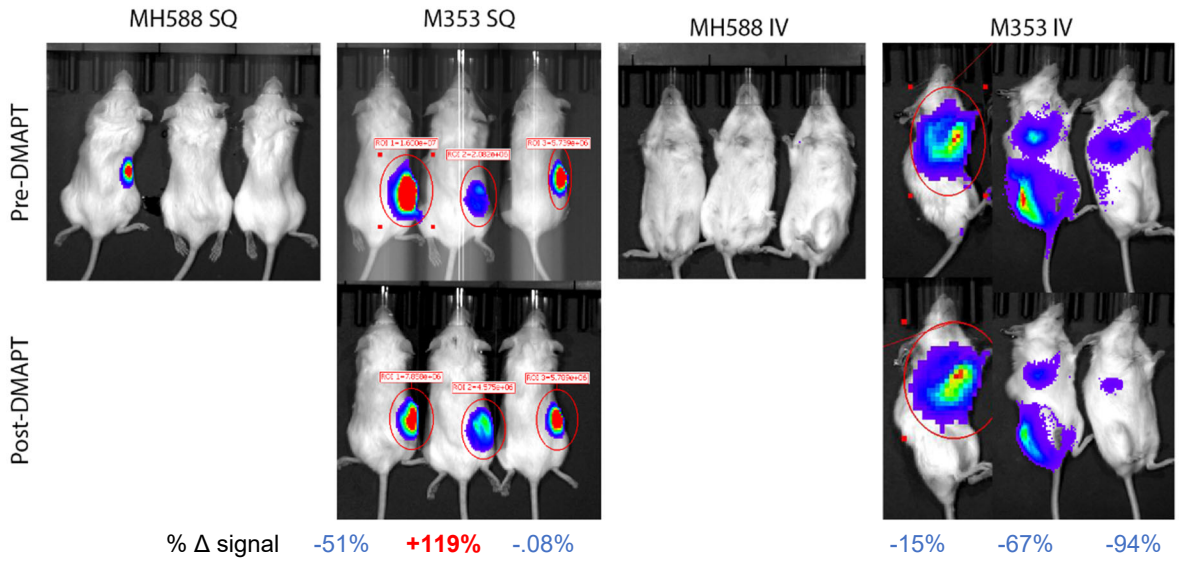

Figure 2.36: Top: Examples of luminescent DH82 HS tumors in mice injected with cells IP HS cells. Because cells were engineered with a p65/relA luciferase reporter plasmid, attenuation of active NF-kB signaling was expected with 4h of DMAPT therapy. Bottom: Left: subcutaneous tumor models in NOD SCID mice. Although MH588 SQ mice developed tumors, only one of these maintained luminescent signal. M353 SQ mice maintained luminescent signal throughout the tumor growth period, but there was an equivocal difference in the luminescent signal pre- and post-DMAPT administration. Right: MH588 IV mice never demonstrated luminescent signal in the lung area, even immediately following injection of tumor cells. M353 IV mice had luminescent signal from lung tumors (and in the middle mouse, from an area of thickened lumbar tissue that may have followed outgrowth from a tumor thrombus in circulation). This signal was attenuated, to varying degrees, with DMAPT therapy. Note that following DMAPT administration, the first mouse in this group had progressive respiratory distress, and euthanasia was performed only one-hour post-gavage. The luminescent signal range was fixed to the same minimum and maximum values in pre- and post-DMAPT images for each mouse.

At day 107, when mice in the MH588 IV group demonstrated no signal, mice were rechallenged with $15x10^6$ DH82 HS/M423 cells IP (cells passaged through a NOD SCID mouse that had an aggressive appearance cytologically). These mice developed malignant effusions at 20 +/- 6.6 days. STR analysis is pending to further define these cells as truly being of DH82 background. Prior to euthanasia, mice were imaged, and tumor cell luminescence was measured in counts. Mice were then dosed via oral gavage with 100 mg/kg fumarate salt DMAPT dissolved in water and were re-imaged four hours later prior to humane euthanasia. On gross examination and via

histopathology, mice had numerous nodules of tumor cells throughout the peritoneal cavity, and one of three mice had evidence of tumor formation in the R caudal lung, as well. The spleen was enlarged, and on histopathology, had evidence of erythroid-predominant extramedullary hematopoiesis, without evidence of tumor formation (**Figure 2.37**). The liver and spleen appeared grossly normal, aside from nodules adhered to the exterior surfaces of these organs. Luminescent images of these mice, pre- and post-DMAPT therapy, are shown in **Figure 2.38**.

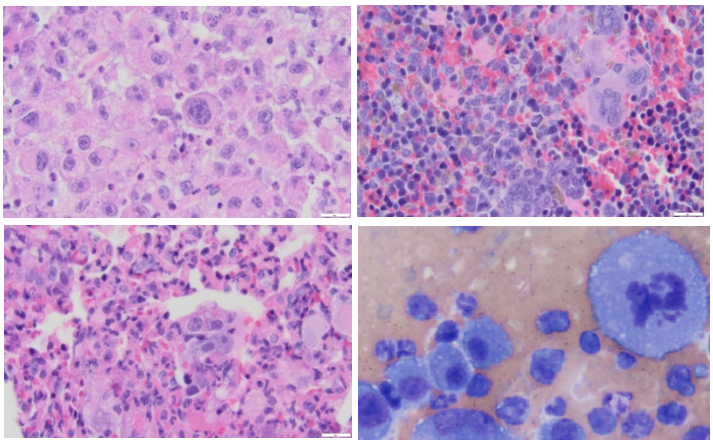

Figure 2.37: Top and bottom left: Histopathology images from M423, 400x, hematoxylin and eosin. Top left: abdominal mass lesion, containing many atypical HS cells. Top right: spleen, demonstrating extramedullary hematopoiesis. Bottom left: lung: demonstrating a marked, neutrophil-rich inflammatory response and infiltration of atypical HS cells. Bottom right: cytocentrifuged preparations of M353 HS cells, modified Wright-Giemsa stain, 1000x. Not the significant cellular pleomorphism in the neoplastic cell population, including a large and bizarre mitotic figure. Not shown: histologically normal liver.

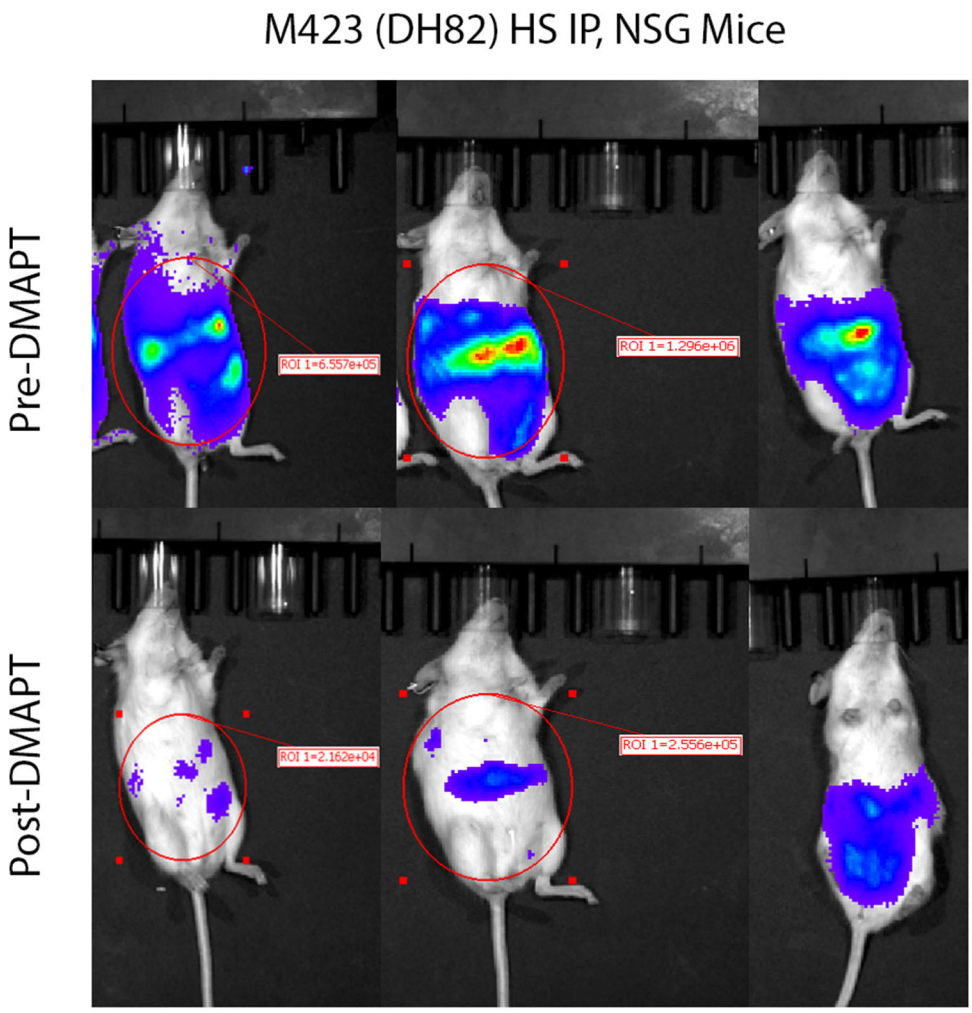

Figure 2.38: Mice imaged prior to (top), and following (bottom), 4 hours of DMAPT therapy. In this experiment, attenuation in luminescent signal was observed in all three mice evaluated. From left to right, the quantified signal attenuation was 97%, 90%, and 58%.

To further validate attenuation of constitutive NF-kB signaling in mice post-DMAPT therapy, cells from malignant effusions were collected at both time points, cytocentrifuged, and stained for RelA immunocytochemistry, as previously described (**Figure 2.39**).

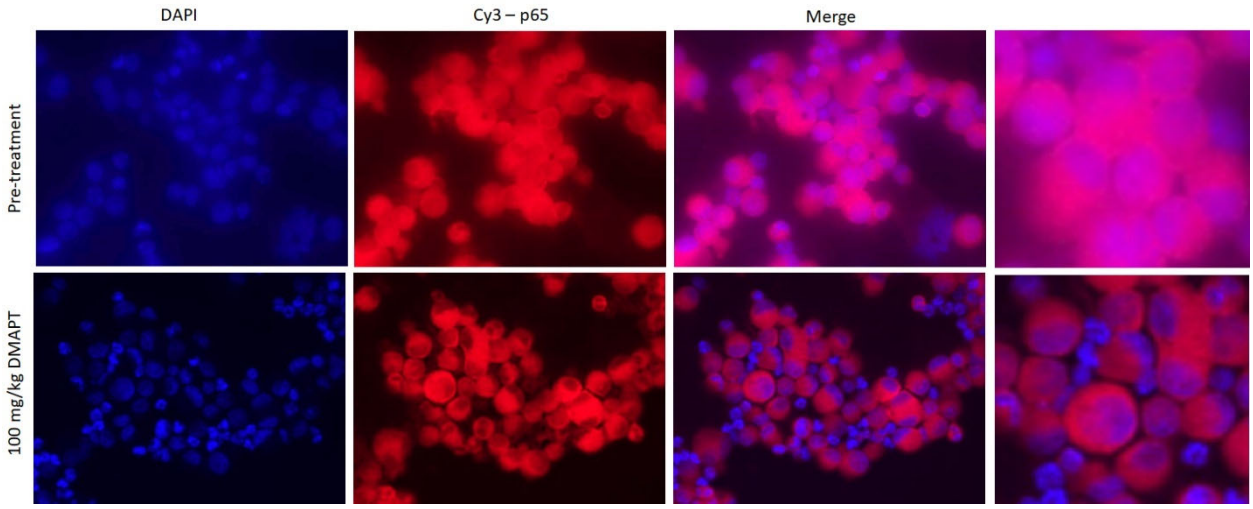

Figure 2.39: Cytocentrifuged cells from the malignant effusion of M421, pre- and post-DMAPT treatment. Note that, within intact cells, there is decreased overlap between red (NF-kB RelA/Cy3) and the cell nucleus (DAPI, blue) with DMAPT treatment, consistent with some inhibition of nuclear RelA translocation.

Discussion and Conclusions

Some outputs from these experiments are expected with PTL therapy. For example, data from RNA sequencing experiments demonstrate that, in canine HS cells treated with PTL for 6h and 24h, there is downregulation of NF-kB signaling, as determined by GSEA pathway analysis and identification of NF-kB target genes within these pathways. Following PTL treatment, canine HS, HSA, MCT, and lymphoma cell lines exhibit dose-dependent ROS generation, which is of much greater magnitude than is observed in normal, peripheral blood mononuclear cells. Some cell lines exhibit nuclear exclusion of p65/RelA with PTL therapy, consistent with downregulation of aberrant NF-kB signaling.

There are some significant limitations to the current study, and many questions remain unanswered.

Low numbers of genes were found to be differentially expressed in comparing PTL-sensitive to PTL-resistant cell lines; however, 3 of 4 identified GSEA Hallmarks pathways contain NF-kB target genes, which is suggestive of an NF-kB-mediated component of sensitivity in canine cancer cell lines.

Although primary patient cells were maintained in culture for a short period of time for collection, cell viability was not as robust as hoped, which limited the number of experiments that could be performed with each aliquot of cells. Most ideally, data would have been generated for each experiment using the same group of patient cells, with multiple replicate experiments, to allow more readily comparison between primary cells and cell lines. However, the data in this study do show that primary cells tend to behave in a similar fashion as compared to cell lines, and therefore are a useful, if imperfect, measure of behavior with PTL therapy.

While PTL exhibited synergism with two standard-of-care chemotherapeutics that were evaluated, the assessment of only two other compounds provides a narrow view of PTL's potential as a therapeutic in canine cancers. In the human literature, as reviewed extensively elsewhere, PTL exhibits broad synergism with a wide range of therapeutic compounds, and for a wide variety of hematopoietic and solid tumors, both *in vitro* and *in vivo*.[32,15,37,27,13,24] Because most canine cell lines are sensitive to PTL at single agent dose concentrations, there are many canine tumor types that may benefit from PTL therapy, alone, and likely in combination with other therapeutics. [24,32,15,37]

Additionally, while HO-1 induction was used as a surrogate measure of PTL's activity in this study, this induction is associated with oxidative resistance and may limit PTL's ultimate clinical application for some cancer types.[32] To interpret any meaningful

trend in oxidative resistance across cancer types, multiple cell lines, and ideally patient-derived samples, would be evaluated with this assay. Mechanisms of resistance may also be studied by evaluating genetic changes in cell lines that are made resistant over time against a chemotherapeutic. Cell lines made resistant to standard-of-care therapeutics and/or PTL may be useful in further understanding how resistance may develop and be overcome in the clinical setting.

While there is evidence that PTL alters cellular redox balance in some canine tumor types, and GSH and GPX activity suggest that mechanisms of action for this drug may be conserved between dogs and humans, this picture is incomplete by virtue of evaluation of only the glutathione system, as PTL isinhibitor of thioredoxin reductase.[39,5] As the thioredoxin system is often upregulated in human cancers, this presents yet another mechanism in which PTL may act and potentially target neoplastic cells in dogs, but was not explored in this study.[17] Additionally, as we were unable to confirm the role of glutathione peroxidases in PTL resistance (as is seen consistently across hundreds of human cancers), evaluation of changes in genetic expression across larger numbers of canine cancers will undoubtedly be beneficial in understanding likely vulnerabilities and mechanisms of resistance for many therapeutics, including PTL.

Although there is tentative success, it took much longer than anticipated to develop a canine xenograft model of disseminated HS in mice. A 4-arm experiment is in progress, in which mice with cells isolated from DH82/M423 have been injected with $15x10^6$ cells IP in 1:1 Matrigel (~4-6 mg/mL). Mice will be treated with vehicle, lomustine only, PTL only, or a combination of lomustine and PTL. For this experiment, survival is

the primary outcome. Following humane euthanasia, tissues will be evaluated for NF-kB localization and cleaved caspase 3 (for evaluation of apoptotic activity within tumors).

In conclusion, mechanistically, there is evidence that PTL inhibits NF-kB signaling in cancer cells, and that constitutive NF-kB activity is present in at least some types of canine cancer, and likely contributes to cancer-associated morbidity and mortality, as is seen in humans. Additionally, PTL's mechanisms of action in canine cells are similar to what has been observed in human tumor cells, namely, that NF-kB inhibition and alteration of redox balance are both evident in canine cancer cells.

PTL remains a promising therapeutic for canine cancers for a variety of reasons: it has multiple mechanisms of action, most canine cells (from cell lines and primary tumor cell samples) are sensitive to PTL at single agent doses that are well-tolerated in dogs *in vivo*, and PTL can readily be combined with standard-of-care chemotherapeutics, often with synergistic outcomes. These data provide a strong rationale for further evaluating DMAPT in murine models of disseminated canine diseases, and ultimately, moving DMAPT forward into clinical trials in dogs with naturally occurring cancers, especially if results from the pending xenograft study are promising.

References

1. Brasier AR. The nuclear factor-kappaB-interleukin-6 signalling pathway mediating vascular inflammation. *Cardiovasc Res*. 2010;86**:** 211-218.

2. Chavez ML, Chavez PI. Feverfew. *Hosp Pharm*. 1999;34**:** 436-461.

3. Dolcet X, Llobet D, Pallares J, Matias-Guiu X. NF-kB in development and progression of human cancer. *Virchows Archiv*. 2005;446**:** 475-482.

4. Drew R, Miners JO. The effects of buthionine sulphoximine (BSO) on glutathione depletion and xenobiotic biotransformation. *Biochem Pharmacol*. 1984;33**:** 2989-2994.

5. Duan D, Zhang J, Yao J, Liu Y, Fang J. Targeting Thioredoxin Reductase by Parthenolide Contributes to Inducing Apoptosis of HeLa Cells. *J Biol Chem*. 2016;291**:** 10021-10031.

6. Duran A, Linares JF, Galvez AS, et al. The signaling adaptor p62 is an important NF-kappaB mediator in tumorigenesis. *Cancer Cell*. 2008;13**:** 343-354.

7. Fang J, Sawa T, Akaike T, et al. In vivo antitumor activity of pegylated zinc protoporphyrin: targeted inhibition of heme oxygenase in solid tumor. *Cancer Res*. 2003;63**:** 3567-3574.

8. Ghantous A, Sinjab A, Herceg Z, Darwiche N. Parthenolide: from plant shoots to cancer roots. *Drug Discov Today*. 2013;18**:** 894-905.

9. Gounder M, Desai V, Kuk D, et al. Impact of surgery, radiation and systemic therapy on the outcomes of patients with dendritic cell and histiocytic sarcomas. *Eur J Cancer*. 2015;51**:** 2413-2422.

10. Guzman ML, Rossi RM, Neelakantan S, et al. An orally bioavailable parthenolide analog selectively eradicates acute myelogenous leukemia stem and progenitor cells. *Blood*. 2007;110**:** 4427-4435.

11. Ito D, Frantz AM, Williams C, et al. CD40 ligand is necessary and sufficient to support primary diffuse large B-cell lymphoma cells in culture: a tool for in vitro preclinical studies with primary B-cell malignancies. *Leuk Lymphoma*. 2012;53**:** 1390-1398.

12. Kayikcioglu E, Aydin AA, Onder AH, Sayiner A, Suren D, Ozturk B. An extremely rare neoplasm, histiocytic sarcoma: A report of two cases with an aggressive clinical course. *J Oncol Sci*. 2017;3**:** 84-86.

13. Kim S-L, Kim SH, Trang KTT, et al. Synergistic antitumor effect of 5-fluorouracil in combination with parthenolide in human colorectal cancer. *Cancer Letters*. 2013;335**:** 479-486.

14. Lai KS, Jin Y, Graham DK, Witthuhn BA, Ihle JN, Liu ET. A kinase-deficient splice variant of the human JAK3 is expressed in hematopoietic and epithelial cancer cells. *J Biol Chem*. 1995;270**:** 25028-25036.

15. Lamture G, Crooks PA, Borrelli MJ. Actinomycin-D and dimethylamino-parthenolide synergism in treating human pancreatic cancer cells. *Drug Dev Res*. 2018;79**:** 287-294.

16. Lim K-H, Tefferi A, Lasho TL, et al. Systemic mastocytosis in 342 consecutive adults: survival studies and prognostic factors. *Blood*. 2009;113**:** 5727-5736.

17. Lincoln DT, Ali Emadi EM, Tonissen KF, Clarke FM. The thioredoxin-thioredoxin reductase system: over-expression in human cancer. *Anticancer Res*. 2003;23**:** 2425-2433.

18. Livak KJ, Schmittgen TD. Analysis of relative gene expression data using real-time quantitative PCR and the 2(-Delta Delta C(T)) Method. *Methods*. 2001;25**:** 402-408.

19. Modi NT, Chen L-F. Measuring NF-κB Phosphorylation and AcetylationAcetylation. In: Franzoso G, Zazzeroni F, eds. *NF-κB Transcription Factors: Methods and Protocols*. New York, NY: Springer US; 2021:3-17.

20. Montagnier L, Olivier R, Pasquier C. *Oxidative Stress in Cancer, AIDS, and Neurodegenerative Diseases*, 1 ed.CRC Press; 1998.

21. Motolani A, Martin M, Sun M, Lu T. Phosphorylation of the Regulators, a Complex Facet of NF-κB Signaling in Cancer. *Biomolecules*. 2021;11**:** 15.

22. O'Donoghue LE, Rivest JP, Duval DL. Polymerase chain reaction–based species verification and microsatellite analysis for canine cell line validation. *J Vet Diagn Invest* 2011;23**:** 780-785.

23. Pareek A, Suthar M, Rathore GS, Bansal V. Feverfew (Tanacetum parthenium L.): A systematic review. *Pharmacogn Rev*. 2011;5**:** 103-110.

24. Patel NM, Nozaki S, Shortle NH, et al. Paclitaxel sensitivity of breast cancer cells with constitutively active NF-κB is enhanced by IκBα super-repressor and parthenolide. *Oncogene*. 2000;19**:** 4159-4169.

25. Pei S, Minhajuddin M, D'Alessandro A, et al. Rational Design of a Parthenolide-based Drug Regimen That Selectively Eradicates Acute Myelogenous Leukemia Stem Cells. *J Biol Chem*. 2016;291**:** 21984-22000.

26. Pradère J-P, Hernandez C, Koppe C, Friedman RA, Luedde T, Schwabe RF. Negative regulation of NF-kB p65 activity by serine 536 phosphorylation. *Sci Signal*. 2016;9**:** ra85-ra85.

27. Rad AT, Hargrove D, Daneshmandi L, Ramsdell A, Lu X, Nieh M-P. Codelivery of Paclitaxel and Parthenolide in Discoidal Bicelles for a Synergistic Anticancer Effect: Structure Matters. *Adv Biomed Res*. 2022;2**:** 2100080.

28. Saccani S, Marazzi I, Beg AA, Natoli G. Degradation of promoter-bound p65/RelA is essential for the prompt termination of the nuclear factor kappaB response. *J Exp Med*. 2004;200**:** 107-113.

29. Serasanambati M, Chilakapati SR. Function of Nuclear Factor Kappa B (NF-kB) in human diseases- A Review. *South Indian J Biol Sci*. 2016;2**:** 368.

30. Sica A, Dorman L, Viggiano V, et al. Interaction of NF-kappaB and NFAT with the interferon-gamma promoter. *J Biol Chem*. 1997;272**:** 30412-30420.

31. Son YH, Jeong YT, Lee KA, et al. Roles of MAPK and NF-kappaB in interleukin-6 induction by lipopolysaccharide in vascular smooth muscle cells. *J Cardiovasc Pharmacol*. 2008;51**:** 71-77.

32. Sztiller-Sikorska M, Czyz M. Parthenolide as Cooperating Agent for Anti-Cancer Treatment of Various Malignancies. *Pharmaceuticals*. 2020;13**:** 194.

33. Tirumurugaan KG, Kang BN, Panettieri RA, Foster DN, Walseth TF, Kannan MS. Regulation of the cd38 promoter in human airway smooth muscle cells by TNF-alpha and dexamethasone. *Respir Res*. 2008;9**:** 26.

34. Vandeputte C, Guizon I, Genestie-Denis I, Vannier B, Lorenzon G. A microtiter plate assay for total glutathione and glutathione disulfide contents in cultured/isolated cells: performance study of a new miniaturized protocol. *Cell Biol Toxicol*. 1994;10**:** 415-421.

35. Vincenti MP, Coon CI, Brinckerhoff CE. Nuclear factor kappaB/p50 activates an element in the distal matrix metalloproteinase 1 promoter in interleukin-1beta-stimulated synovial fibroblasts. *Arthritis Rheum*. 1998;41**:** 1987-1994.

36. Wiedhopf RM, Young M, Bianchi E, Cole JR. Tumor Inhibitory Agent from Magnolia grandiflora (Magnoliaceae) I: Parthenolide. *J Pharm Sci*. 1973;62**:** 345.

37. Wyrebska A, Gach K, Janecka A. Combined Effect of Parthenolide and Various Anti-cancer Drugs or Anticancer Candidate Substances on Malignant Cells in vitro and in vivo. *Mini Rev Med Chem*. 2014;14**:** 222-228.

38. Yun B-R, Lee M-J, Kim J-H, Kim I-H, Yu G-R, Kim D-G. Enhancement of parthenolide-induced apoptosis by a PKC-alpha inhibition through heme oxygenase-1 blockage in cholangiocarcinoma cells. *Exp Mol Med*. 2010;42**:** 787-797.

39. Zhang J, Duan D, Osama A, Fang J. Natural Molecules Targeting Thioredoxin System and Their Therapeutic Potential. *Antioxid Redox Signal*. 2021;34**:** 1083-1107.

CHAPTER 3: IMMUNOHISTOCHEMICAL CHARACTERIZATION OF NF-KB ACTIVATION IN CANINE NEOPLASMS

Overview

NF-kB proteins are a family of structurally related, eukaryotic transcription factors that have 400+ genetic targets, and are involved in many vital cellular processes, including innate immunity, inflammatory responses, development, cellular growth, and survival. Not surprisingly, overactivation of NF-kB is a feature of many chronic disease processes, including cardiac disease, neurodegenerative disease, immune-mediated disease, and cancer. While NF-kB overactivation has been documented extensively in human oncology, there is a relative paucity of data documenting the same phenomenon in veterinary medicine. Therefore, large scale validation of NF-kB performed via immunohistochemistry of 215 tumor samples (lymphoma, HS, HSA, and MCT). Antibodies were validated for use via western blot, immortalized cell pellets, and evaluation of normal canine tissues. Results of this study show that many spontaneous canine tumor samples have nuclear p65 and p100/p52 IHC staining that is of greater magnitude than observed in comparable, normal cell populations, indicating the promise of therapeutics that target aberrant NF-kB signaling, including parthenolide.

Introduction

As previously discussed, disseminated neoplasms pose a significant challenge in both humans and animals. More specifically, disseminated mast cell neoplasia (MCT), hemangiosarcoma (HSA), and histiocytic sarcoma (HS) are uniformly deadly in both

humans and dogs, despite medical interventions available for these diseases.[1,2,4,5,12,13,17,16,18,27,21,28,29,32,36] while actively benefitting the canine population. Other diseases, such as lymphoma, while common in both humans and dogs, share remarkable cross-species similarities.[10,15] The use of naturally occurring canine cancers can be used as a model to accelerate research for diseases that otherwise receive little attention in humans (so called “orphan diseases”[22]), and for diseases that are more common, but are biologically and molecularly similar.[10,15]

Some evidence in canine cell lines and in the literature, as outlined in Chapters 1 and 2, supports constitutive NF-kB signaling as a druggable target in both canine and human tumors. To further demonstrate the potential roles of these proteins in canine cancer, large-scale validation of NF-kB as a potential therapeutic target was undertaken across 215 tumors in dogs, including 29 MCTs, 91 HS, 85 lymphomas, and 10 HSAs. To further understanding of the implications of NF-kB overactivation in canine tumors, outcome data, when available, and other tumor features (such as mitotic index, anatomic location), were evaluated in combination with tumor NF-kB immunohistochemical (IHC) nuclear staining grade and nuclear to cytoplasmic (N:C) ratio staining.

Relative to normal mast cells, dendritic cells, endothelial cells, and lymphocytes, respectively, NF-kB p65 and p52 nuclear staining were more prevalent in histologically diverse tumor types, further documenting overactive NF-kB signaling in canine tumors. Greater nuclear p65 staining was associated with a shorter progression free interval (PFS) and overall survival (OS) in canine lymphomas and correlated with Ki67 IHC (a proliferative marker) in canine MCTs.

Materials and methods

Cell lines

The canine cancer cell lines utilized in this study were generously provided by researchers at other institutions, purchased from the American Type Culture Collection (ATCC), or established from tumor samples in-house (**Table 3.1**). Note that the information in Table 3.1 is repeated from Chapter 1 but has been repeated here for reference to the specific cell types used in this study. Cells were maintained in appropriate media for the cell line, as previously detailed in Chapter 1. Cell lines were authenticated via short tandem repeat analysis and a multispecies multiplex PCR assay (as previously described),[20] and confirmed to be mycoplasma-free prior to use in assays.

Table 3.1: Canine cell lines evaluated in this study.

CELL LINE NAME	CANCER TYPE	SOURCE	BREED
SB-HSA	Hemangiosarcoma	UWM (E. Dickerson)	German Shepherd
DH82	Histiocytic Sarcoma	ATCC	Golden Retriever
NIKE / MH	Histiocytic Sarcoma	MSU (B. Kitchell)	Not collected
CLL1390	Leukemia	UCD (P. Moore)	Not collected
1771	Lymphoma	UPENN (K.A. Jeglum)	Not collected
CLBL1	Lymphoma	Aus (B. Rutgen)	Bernese Mountain Dog
BRMCT	Mast Cell	UCSF (W. Gold)	Not collected
C2MCT	Mast Cell	UCSF (W. Gold)	Not collected

Aus: Veterinary University of Austria. MSU: Michigan State University. UCSF: University of California San Francisco. UCD: University of California-Davis. UPENN: University of Pennsylvania. UWM: University of Wisconsin-Madison.

Antibodies

The following are antibodies that were used in this study. Because no NF-kB pathway antibodies had been evaluated by Abcam for efficacy in canine cells, all antibodies used were purchased as part of the Abtrial or Novus Biologics trial program, and expression was successful to varying degrees.

Table 3.2: Antibodies

ANTIBODY CATALOG NUMBER	SOURCE	TARGET	NF-KB PATHWAY	DILUTION(S) USED	ANTIGEN RETRIEVAL
AB16502	Abcam	p65/RelA	Canonical	0.5 ug/mL (WB), 1:5,000 (IHC)	Heat
NB100-82063	Novus Biologics	p100/p52	Alternative	1:1,000 (WB), 1:200 (IHC)	Heat
AB8227	Abcam	Beta-Actin	N/A	1:2,500 (WB)	

Western blot

Cells were plated at ~75% confluency in T25 flasks with C/10 media 24 hours prior to treatment. The following day, cells were washed with PBS, collected either via cell scraping (CLBL1, C2 cells) or trypsinization (DH82, SB), as appropriate. For DH82 and SB, cells were washed with PBS and then exposed to 1 mL trypsin for 5 minutes to detach them from the culture plate. 2 mL C/10 media were added to neutralize trypsin. Collected cells were centrifuged at 1,400 rpm for 5 minutes. The trypsin/media supernatant was removed from pelleted cells, and cell pellets were resuspended in 1 mL PBS in a 1.5 mL Eppendorf tube. Cells were then centrifuged at 10,000 rpm at 4 degrees Celsius for 5 minutes. After discarding the PBS supernatant, cells were homogenized with 150 µL of buffer containing M-PER protein extraction reagent (Pierce), 1 mM $NaVO_4$, 1 mM PMSF, Complete Mini Protease Inhibitor (Roche), and 1%

SDS. The cell homogenate was placed on ice for 10 minutes, and lysates were passed through a 25-gauge needle 5 times. Following centrifugation at 10,000 rpm at 4 degrees Celsius for 5 minutes, the supernatant was used to measure cellular protein concentrations, using the BCA protein kit (Bichinchoninic Acid kit, Pierce, Rockford, IL). For evaluation of NF-kB p65 and IKBa expression, 25-30 ug samples of cells were electrophoresed into a denaturing 4-12% Bis-Tris gel (Invitrogen, Carlsbad, CA), and were transferred electrophoretically to a polyvinylidene difluoride (PVDF) membrane. Membranes were blocked with SuperBlock™ (PBS) Blocking Buffer (Thermo Fisher Scientific, Waltham, MA) for one hour at room temperature, followed by incubation of primary antibody (as indicated in **Table 3.2**) overnight on a rocker, in blocking solution at 4 degrees Celsius. After three washes in TBST, membranes were incubated in a 1:20,000 dilution of HRP-conjugated goat anti-rabbit IgG for 1 hour at room temperature. Immunoreactive proteins were detected using SuperSignal® West Pico Chemiluminescent Substrate (Pierce) and was analyzed via autoradiography. Beta-Actin was used as a loading control; this antibody was incubated for 1 hour at room temperature followed by incubation with secondary antibody, as previously described. Relative band intensity was measured in ImageLab computer software (Bio-Rad Laboratories, Hercules, CA).

Determination of c-kit mutation status, Ki67 IHC, and c-kit IHC

Many of the MCTs identified for use in this study were diagnostic samples from the CSU diagnostic laboratory, and had pre-existing MCT panel data available, which included mitotic index, *c-kit* mutation status, Ki67 IHC, and KIT IHC. For tumors in which

these data were not readily available, tumor blocks were given to the CSU diagnostic laboratory and Clinical Immunology Laboratory (A. Avery) to complete these tests, as had been done previously for other tumor blocks in this set.

Preparation of cell blocks for immunohistochemistry

Cells were grown to near confluence (~90%) in T175 culture flasks and were treated with DMSO (vehicle control) or 10 μM parthenolide (PTL) for 6 hours. Cells were harvested (via cell scraping or trypsinization, as appropriate), then washed with PBS. Cells were suspended in 10% buffered formalin in an Eppendorf tube for 15 minutes to ensure fixation. Following fixation, cells were rinsed in PBS, centrifuged, then resuspended in ~150 μL of 1% agarose gel. Pellets of gel containing cells were pipetted into the caps of fresh Eppendorf tubes and allowed to cool on ice. Following cooling, gel discs were pipetted into the caps of Eppendorf tubes, then gently removed with a #10 blade. Gel discs were paraffin-embedded using standard methods, by the Colorado State University histopathology laboratory.

Preparation of tissue microarrays

The Colorado State University Veterinary Diagnostic Laboratory database was searched to identify histologically normal tissues, as well as histiocytic sarcoma and mast cell tumor cases. Mast cell tumor cases were selected to have tumors of varying histologic grades (Patnaik and Kuipel), as well as representation of cutaneous and non-cutaneous tumors. Histiocytic sarcoma cases were selected to ensure broad

representation across anatomical locations, and to the extent possible, breeds of dogs. Lymphoma and hemangiosarcoma blocks were available from previous patient study populations.

Tissue microarrays were prepared using EZ-TMA 120-well, 1.5 mm, recipient blocks (IHC World, Woodstock, MD). Tumor cores were taken with a 1.5 mm biopsy punch and were gently extruded with a metal stylette. Paraffin embedding was performed by the Colorado State University Veterinary Diagnostic Laboratory, as per recipient block manufacturer instructions.

Immunohistochemistry

Tissue blocks were sectioned at 5 microns, then mounted on Superfrost Plus slides (Fisher Scientific, Hampton, NH) and immunolabeling for p65 and p100/p52 was performed using standard methods. Tissue slides were de-paraffinized in xylenes and re-hydrated with a series of graded alcohols. Briefly, antigen retrieval was performed, as outlined in **Table 3.1**. Tissues were blocked for endogenous peroxidase by incubation in 3% hydrogen peroxide for 5 minutes. Sections were incubated with primary antibodies, as outlined in **Table 3.1**. Detection was performed using the universally labeled streptavidin-biotin2 system (Dako, Carpinteria, CA), which uses a mixture of biotinylated goat anti-mouse and anti-rabbit IgG secondary antibodies followed by horseradish-labeled streptavidin. A universal negative control was used for each antibody evaluated. Positive staining was visualized with DAB chromogen substrates.

Semi-quantitative grading of IHC staining

Immunohistochemical grading was performed using a semi-quantitative scoring scheme for nuclear and cytoplasmic staining. For assessment of both normal tissues and tumor tissues, a semi-quantitative grading scheme was developed and used, with all grading performed by one observer (LJS). To ensure reproducibility, cores to be graded were determined via a random number generator. In each core, 200 cells were graded according to the scheme outlined in **Figure 3.1** for nuclear and cytoplasmic reactivity. Cells were considered negative for IHC staining if they appeared similar to the universal negative controls for those antibodies. The number of cells mildly/slightly, moderately, or strongly immunoreactive for the antibodies in question were recorded. Using the following equation, nuclear and cytoplasmic scores were calculated for each tumor core within these microarrays:

*IHC score = (# of negative cells * 0) + (# of 1+ cells *1) + (# of 2+ cells * 2) + (# of 3+ cells * 3)*

Based on the IHC scores generated for normal tissues, thresholds were set for low, moderate, and high nuclear and cytoplasmic staining, respectively. Each core was graded twice, to ensure that the overall grading nuclear and cytoplasmic scores did not differ among assessments. If a tumor core's nuclear or cytoplasmic score was not in agreement between these two scoring events, it was regraded.

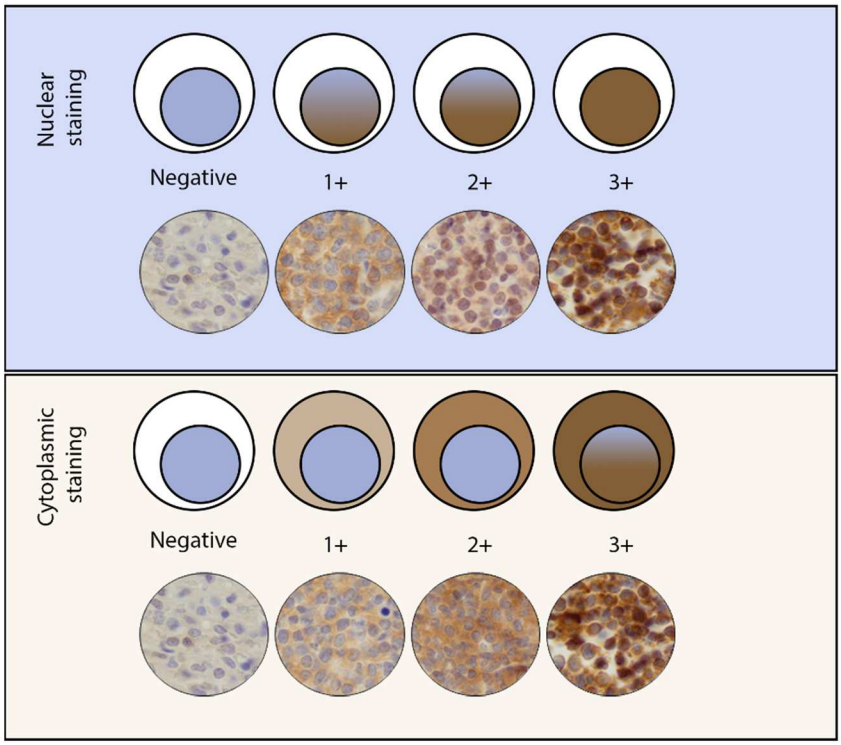

Figure 3.1: Graphic and microscopic examples (Hematoxylin and DAB, 400x) of criteria used to score each cell for nuclear and cytoplasmic reactivity.

Control tissues

Immunohistochemistry of lymphocytes within normal lymphoid tissues was used to set the threshold for evaluation of neoplastic lymphocyte activation of NF-kB.

Because some of the normal cell counterparts are found in relatively low numbers in the normal canine body, it was initially challenging to identify appropriate controls. For example, although large numbers of mast cells may be present in atopic skin, which could potentially be used as a “normal” tissue control, the NF-kB activation status of mast cells in this environment may be increased relative to normal, resting mast cells. While dendritic cells are ubiquitous in the body, locating large numbers of these cells is challenging.

As most HS are derived from antigen presenting cell (APC) dendritic cells, normal dendritic cells were identified in lymphoid tissues (spleen and peripheral lymph nodes), based on their location relative to lymphoid follicles, as well as physical appearance. Normal mast cells were identified in lymphoid tissues, as well as perivascularly in normal canine skin sections. For HSA, normal endothelial cells within lymph nodes were used as staining controls.

Correlation with other case data

The relative staining intensities of tumors for NF-kB signaling partners were compared with factors that may influence a tumor's biologic behavior, either in theory or as previously demonstrated in the literature or by patient outcomes in our data sets.

For lymphoma microarrays, tumor cores were taken from a pre-curated set of paraffin-embedded tissues that had been used previously in another study. In this previous study, tissues from sixty-four dogs with naïve multicentric B-cell lymphoma were treated with a standardized, 19-week, CHOP (cyclophosphamide, doxorubicin, vincristine, and prednisone) chemotherapy protocol, and outcome data were recorded for these patients.[35]

HS and HSA samples were taken from diagnostic laboratory biopsy and necropsy samples, and thus, follow-up data were largely unavailable. When available, IHC grading was evaluated with respect to the anatomic location of the tumor and/or the mitotic index.

Outcome data were similarly not available with respect to the MCTs used in this study; however, for most tumors evaluated, we had access to KIT IHC localization data,

c-kit mutational status, Kuipel and Patnaik grades (for cutaneous tumors), mitotic index, and anatomic location of the tumor.

Statistical analyses

Correlations between continuous variables (MI and nuclear p65 score, as well as nuclear to cytoplasmic p65 ratio) were computed by means of the Spearman rank-correlation coefficient. The Kruskal-Wallis nonparametric analysis of variance was used to determine the significance levels of differences between groups of continuous variables after stratification on categorical variables (such as tumor grade or anatomical site of origin). When two groups of continuous variables were used after stratification on categorical variables, a Mann-Whitney nonparametric test was used. Pre- and post-CHOP treatment immunoreactivity was compared in lymphoma cores using a 2-tailed, paired Mann-Whitney test. The Kaplan-Meier method was used to estimate progression free interval (PFI) and overall survival time (OST). Impact of p65 score and ratio on outcome (PFI and OST) were assessed using log rank and Cox proportional hazards methods. Statistical analyses were performed in SPSS Software (Armonk, NY) and GraphPad Prism Software (San Diego, CA).

Results

Western analysis

The antibody for total NF-kB RelA/p65 (ab16502) had been previously validated in canine cell lines while investigating phospho-RelA and phospho-IKBa activity in the

previous chapter (see **Figure 2.5**). Multiple antibodies for the alternative NF-kB signaling pathway (p100, p52, or both p100 and p52) were initially evaluated on a trial basis. The antibody with the strongest signal is presented in **Figure 3.2** and was used for subsequent evaluation. Based on this initial screening experiment, most canine hematopoietic cell lines had evidence of p100 and p52 proteins with this antibody, to varying degrees.

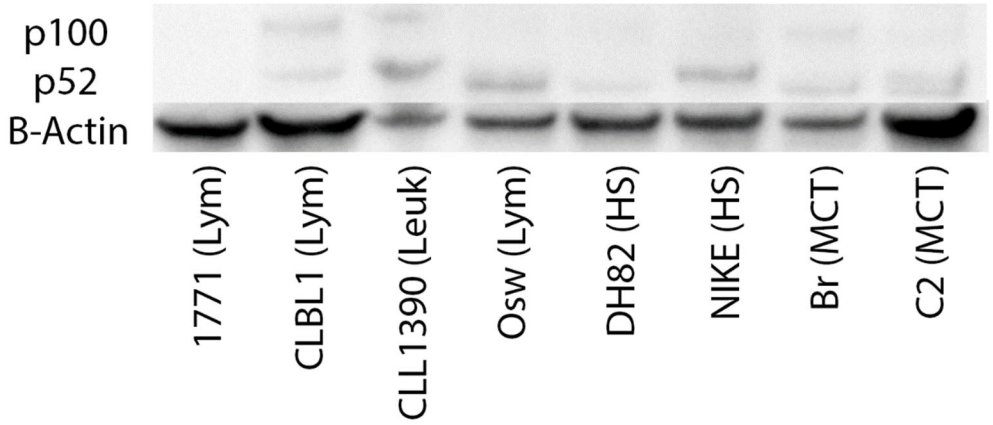

Figure 3.2: Western blot: For multiple canine hematopoietic cell lines, bands were observed at molecular weights of 100 and ~52 kDa, consistent with the molecular weights of NF-kB p100 and p52, respectively.

Cell pellet immunohistochemistry

Cell pellets from various canine cell lines (as shown in **Figure 3.3**) were evaluated for expression of NF-kB RelA/p65 and p100/p52 via IHC. It appeared that there was some noticeable decrease in nuclear p65 staining intensity with PTL treatment in DH82 (HS) and SB (HSA) cell lines. There was, perhaps, a slight difference in p65 nuclear staining intensity in the other cell lines. These results appear consistent with ICC using the same antibody (see **Figure 2.8**, previous chapter), except that in the

SB cell line, the result via IHC appears slightly more dramatic than is observed via ICC. All cell lines evaluated appeared to have strong nuclear staining localization of p100/p52. IHC pellets from cells treated with PTL appeared similar to vehicle control. This is expected since, to the author's knowledge, PTL is not an inhibitor of the alternative NF-kB signaling cascade.

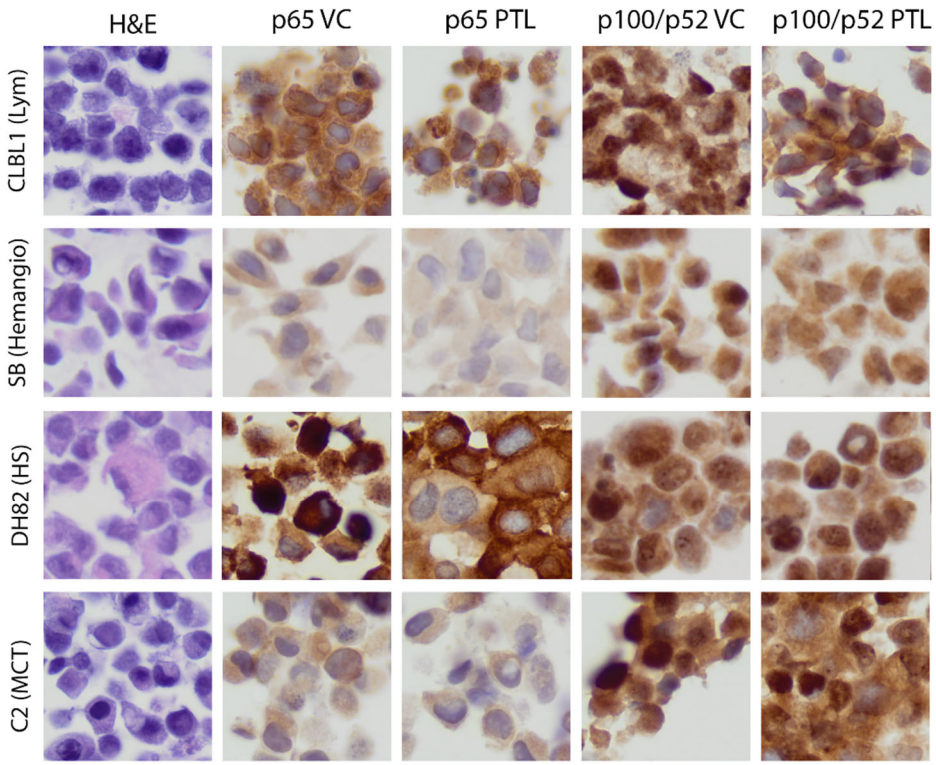

Figure 3.3: Hematoxylin and eosin (left-most panel) and DAB chromogen immunohistochemistry (IHC) (remaining panels), 400x. IHC of canine cell line cell pellets. Inhibition of nuclear translocation with NF-kB canonical signaling is evident in DH82 (HS) and to a lesser extent, in SB (HSA) cells. There is a possible slight difference in nuclear p65 staining in the other two cell lines (versus normal variation in staining). Staining for alternative NF-kB signaling cascade members (p100/p52) appears similar between control and treatment conditions for PTL, as expected (as PTL is only documented to inhibit the canonical pathway).

Assessment of normal and tumor tissues with IHC

Examples of normal tissue controls are shown in **Figure 3.4**.

Tumor	Normal tissue control	Normal tissue stained with p65	Normal tissue stained with p100/p52
Lymphoma	Normal lymph node	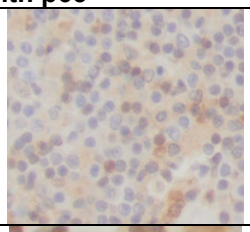	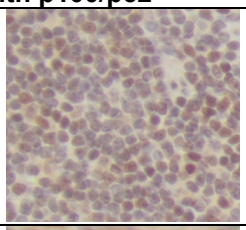
Histiocytic Sarcoma	Dendritic cells from the light zones of germinal follicles in spleen and lymph node	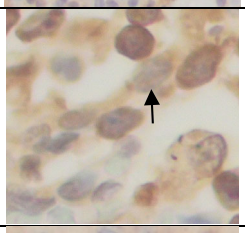	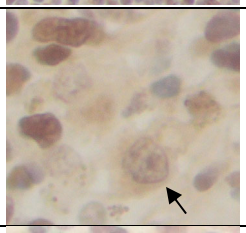
Mast Cell Tumor	Normal mast cells from skin, lymph nodes	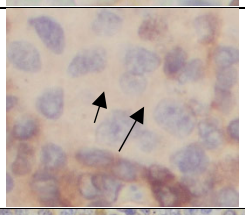	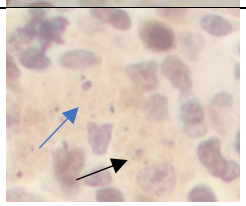
Hemangiosarcoma	Normal endothelial cells	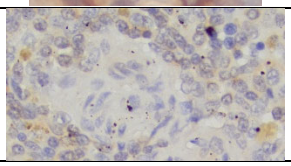	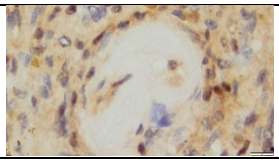

Figure 3.4: Examples of immunostaining for p65 and p100/p52 in normal canine tissues.

IHC grading of tissue microarrays

Figure 3.5 shows the arrangement of tumor cores in tissue microarrays. Each microarray is placed on a single microscopic slide, which allows staining of multiple tumor cores for high throughput IHC assessment.

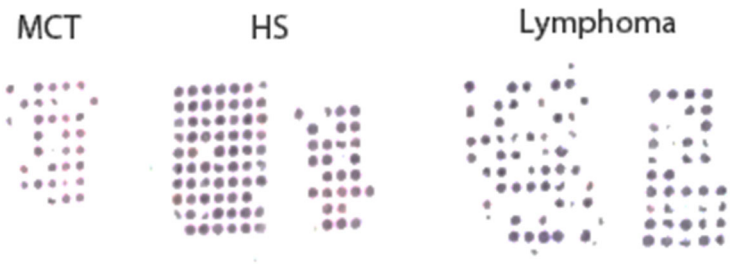

Figure 3.5: Images of 1.5 mm tissue microarray cores, as arranged on glass slides, which were constructed and used for this study.

Table 3.3 shows the cytoplasmic and nuclear scores for normal tissue cells. These values were subsequently used as a threshold to determine whether tumor tissues had greater relative overactivation of NF-kB signaling pathways. **Table 3.4** shows the numbers of tumors that were ultimately classified as having low, moderate, or high nuclear NF-kB pathway staining. Tumors staining was then compared to the threshold set by grading normal tissues. These data are presented graphically in **Figure 3.6.**

Table 3.3: Normal cell thresholds established via IHC grading.

Normal cell type	*P65 nuclear score*	*P100/p52 nuclear score*	*# of cells evaluated*
Lymphocytes	60	74	2,000
Dendritic cells	20	93	200
Mast cells	50	80	200
Endothelial cells	8	21	200

Table 3.4: IHC grading of tumor tissues.

Stain	*Tumor type*	*Negative*	*Low*	*Moderate*	*High*	*Positive*
p65	Lymphoma	2	1	34	48	83
	Histiocytic sarcoma	11	42	31	5	78
	Mast cell tumor	19	13	7	2	9
	Hemangiosarcoma	0	1	4	5	10
p100/p52	Lymphoma	4	0	36	40	76
	Histiocytic sarcoma	16	0	47	28	75
	Mast cell tumor	0	0	3	26	29
	Hemangiosarcoma	0	1	5	4	10
p65	Lymphoma	2.4%	1.2%	40.0%	56.5%	97.6%
	Histiocytic sarcoma	12.4%	47.2%	34.8%	5.6%	87.6%
	Mast cell tumor	67.9%	46.4%	25.0%	7.1%	32.1%
	Hemangiosarcoma	0%	40.0%	30.0%	30.0%	100%
p100/p52	Lymphoma	5.0%	5.0%	45.0%	50.0%	95%
	Histiocytic sarcoma	14.9%	17.6%	51.6%	30.8%	85.1%
	Mast cell tumor	0.0%	0.0%	10.3%	89.7%	100%
	Hemangiosarcoma	0.0%	10.0%	50.0%	40.0%	100%

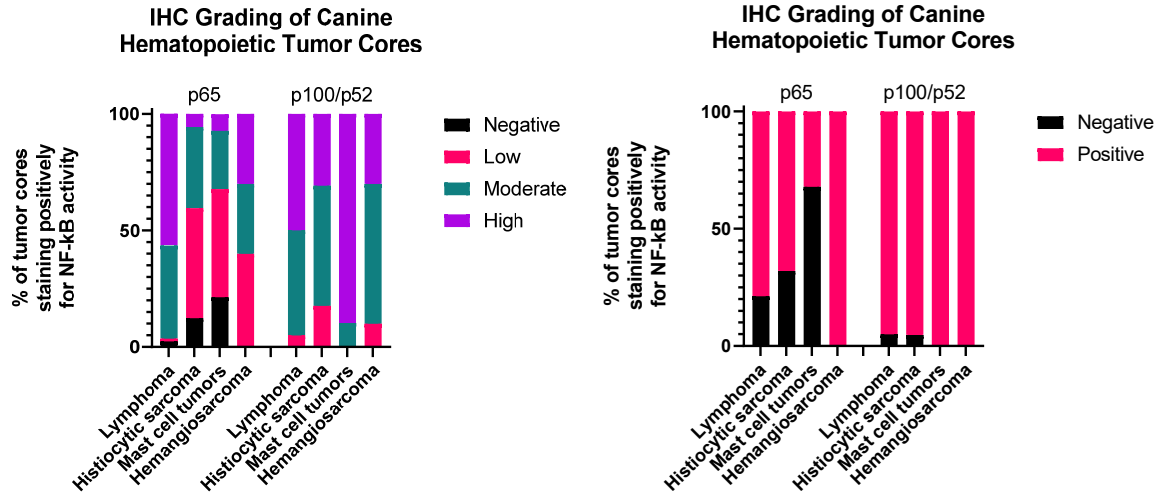

Figure 3.6: Summary data showing numbers of canine hematopoietic tumor cores with IHC nuclear grades (left) and the percentage of tumors with positive staining relative to control tissues in each category (right).

Relative to control tissues, many tumor types exhibited some overactivation (nuclear staining) of p65 and/or p100/p52. This indicates that inhibitors of both NF-kB pathways may be of some therapeutic benefit to patients with these diseases. For example, the plant-derived, secondary metabolite PTL is a canonical NF-kB inhibitor shown to be effective *in vitro* in many different canine cell lines, including the cell lines that were evaluated immunohistochemically in this study. In the following sections, NF-kB activation status is evaluated with respect to other available data points (survival data, mitotic index, etc., as available) for each tumor type.

Lymphoma

As previously noted, pre- and post-CHOP-treatment (relapsed) data were available for lymphoma cores, as well as survival data. There was no difference in nuclear p65 staining or p65 nuclear/cytoplasmic staining intensity for pre- vs post-treatment patients in this study. There was a trend toward increased nuclear p65 and the p65 nuclear/cytoplasmic ratio for B vs T cell lymphomas, but this difference was not statistically significant ($p = 0.07$ and $p = 0.1$), respectively. There was no significant correlation between nuclear p65 staining and survival metrics (PFS, OST). However, there were significant correlations between p65 nuclear/cytoplasmic ratio staining and these metrics via Cox regression, as follows:

Progression free survival: $p = 0.011$, HR (95% CI) = 1.124 (1.002 – 1.228)

Overall survival: $p = 0.021$, HR (95% CI) = 1.107 (1.016-1.206)

No significant correlations were identified in this data set for p100/p52 IHC staining.

Histiocytic Sarcoma

There was not a statistically significant difference in the mitotic index (MI) that could be predicted by a tumor's anatomical site of origin in this data set. There was no significant correlation (Spearman's r) between a tumor's MI and nuclear p65 or p100/p52 staining intensity, nor between the MI and the N:C staining ratio. Summary statistics from these analyses are shown in **Figure 3.7.**

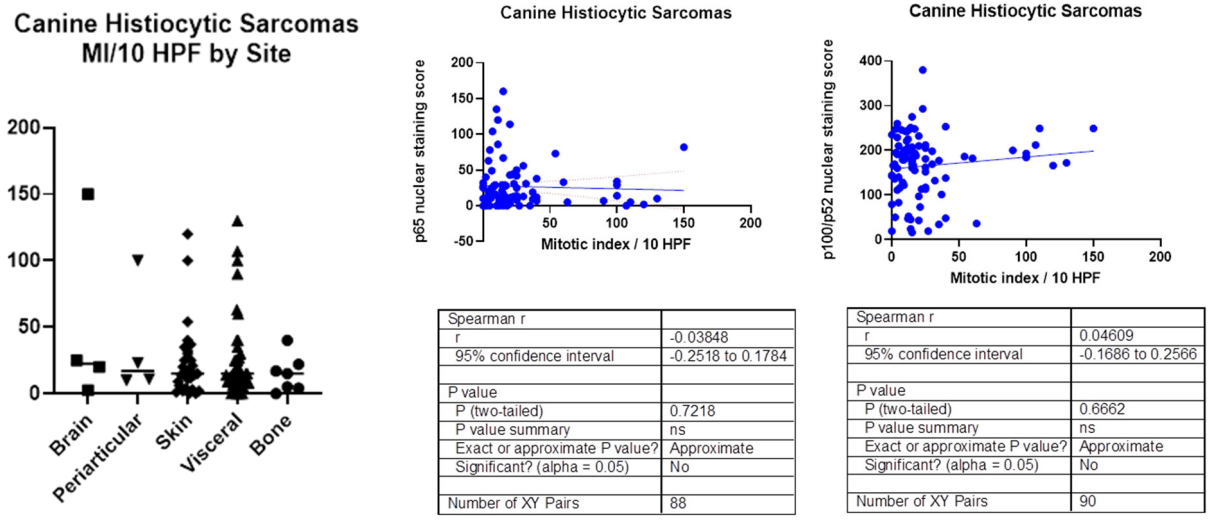

Spearman r	
r	-0.03848
95% confidence interval	-0.2518 to 0.1784
P value	
P (two-tailed)	0.7218
P value summary	ns
Exact or approximate P value?	Approximate
Significant? (alpha = 0.05)	No
Number of XY Pairs	88

Spearman r	
r	0.04609
95% confidence interval	-0.1686 to 0.2566
P value	
P (two-tailed)	0.6662
P value summary	ns
Exact or approximate P value?	Approximate
Significant? (alpha = 0.05)	No
Number of XY Pairs	90

Figure 3.7: Selected outputs from statistical analyses of mitotic index and NF-kB IHC nuclear staining intensity. The mitotic index was not statistically correlated with either p65 or p100/p52 nuclear staninig intensity in HS tumor cores.

Mast Cell Tumor

There was not a statistically significant difference in the mitotic index (MI) that could be predicted by a tumor's anatomical site of origin in this data set. There was no

significant correlation (Spearman's r) between a tumor's MI and the nuclear p65 or p100/p52 staining intensity, nor between the MI and the N:C staining ratio. Summary statistics from these analyses are shown in **Figure 3.8.**

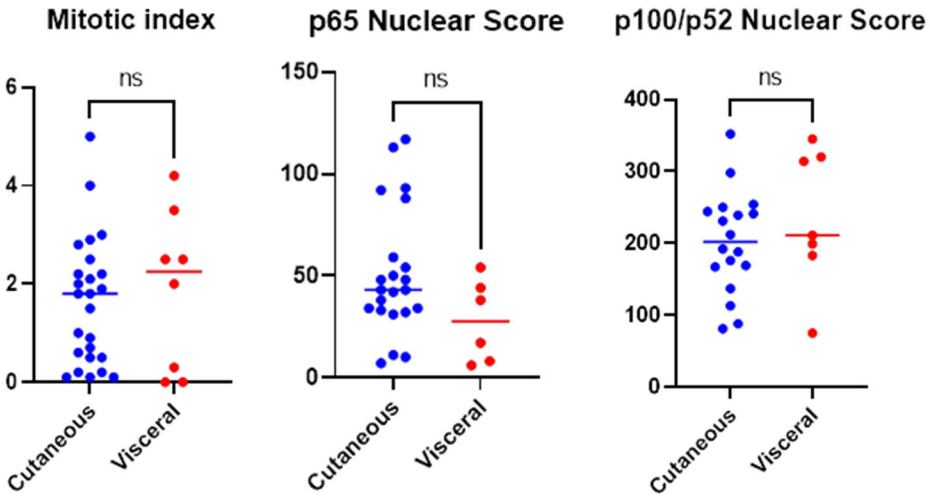

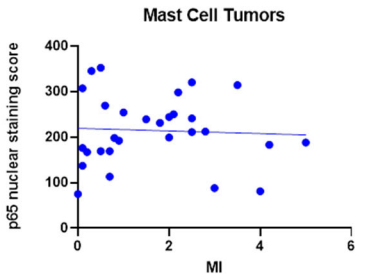

Spearman r	
r	0.2716
95% confidence interval	-0.1167 to 0.5878
P value	
P (two-tailed)	0.1542
P value summary	ns
Exact or approximate P value?	Approximate
Significant? (alpha = 0.05)	No
Number of XY Pairs	29

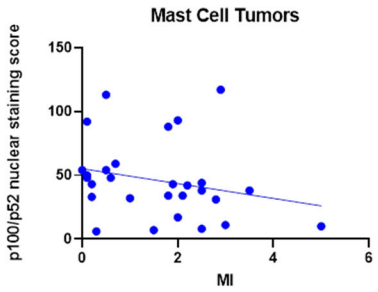

Spearman r	
r	-0.3351
95% confidence interval	-0.6364 to 0.05500
P value	
P (two-tailed)	0.0813
P value summary	ns
Exact or approximate P value?	Approximate
Significant? (alpha = 0.05)	No
Number of XY Pairs	28

Figure 3.8: Top: there was no statistical difference in the mitotic index, p65, or p100/p52 staining properties of cutaneous vs. visceral MCTs from dogs. Bottom: A statistically significant correlation was not identified between NF-kB nuclear staining intensity and mitotic index in canine mast cell tumors.

For the MCTs evaluated in this study, as previously noted, multiple criteria were available to test statistical correlation with NF-kB IHC staining intensity. Although cutaneous MCTs are one of the most common neoplasms to affect dogs, their biologic behavior is quite variable, and various grading schemes and molecular markers have been studied to attempt higher precision in prognostication and optimization of treatment regimens.[34]

For cutaneous MCTs in dogs, two histologic grading schemes are commonly in use. The Patnaik system (1984) divides MCTs into three histologic grades,[23] while the more recent Kuipel system (2011) uses a two-tiered scheme to avoid challenges in interpreting moderately differentiated, or "intermediate grade" lesions.[19,11,7] **Figure 3.9** shows summary statistics correlating the two aforementioned MCT grading schemes with NF-kB nuclear staining intensity. There were no statistically significant correlations identified, although there was a trend toward greater nuclear p65 staining with higher Patnaik and Kuipel grade.

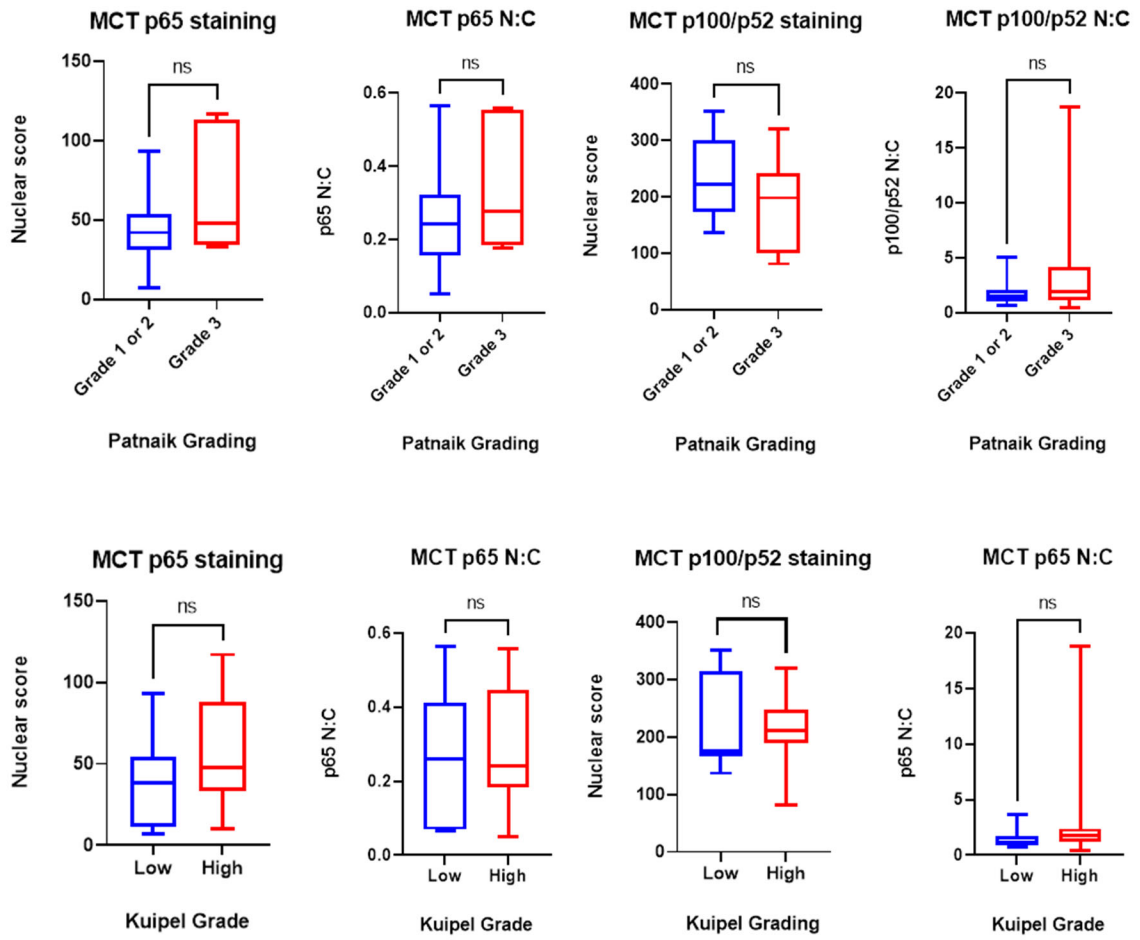

Figure 3.9: There were no statistically significant associations between histologic grading schemes and p65 or p100/p52 IHC staining scores. Selected data are shown.

Measures of proliferation have been used in both human and veterinary medicine to attempt more accurate prognostication in various neoplastic diseases. Ki67 is a nuclear protein that is expressed in all phases of the cell cycle, but is not expressed in noncycling cells, and therefore, the proportion of positive Ki67 cells in tissue can be used to determine the proliferative index or "growth fraction" within a tissue.[6,26] Summary data for Ki67 staining in the current study data set are shown in **Figure 3.10.** There was a significant correlation between Ki67 stain grade and p65 nuclear grading (Mann Whitney test, p = 0.0257). A statistically significant correlation was not observed

between MI and Ki67 staining, nor between p65 or p100/p52 and MI in this study, although there was a trend toward higher MI for tumors with high Ki67 staining, as well as a trend for greater p65 nuclear staining with higher MI.

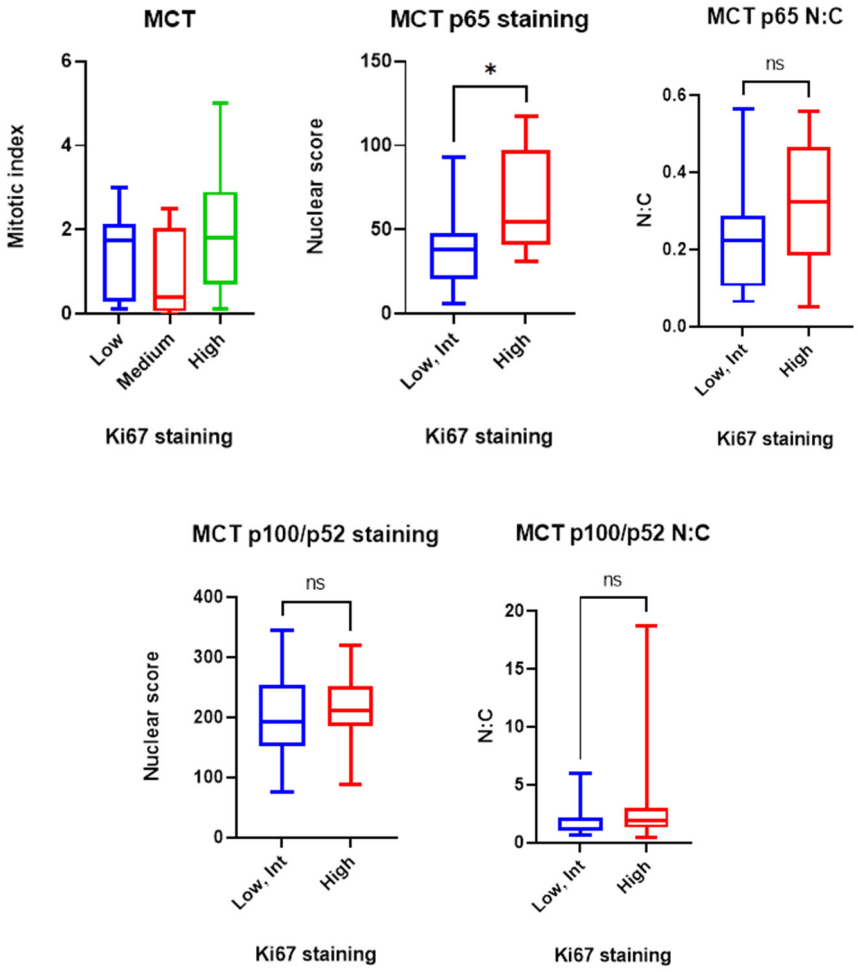

Figure 3.10: The correlation between Ki67 and p65 nuclear staining in canine MCTs is statistically significant. While the mitotic index and p65 N:C showed positive trends with greater Ki67 staining, these changes were not statistically significant. P100/p52 immunostaining and Ki67 do not appear to correlate in canine MCTs.

The KIT protein is a tyrosine kinase receptor is a product of the c-kit proto-oncogene. Of many potential markers, *c-kit* has been consistently identified as a key player in MCT development, and its constitutive activation is associated with tyrosine

receptor kinase-mediated cellular survival, proliferation, and motility via multiple downstream pathways, including the RAS/mitogen-activated protein kinase pathway, PI3-kinase, and Src family of kinases (SFK) pathways.[7]

Mutations of the *c-kit* gene can lead to constitutive KIT activation, independent of ligand binding, and in one study, exon 11 mutations have been documented as occurring more frequently in grade II or III tumors.[37] A statistically significant correlation was not identified between *c-kit* mutation status and NF-kB IHC staining intensity; however, only low numbers of tumors in this study had detectable mutations (**Figure 3.11**).

IHC detection of KIT has been well established in veterinary medicine, and different patterns of KIT expression have been described in normal mast cells (membranous, pattern I) and neoplastic mast cells (occasionally membranous, but often cytoplasmic, often adjacent to the cell nucleus, patterns II and III).[24] Data evaluating KIT and NF-kB IHC staining are shown in **Figure 3.11.** No statistically significant associations were identified in this data set.

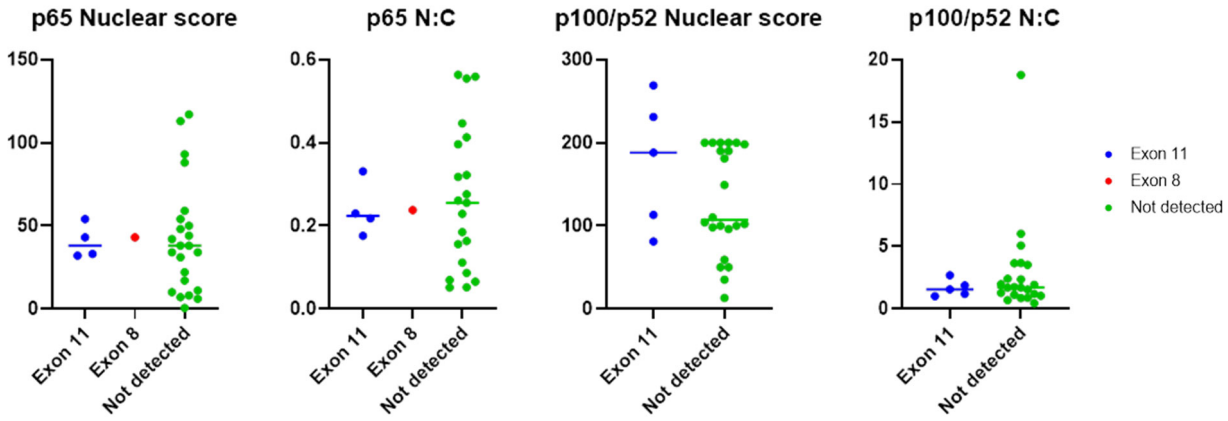

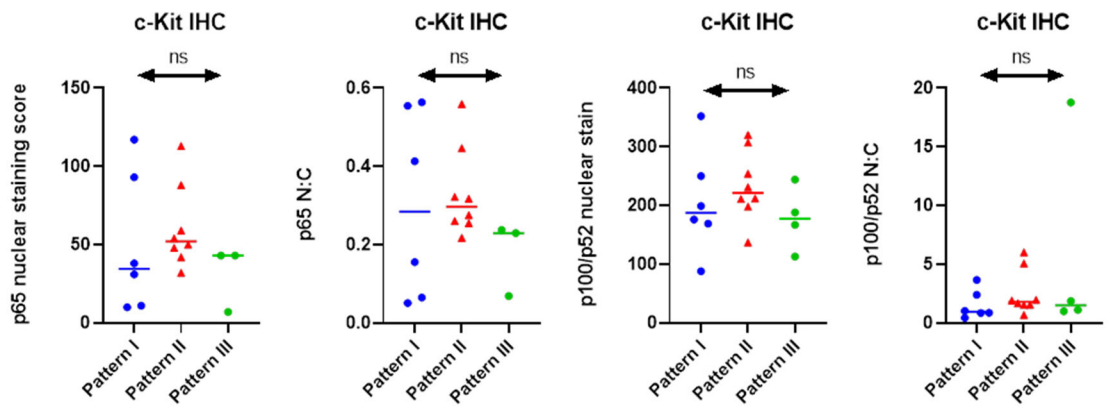

Figure 3.11: Top: c-Kit ITD mutations identified in canine MCTs and NF-kB staining. Bottom: correlations between c-Kit staining patterns and NF-kB staining. No statistically significant correlations were identified in this data set.

Hemangiosarcoma

None of the immunostaining performed on this tumor set yielded a statistically significant correlation with mitotic index (**Figure 3.12**).

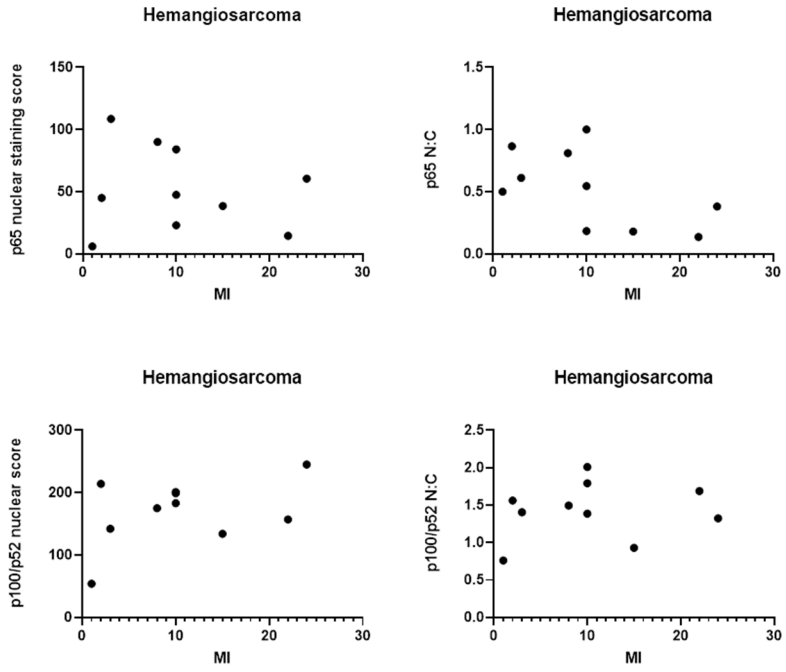

Figure 3.12: p65 and p100/p52 nuclear staining plotted against mitotic index for HSA tumors. No statistically significant Spearman correlations were identified.

Discussion and Conclusions

Overall, findings from this study support overactive NF-kB signaling as a common aberration in a variety of tumor types, and importantly, in types of cancer that are overrepresented in some dog breeds but are considered orphan diseases in humans. For HS, HSA, and MCT, this study suffers from the usual problems affecting studies that utilize biopsy and necropsy specimens, which include variable time of formalin fixation prior to embedding (which can, in theory, affect immunohistochemical staining properties of cells[33]), incomplete information regarding disease presentation (for biopsy specimens), and lack of outcome data.

Based on the canine lymphoma data, p65 nuclear staining has potential as a predictor of progression free interval and overall survival in dogs with this cancer type. This finding is not surprising, since p65 activation has been documented in human ABC diffuse large B cell lymphoma, which is a biologically similar disease to cases of canine lymphoma.[3 8] Although lymphoma is a heterogeneous disease with variable biologic behavior, inadequate numbers of tumors were available to assess NF-kB staining with respect to histologic subtype. Additionally, inadequate sample numbers were available to assess staining differences with respect to T vs. B cell immunophenotype. Ideally, data from this preliminary study could be used to further evaluate the NF-kB activation status of a larger number of lymphomas for which additional data are available for correlation (immunophenotype, histologic subtype, and outcome).

Since there is evidence of documented crosstalk between NF-kB signaling and PI3-Kinase/AKT, JAK-STAT, and MAPK signaling pathways, and these pathways are

downstream of KIT signaling, we initially expected to see more evidence of p65 nuclear staining in MCTs.[1,2,12,25,31,36]

The significance of this seeming discrepancy is unknown at the time of writing. Since this was a relatively small dataset, perhaps the data are not fully representative of p65 activation status. Alternatively, this could be a real finding, as MCT cell lines are more resistant to the NF-kB inhibitor PTL (Chapter 2) as compared to other tumor types. Ideally, larger numbers of MCTs would be assessed to make this determination with more confidence.

As previously noted, one substantial challenge in histologic grading of MCTs is that in the Patnaik system, more than 40% of tumors are classified as being of "intermediate" grade, yet these tumors demonstrate significantly variable biologic behavior, and problematically, there is significant pathologist interobserver variability in this grading scheme.[19] Many of the studies evaluating additional biologic markers for MCTs, including proliferative indices, have been aimed at overcoming the limitations that are evident in existing histologic grading schemes. In a study evaluating multiple proliferative markers in canine MCTs, Ki67 staining had a distinct cut-off value that allowed for discrimination of tumors with an increased incidence and rate of tumor recurrence at the original surgical site, as well as increased incidence of MCT-related mortality.[34] Especially with respect to grade II tumors in the Patnaik system, several other studies have demonstrated that the Ki67 index and MI may aid in predicting MCT prognosis, but overall, a high Ki67 index should not, on its own, be considered a poor prognostic indicatior.[25,34,14,31,9] The Ki67 index is one of many factors that may be useful in understanding MCT behavior, but no single prognostic marker is currently considered

to be definitive.[30] The association between Ki67 and p65 nuclear staining in the current study suggests that at least some MCT proliferation may be due to p65 overactivation. Again, evaluation of a larger number of MCTs, especially for which treatment is standardized and outcome data are known, may be beneficial, to further document NF-kB signaling overactivation, as well as determine its significance with respect to patient outcome.

Overall, data from this study demonstrate that NF-kB overactivation, both via the canonical and alternative signaling pathways, is present in a wide variety of canine tumor types and is a viable therapeutic target. Additional studies are needed to understand the biological implications of these signaling abnormalities, as well as the genetic bases of mutations or non-mutational processes that may give rise to aberrant signaling in these tumors. Such studies may ultimately provide necessary data for improving our understanding of tumor biology, as well as an improved understanding of therapeutics that may be useful for these tumors.

References

1. Ahmad SF, Ansari MA, Zoheir KMA, et al. Regulation of TNF-α and NF-κB activation through the JAK/STAT signaling pathway downstream of histamine 4 receptor in a rat model of LPS-induced joint inflammation. *Immunobiology*. 2015;220: 889-898.

2. Bai D, Ueno L, Vogt PK. Akt-mediated regulation of NFkappaB and the essentialness of NFkappaB for the oncogenicity of PI3K and Akt. *Int J Cancer*. 2009;125: 2863-2870.

3. Cannon C, Borgatti A, Henson M, Husbands B. Evaluation of a combination chemotherapy protocol including lomustine and doxorubicin in canine histiocytic sarcoma. *J Small Anim Pract.* 2015;56: 425-429.

4. Cohen SM, Storer RD, Criswell KA, et al. Hemangiosarcoma in rodents: mode-of-action evaluation and human relevance. *Toxicol Sci.* 2009;111: 4-18.

5. Davis RE, Brown KD, Siebenlist U, Staudt LM. Constitutive Nuclear Factor κB Activity Is Required for Survival of Activated B Cell–like Diffuse Large B Cell Lymphoma Cells. *Exp Med.* 2001;194: 1861-1874.

6. Dervisis NG, Kiupel M, Qin Q, Cesario L. Clinical prognostic factors in canine histiocytic sarcoma. *Vet Comp Oncol.* 2017;15: 1171-1180.

7. Dickerson EB, Thomas R, Fosmire SP, et al. Mutations of Phosphatase and Tensin Homolog Deleted from Chromosome 10 in Canine Hemangiosarcoma. *Vet Pathol*. 2005;42: 618-632.

8. Gerdes J, Lemke H, Baisch H, Wacker HH, Schwab U, Stein H. Cell cycle analysis of a cell proliferation-associated human nuclear antigen defined by the monoclonal antibody Ki-67. *J Immunol.* 1984;133: 1710-1715.

9. Gil da Costa RM. C-kit as a prognostic and therapeutic marker in canine cutaneous mast cell tumours: From laboratory to clinic. *Vet J.* 2015;205: 5-10.

10. Grimm T, Schneider S, Naschberger E, et al. EBV latent membrane protein-1 protects B cells from apoptosis by inhibition of BAX. *Blood.* 2005;105: 3263-3269.

11. Horta RS, Lavalle GE, Monteiro LN, Souza MCC, Cassali GD, Araújo RB. Assessment of Canine Mast Cell Tumor Mortality Risk Based on Clinical, Histologic, Immunohistochemical, and Molecular Features. *Vet Pathol*. 2018;55: 212-223.

12. Ibrahim SSA, Salama MA, Selima E, Shehata RR. Sitagliptin and tofacitinib ameliorate adjuvant induced arthritis via modulating the cross talk between JAK/STAT and TLR-4/NF-κB signaling pathways. *Life Sci*. 2020;260: 118261.

13. Ito D, Frantz AM, Modiano JF. Canine lymphoma as a comparative model for human non-Hodgkin lymphoma: recent progress and applications. *Vet Immunol Immunopathol*. 2014;159: 192-201.

14. Kiupel M, Webster JD, Bailey KL, et al. Proposal of a 2-tier histologic grading system for canine cutaneous mast cell tumors to more accurately predict biological behavior. *Vet Pathol*. 2011;48: 147-155.

15. Kommalapati A, Tella SH, Durkin M, Go RS, Goyal G. Histiocytic sarcoma: a population-based analysis of incidence, demographic disparities, and long-term outcomes. *Blood*. 2018;131: 265-268.

16. Lamerato-Kozicki AR, Helm KM, Jubala CM, Cutter GC, Modiano JF. Canine hemangiosarcoma originates from hematopoietic precursors with potential for endothelial differentiation. *Exp Hematol.* 2006;34: 870-878.

17. Maglennon GA, Murphy S, Adams V, et al. Association of Ki67 index with prognosis for intermediate-grade canine cutaneous mast cell tumours. *Vet Comp Oncol*. 2008;6: 268-274.

18. Marconato L, Gelain ME, Comazzi S. The dog as a possible animal model for human non-Hodgkin lymphoma: a review. *Hematol Oncol*. 2013;31: 1-9.

19. Moirano SJ, Lima SF, Hume KR, Brodsky EM. Association of prognostic features and treatment on survival time of dogs with systemic mastocytosis: A retrospective analysis of 40 dogs. *Vet Comp Oncol.* 2018;16: E194-E201.

20. Moore PF. A Review of Histiocytic Diseases of Dogs and Cats. *Vet Pathol.* 2014;51: 167-184.

21. Murai A, Asa SA, Kodama A, Hirata A, Yanai T, Sakai H. Constitutive phosphorylation of the mTORC2/Akt/4E-BP1 pathway in newly derived canine hemangiosarcoma cell lines. *BMC Vet Res.* 2012;8: 128.

22. Northrup NC, Harmon BG, Gieger TL, et al. Variation among pathologists in histologic grading of canine cutaneous mast cell tumors. *J Vet Diagn Invest*. 2005;17: 245-248.

23. O'Donoghue LE, Rivest JP, Duval DL. Polymerase chain reaction–based species verification and microsatellite analysis for canine cell line validation. *J Vet Diagn Invest*. 2011;23: 780-785.

24. Pardanani A. Systemic mastocytosis in adults: 2013 update on diagnosis, risk stratification, and management. *Am J Hematol*. 2013;88: 612-624.

25. Park S, Zhao D, Hatanpaa KJ, et al. RIP1 activates PI3K-Akt via a dual mechanism involving NF-kappaB-mediated inhibition of the mTOR-S6K-IRS1 negative feedback loop and down-regulation of PTEN. *Cancer Res*. 2009;69: 4107-4111.

26. Parrales A, McDonald P, Ottomeyer M, et al. Comparative oncology approach to drug repurposing in osteosarcoma. *PLoS One*. 2018;13: e0194224.

27. Patnaik AK, Ehler WJ, MacEwen EG. Canine cutaneous mast cell tumor: morphologic grading and survival time in 83 dogs. *Vet Pathol*. 1984;21: 469-474.

28. Reguera MJ, Rabanal RM, Puigdemont A, Ferrer L. Canine mast cell tumors express stem cell factor receptor. *Am J Dermatopathol*. 2000;22: 49-54.

29. Scase TJ, Edwards D, Miller J, et al. Canine mast cell tumors: correlation of apoptosis and proliferation markers with prognosis. *J Vet Intern Med*. 2006;20: 151-158.

30. Scholzen T, Gerdes J. The Ki-67 protein: From the known and the unknown. *J Cell Physiol*. 2000;182: 311-322.

31. Schulze-Osthoff K, Ferrari D, Riehemann K, Wesselborg S. Regulation of NF-κB Activation by MAP Kinase Cascades. *Immunobiology*. 1997;198: 35-49.

32. Skorupski KA, Clifford CA, Paoloni MC, et al. CCNU for the Treatment of Dogs with Histiocytic Sarcoma. *J Vet Intern Med*. 2007;21: 121-126.

33. Takada M, Smyth LA, Thaiwong T, et al. Activating Mutations in PTPN11 and KRAS in Canine Histiocytic Sarcomas. *Genes*. 2019;10: 505.

34. Tate G, Suzuki T, Mitsuya T. Mutation of the PTEN gene in a human hepatic angiosarcoma. *Cancer Genet Cytogenet.* 2007;178: 160-162.

35. Thamm DH, Avery AC, Berlato D, et al. Prognostic and predictive significance of KIT protein expression and c-kit gene mutation in canine cutaneous mast cell tumours: A consensus of the Oncology-Pathology Working Group. *Vet Comp Oncol*. 2019;17: 451-455.

36. Torres J, Enríquez-de-Salamanca A, Fernández I, et al. Activation of MAPK Signaling Pathway and NF-κB Activation in Pterygium and Ipsilateral Pterygium-Free Conjunctival Specimens. *Investig Ophthalmol Vi. Sci.*. 2011;52: 5842-5852.

37. van Lelyveld S, Warland J, Miller R, et al. Comparison between Ki-67 index and mitotic index for predicting outcome in canine mast cell tumours*. J Small Anim Pract*. 2015;56: 312-319.

38. Wang G, Wu M, Durham AC, et al. Molecular subtypes in canine hemangiosarcoma reveal similarities with human angiosarcoma. *PLoS One*. 2020;15: e0229728.

39. Webster JD, Miller MA, DuSold D, Ramos-Vara J. Effects of Prolonged Formalin Fixation on Diagnostic Immunohistochemistry in Domestic Animals. *J Histochem Cytochem*. 2009;57: 753-761.

40. Webster JD, Yuzbasiyan-Gurkan V, Miller RA, Kaneene JB, Kiupel M. Cellular Proliferation in Canine Cutaneous Mast Cell Tumors: Associations with c-KIT and Its Role in Prognostication. *Vet Pathol*. 2007;44: 298-308.

41. Wolf-Ringwall A, Lopez L, Elmslie R, et al. Prospective evaluation of flow cytometric characteristics, histopathologic diagnosis and clinical outcome in dogs with naïve B-cell lymphoma treated with a 19-week CHOP protocol. *Vet Comp Oncol.* 2020;18: 342-352.

42. Yang J, Kantrow S, Sai J, et al. Ikk4a/Arf Inactivation with Activation of the NF-κB/IL-6 Pathway Is Sufficient to Drive the Development and Growth of Angiosarcoma. *Cancer Res.* 2012;72: 4682-4695.

43. Zemke D, Yamini B, Yuzbasiyan-Gurkan V. Mutations in the juxtamembrane domain of c-KIT are associated with higher grade mast cell tumors in dogs. *Vet Pathol*. 2002;39: 529-535.

CHAPTER 4: CONCLUSIONS AND FUTURE DIRECTIONS

General Conclusions

The studies contained within this dissertation evaluate the NF-kB activation status of many canine tumors, of varying histologic types. Aberrant, overactive, NF-kB signaling has been characterized extensively across many types of cancer in human medicine, and to some degree in veterinary medicine as well, as reviewed in Chapter 1. In Chapters 2 and 3, studies with canine cell lines, primary cells from patients, and biopsy specimens often demonstrate overactive NF-kB signaling. Because there are many pro-tumorigenic effects of NF-kB activity, including cell survival, proliferation, angiogenesis, inflammation, invasion, and metastasis, the effect of constitutive NF-kB activation can be devastating to the host. This work further corroborates NF-kB overactivation as an important signaling aberration in canine cancer, and importantly, in human “orphan diseases” as well as lymphoma; the latter, as previously noted, is an incredibly common cancer in both dogs and humans. NF-kB overactivation is yet another molecular similarity that canine cancers share with their human counterparts. Importantly, these data were able to demonstrate a correlation between p65/RelA nuclear immunostaining intensity and decreased survival in lymphoma patients, as well as correlation with Ki67, a proliferative and prognostic indicator in MCT. Although additional studies are needed, these data suggest that aberrant NF-kB signaling is not just a feature of canine cancer, but has measurable cellular and organism-level consequences, and that therapeutic targeting that alters this signaling may be beneficial for some tumor types.

An additional goal of this research was to evaluate the compound parthenolide (PTL) as a potential therapeutic in canine cancer. Data from canine cell lines, primary cells, and preliminarily in mice are all indicative of PTL being a viable therapeutic compound, which exerts its action, in part, via NF-kB inhibition and perturbation of cellular redox balance in canine cancers. A pending mouse experiment will evaluate the effectiveness of PTL in an *in vivo* xenograft model of canine HS.

Future Directions

There are numerous potential future directions for this work. As there are few viable treatment options for canine HS, HSA, and disseminated MCT, PTL is worth investigating as an adjuvant therapeutic to existing chemotherapeutic protocols. As previously stated, an additional, four-arm mouse experiment is pending in which combination therapy with CCNU/lomustine will be evaluated in a xenograft model of canine HS. If warranted, additional mouse experiments and potentially, canine clinical trials, may be beneficial in further evaluating PTL's promise as a therapeutic in dogs.

To this end, given the broad activity of PTL in tumor types of quite variable histologic backgrounds, an obvious set of follow-up experiments for PTL would be evaluation of combination therapies with other standard-of-care drugs that are in use for various cancer types. A CRISPR-Cas9 whole genome library has been constructed and is currently undergoing evaluation in the Duval laboratory. A stated goal of the library is to use CRISPR-Cas9 knockout genes to identify drug targets that may be synthetic lethal when combined with other therapeutics; the library could be used to identify potential synthetic lethal targets with PTL, if it is used in this fashion.

The NF-kB immunostaining in canine tumors lays the groundwork for investigation of additional therapeutics that may target aberrant canonical and alternative NF-kB signaling. In addition, further evaluation of genetic expression data across many canine cell lines will likely identify anomalies that are linked to NF-kB overactivation, which may help researchers understand how best to target aberrant signaling. Creation and study of cell lines that are resistant to standard-of-care chemotherapeutics may help to elucidate mechanisms of resistance that may be linked to NF-kB signaling, and evaluation of PTL as a compound in this scenario could provide an *in vitro* model of treatment for drug-resistant neoplasms.